A COMPARATIVE STUDY AND ANALYSIS OF PHES AND UGPHES SYSTEMS

by

Shiraz Yusuf Khan

Submitted in partial fulfillment of the requirements for the degree of

Master of Science in Power and Energy Systems

School of Electrical, Electronic and Computer Engineering

University of KwaZulu-Natal

Durban

October 2015

ABSTRACT

Underground Pumped Hydroelectric Energy Storage (UGPHES) is a similar energy storage concept to the conventional Pumped Hydroelectric Energy Storage (PHES) with the major difference being that the lower reservoir is in an underground cavern system. Electricity is stored in the form of gravitational potential energy between a surface reservoir and an underlying subterranean reservoir. In this study, various existing energy storage systems are examined with the UGPHES introduced as an alternative technology for bulk energy storage in South Africa to contribute to the constrained electricity network with environmental and economic benefits. The use of existing infrastructure for the implementation of UGPHES systems is explored, which includes the use of aquifers and abandoned mines. South Africa has large amounts of groundwater as well as transboundary aquifers which may be used for UGPHES systems. A mathematical model is presented which highlights the considerations for the implementation of an aquifer UGPHES system including head and aquifer transmissivity. The use of abandoned mines in South Africa is also explored as it presents an existing underground cavern as well as large amounts of groundwater. Finally, a mathematical model is presented to provide an analysis of the water hammer phenomenon as well as an economic analysis for the use of abandoned mines for UGPHES systems.

I dedicate my dissertation to my wife Farzana Banu and our four children, Muhammed Suhail, Mariam Bibi, Muhammed Hussain and Faatimah Zahra. They all provided me with the support and encouragement that I needed to work hard to complete this dissertation, including sacrificing weekends, holidays and valuable family time. I also dedicate my dissertation to my research supervisor Dr. Innocent Davidson who always found the time in his hectic schedule to provide me with direction, support and encouragement required to make this dissertation a success.

PREFACE

This mini-dissertation is the own work of Shiraz Yusuf Khan, Student No. 951031135, and has not been submitted in part or in whole to any other University. The research work was carried out in Sarnia, Ontario, Canada under the supervision of Dr. I.E. Davidson based in South Africa, in partial fulfillment of the requirements for the degree of Master of Science in Power and Energy Systems.

Signed by …… at …… on ……...

ACKNOWLEDGEMENTS

The author would like to thank the following people and entities for their support and assistance in the development of this dissertation:

Dr. I.E. Davidson

Department of Environmental Affairs and Tourism (DEAT) – South Africa

Department of Mineral Resources (DMR) – South Africa

Department of Water Affairs and Forestry (DWAF) – South Africa

Eskom

Energy Storage Association (ESA)

Institute of Electrical and Electronic Engineers (IEEE)

Massachusetts Institute of Technology (MIT)

Ministry of Mines and Energy (MME) - Namibia

The University of KwaZulu Natal (UKZN)

TABLE OF CONTENTS

LIST OF TABLES

LIST OF FIGURES

LIST OF ABBREVIATIONS

°C	Degree Celsius
a	annum
A	Ampere
AC	Alternating Current
AGEP	Average Groundwater Exploitation Potential
AMD	Acid Mine Drainage
ATES	Aquiferous Thermal Energy Storage
BIC	Bushveld Igneous Complex
Br	Bromine
c	cent
CAES	Compressed Air Energy Storage
CEB	Cuvelai-Etosha Basin
CHES	Carbon-Hydride Energy Storage
Cd	Cadmium
CES	Cryogenic Energy Storage
CO_2	Carbon Dioxide
CSP	Concentrating Solar Power
d	day

DC	Direct Current
DMR	Department of Mineral Resources
DWA	Department of Water Affairs
DWR	Deep Water Research
EQPS	Elmhurst Quarry Pumped Storage
FEM	Finite Element Method
FWT	Floating Wind turbine
GHG	Greenhouse Gas
GIS	Geographic Information System
GMNN	Groundwater Management North Namibia
GPM	Gravity Power Module
GRP	Groundwater Resource Potential
GSHP	Ground Source Heat Pump
GW	Gigawatt
GWh	Gigawatt hour
h	hour
hp	horsepower
HPS	Highview Power Storage
HVAC	Heating, Ventilation and Cooling

kg	kilogram
kJ	kilojoule
km	kilometer
km^2	square kilometer
kV	kilovolt
kW	kilowatt
kWh	kilowatt hour
l	litre
LANL	Los Alamos National Laboratory
lb	pound
Li	Lithium
m	meter
mAh	milliampere hour
mm	millimeter
m^2	square meter
m^3	cubic meter
MJ	Mega Joule
Mm^3	Mega cubic meter
ML	Mega Litre

MCH	Methylcyclohexane
MP&L	Metlakatla Power and Light
MPa	Megapascals
MPSP	Mineville Pumped Storage Project
MW	Megawatt
MWh	Megawatt hour
Na	Sodium
Ni	Nickel
nm	nanometer
Nm^3	Newton cubic meter
NO_x	Nitrogen Oxide
OCAES	Ocean Compressed Air Energy Storage
OCGT	Open Cycle Gas Turbine
ORES	Ocean Renewable Energy Storage
PCM	Phase Change Material
PHES	Pumped Hydroelectric Energy Storage
R	Rand
RDP	Reconstruction and Development Programme
RE	Renewable Energy

RWEC	Riverbank Wiscasset Energy Centre
rpm	revolutions per minute
RTIL	Room Temperature Ionic Liquid
s	second
S	Sulphur
SAHPS	Solar-Assisted Heat Pump System
SATVLA	South African Transvaal Aquifer
SGCHPS	Solar-Ground Coupled Heat Pump System
SMES	Superconducting Magnetic Energy Storage
SO_x	Sulphur Oxide
TES	Thermal Energy Storage
UK	United Kingdom
UGPHES	Underground Pumped Hydroelectric Energy Storage
UPS	Uninterruptable Power Supply
US	United States
V	Volt
VAR	Volt Ampere Reactive
VRLA	Valve Regulated Lead Acid
W	Watt

Wh	Watt hour
Zn	Zinc

CHAPTER 1

INTRODUCTION

The last century has demonstrated that every facet of human development is woven around a sound and stable energy supply regime [1]. Fossil fuels have for a long time been regarded as the primary energy resource used for bulk electric power generation, beside large hydro electric power schemes which use water. However, this has brought with it health and environmental issues which is considered to be a contributor to global warming [2]. Fossil fuels are depletable resources. The real challenge lies in producing electricity supplies through renewable energy and clean energy sources. While renewable energy (RE) sources such as wind and solar energy are seen to be inexhaustible, the amount of energy that we use ultimately needs to be regulated, hence the adoption of energy efficiency measures which include demand-side management. This also presents opportunities for improving the energy infrastructure through the use of distributed generation technologies and provisions for energy storage which ultimately contributes to the level of reliability and security of the electric power supply network [3].

The South African electricity supply industry is evolving to allow for major ongoing changes. The main drivers include system reliability, climate, environmental, regulatory and economic challenges, as well as the fundamental goal of reducing transmission/distribution losses. While the new Kusile and Medupi coal-fired power stations are on the horizon to inject some much needed capacity to the electric power generation capacity, they are fossil fueled power stations which is certainly not in keeping with the drive towards renewable or clean energy technologies. South Africa's geographical positioning allows the country access to an abundance of coal, sunshine and coastal wind, and neighboring countries with vast hydro reserves. It would appear to be a valuable opportunity for South Africa to drive the concept and development of useful renewable energy technologies which will not only alleviate some of the current electrical power supply constraints but ultimately contribute to economic growth and provide more stable and secure energy resources to the ever growing demand. This will also create the unique opportunity to develop methods that will involve the use of all the available technologies together for the overall benefit of customers and consumers.

The future of the energy industry needs to be quickly geared towards alleviating the current energy crisis. This is a technology that must be further developed in order to produce more efficient and cleaner energy as well as minimize energy wastage. Electrical transmission and distribution systems is evolving and to be optimized in support of the new smart grid technologies and harnessing diversified RE generation sources and load management. The combined use of renewable and conventional technologies is becoming common place. Current renewable energy technologies in the form of wind and solar will have to continue to grow while the demand for energy and usage will need to focus on efficiency and be optimized through time-of-use energy management amongst other measures [3].

For South Africa, there will be challenges with the growth of RE in the form of integration into the existing system. Wind and solar energy are intermittent sources requiring intricate planning, processing and control and management to support the traditional AC power grid. Conventional power generation infrastructure will continue to be used however it will have to be more controlled and with a concerted effort on the reduction in use of fossil fuels. It must however be noted that RE technologies will not simply replace conventional power generation infrastructure. The use of solar and wind sources must be controlled and a concerted effort placed on energy storage as a critical component for effective control.

An additional method of energy storage being proposed in South African is the Underground Pumped Hydroelectric Energy Storage (UGPHES), as a compliment to existing storage systems such as the conventional hydro dams and pumped storage systems. This proposed system has been identified as an effective method for bulk energy storage by using existing infrastructure in the form of abandoned mines and aquifers.

1.1 Purpose and scope of research

Pumped Hydroelectric Energy Storage (PHES) is a conventional method of energy storage that is used throughout the world. South Africa has the Drakensberg Pumped Storage Scheme which has been in operation since 1981 and has a capacity of 1,000 MW [4]. The Ingula Pumped Storage Scheme is currently under construction with scheduled completion in 2015 with a capacity of 1,332 MW [5]. PHES has now attained efficiencies of between 70 and 85 percent [6]. The overall contribution globally of PHES installations is

approximately three percent of generating capacity [6]. PHES is reliant on geographic parameters which often times has proven to be quite restrictive in that it is required to use the height difference between two artificial reservoirs or natural bodies of water.

Eskom maintains a varied portfolio of plants: coal fired, hydroelectric power, pumped storage, open cycle gas turbine (OCGT), nuclear and wind power as shown in Table 1-1. Eskom, South Africa's dominant electric utility owns most power stations in the country and accounts for over 95% of all electricity produced in South Africa. Eskom's generation pool comprises of 85% coal, 4.5% hydro, 5.5% gas, 4.4% nuclear and wind accounts for the balance [7].

Table 1-1 – Eskom's power stations [7]

Name of Station	Type of Station	Sets (MW)	Total Capacity (MW)	Year of Operation
Arnot	Coal		2,352	1975
Camden	Coal		1,510	1967
Duvha	Coal		3,600	1980
Grootvlei	Coal		1,200	1969
Hendrina	Coal		1,965	1970
Kendal	Coal		4,116	1988
Komati	Coal		940	1961
Kriel	Coal		3,000	1976
Lethabo	Coal		3,708	1985
Majuba	Coal		4,110	1996
Matimba	Coal		3,990	
Matla	Coal		3,600	1983
Tutuka	Coal		3,654	1985

Name of Station	Type of Station	Sets (MW)	Total Capacity (MW)	Year of Operation
Koeberg	Nuclear	2 x 960	1,920	1984
Gariep	Hydro		360	1971
Vanderkloof	Hydro		240	1977
Drakensberg	Pumped Storage		1,000	1981
Palmiet	Pumped Storage		400	1988
Darling	Wind		5.2	2008
Klipheuwel	Wind		3.2	2002
Acacia	OCGT		171	1976
Port Rex	OCGT		171	1976
Ankerlig	OCGT		1,338	2007
Gourikwa	OCGT		746	2007
Total Installed Capacity			44,032.40 MW	

This dissertation report presents a new adaptation of the pumped hydroelectric method of storing energy which is known as underground pumped hydroelectric energy storage (UGPHES). UGPHES uses an underground water structure in the form of an aquifer or cavern as a lower reservoir which therefore eliminates the dependence on surface topology and minimizes environmental impacts [8]. The primary consideration as part of this research investigation is to consider UGPHES as a potential bulk energy storage system ranging from 1,000 to 3,000 MW to be used during times of high electricity demand similar to the applications of PHES. Furthermore, UGPHES can also be used in smaller applications from as small as 10 kW to 0.5 MW as a cost effective and environmentally benign method of energy storage [3]. Consideration will therefore also be given to schemes of this size for use as an example in agricultural irrigation.

1.2 Methodology

This dissertation considers the value of UGPHES in South Africa as a practical and sustainable alternative to PHES. The practical limitations is explored, including current developments and progress made to date with this prototype concept. This dissertation assesses the availability of South African energy storage systems and provides a comprehensive review of the consideration of implementing such a system. Hydrogeology, electrical and mechanical technologies, legal considerations, system design, operation and economics are all considered. Specific consideration is also given to the practicality and viability of using abandoned mines in South Africa as well as aquifers [3]. Finally, it offers recommendations for further development within the field.

Key questions to be addressed are as follows:

1. What are the advantages and disadvantages of using UGPHES as compared to the conventional PHES?
2. What is the progress being made globally in UGPHES schemes?
3. What is the expected contribution of UGPHES to the electricity grid?
4. What are the practical limitations of UGPHES in South Africa?
5. What are the economic implications? Is UGPHES a financially viable option in South Africa?
6. What are the steps required going forward for UGPHES to be considered as a viable renewable energy alternative for implementation in South Africa?
7. Can South Africa benefit from the groundwater aquifers of Namibia [9]?

This dissertation consists of four major chapters. Chapter 2 is a comprehensive literature review of available energy storage technologies and schemes available including PHES with a model for the scheme. Chapter 3 examines UGPHES together with a model for the scheme. Chapter 4 introduces the aquifer UGPHES system, and provides a design and performance model of the system. It also considers groundwater and aquifers in South Africa and Namibia and the opportunity and feasibility of South Africa benefitting from harnessing this resource. Chapter 5 considers the use of abandoned mines in South Africa for UGPHES schemes. The goal of this dissertation is to provide a framework and

methodology for assessing the use of UGPHES as a viable energy storage scheme in the South African context.

CHAPTER TWO

LITERATURE REVIEW

ENERGY STORAGE SCHEMES AND TECHNOLOGIES

A sustainable energy future is dependent on the ability to store energy on a large scale in an effort to cope with the ever growing demand for energy and to liberate the effect on the utility industry [3].

One of the primary reasons behind energy storage is the fast response time required during peak demand which the conventional coal and nuclear plants cannot deal with efficiently, resulting in wasted energy [3]. Furthermore, the current renewable energy technologies of wind and solar power have no means of storing the energy produced resulting in any excess energy that may be produced, being wasted. While there are many methods of energy storage available and with the development of renewable energy sources, the real challenge however lies in being able to store large amounts of energy in an efficient and cost effective manner.

In the recent past, existing energy storage technologies have been improved and many new storage technologies have been developed. Following is a brief discussion on the various energy storage technologies available.

2.1 Compressed air energy storage (CAES)

Compressed Air Energy Storage (CAES) is a technology whereby electrical energy is stored in the form of high pressure air and is suitable for long duration utility scale applications. It is a technology similar to that of the conventional gas turbine and is seen as a hybrid form of storage. CAES is a proven technology that is both scalable and economical [10].

Off-peak power is used to drive a motor which in turn drives a compressor which compresses air into the underground reservoir. CAES is flexible in its ability to use a broad range of reservoirs for storage of large amounts of air typically in underground geologic

formations [8], saline aquifers and abandoned mines, which therefore results in it having a modest surface footprint. The type of storage bed used influences the dynamics of the CAES system [11]. The stored compressed air energy is used whereby the compressed air is expanded through a high pressure air turbine. The mixture of natural gas with the exhaust from the high pressure turbine is fired in a low pressure natural gas turbine. The natural gas used by the CAES turbine to heat the compressed air that drives the turbine is only one third the requirement of a conventional combustion turbine [11]. The compressed air can also be used whereby the adiabatic pressure change and expansion volume can generate power in a gas turbine [12, 13]. The energy content in this case however, is low [14]. The operation of a CAES system is shown in Figure 2-1.

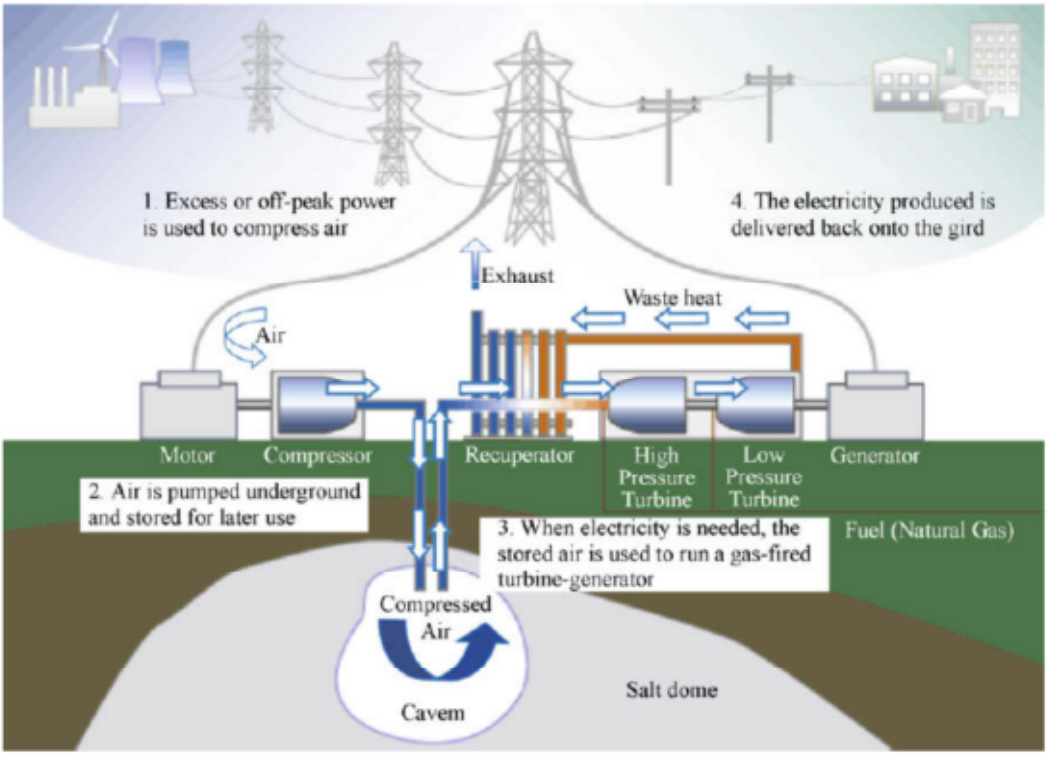

Figure 2-1 – Schematic of CAES [24]

A primary application for CAES is the storage of wind energy which can later be used during times of shortfalls in wind output due to its long duration storage and fast output response times [8]. Another very important consideration for the use of CAES is the fact that it has a low greenhouse gas emission rate and would therefore be an ideal application for reducing the carbon footprint while at the same time maintaining its efficiency [8].

Underground CAES systems are able to store up to 400 MW or 8-26 h of discharge while aboveground systems have a capacity that is significantly lower in the order of 3-15 MW or 2-4 h of discharge [15]. CAES plants have a fast start-up in the order of 12 minutes under normal conditions and 9 minutes for an emergency start [16].

Other adaptations of the CAES system include Ocean Compressed Air Energy Storage (OCAES) whereby a container used for the storage of air is installed on the ocean floor thereby making use of hydrostatic pressure on the seabed which keeps the high pressure compressed air under storage [17]. Adiabatic CAES is a system whereby a combustion chamber is replaced by the use of a thermal energy storage system, and recycling compression heat in order to increase overall efficiency [17]. The isothermal CAES system allows for the compression of air without a rise in temperature thereby eliminating the requirement for thermal energy storage, a combustor, or a series of intercoolers. Isothermal compression requires minimum work for the compression process [17].

2.1.1 Cost of CAES

The construction of the air storage infrastructure and the required air storage volume are the primary factors that determine the capital cost of the CAES system [18]. Compared to other energy storage technologies, CAES requires a fairly low capital cost which is only slightly more than a conventional natural gas turbine and only about half that of lead-acid batteries, adding 3-4 c/kWh [19]. The cost of a CAES installation is in the order of 672–784 R/kW [20]. CAES can be compared to pumped hydroelectric energy storage in that they are both high power, high energy types of storage that are used on a timescale of hours to days ideally suited to utility scale energy storage [21].

2.1.2 CAES site requirements

The primary requirements for a CAES site is for the operation of a gas turbine and a reservoir for compressed air storage with a further consideration of the availability of a natural gas line [21].

Three different geological formations in the form of salt, aquifer or hard rock can host a CAES with salt caverns being the most cost effective cavern option [21]. An aquifer is another option that can also be considered. Hard rock mining is a possible option but the

costs associated with having to excavate a mine make it the least attractive of the three options [21]. Rock caverns are around 60% more expensive to mine as compared to salt caverns for CAES purposes [16]. The use of an abandoned mine is an option for consideration.

2.1.3 CAES performance

The operating temperature and pressure inside the CAES cavern affect the operating capacity of the cavern storage [11]. The energy density for a CAES system is in the order of 12 kWh/m^3 with an estimated efficiency of around 70% [22]. CAES is distinguished from other storage technologies by two characteristics. Firstly, fuel is used during the generation phase, however the net output from the turbines is increased which ultimately means that the fuel efficiency is greatly increased. Secondly, the output electrical energy exceeds the input energy [8]. CAES performance is therefore characterized by the following [8]:

$$ER = \frac{E_{gen}}{E_{comp}} \qquad (2.1)$$

Where,

ER represents the energy ratio

E_{gen} is the Electrical Energy Output

E_{comp} is the Electrical Charge Energy

In a pure storage scheme, the ER would be identical to the storage efficiency.

$$HR = \frac{combustion\ fuel\ consumed}{electrical\ energy\ output} kJ/kWh \qquad (2.2)$$

Where,

HR is the Heat Rate.

The fuel heat rate for a generating plant is (3600/thermal efficiency) kJ/kWh [8].

The turnaround efficiency of a CAES system which is represented by equation (2.3) is based on the overall efficiency of the system taking into consideration the power produced and the usage of gas and off-peak power [23]:

$$Eff = \frac{1}{ER + HR} \qquad (2.3)$$

Where,

Eff is the Turn-Around Efficiency

Equations (2.4) and (2.5) show the mass and energy balance over the control volume enclosing the air in the cavern respectively [11]:

$$\frac{d\rho}{dt} = \frac{\dot{m}_{in} - \dot{m}_{out}}{V} \qquad (2.4)$$

Where,

ρ is the cavern air density

$\dot{m}_{in}$ is the incoming air from the compressor mass flow rate

$\dot{m}_{out}$ is the out-going air to the turbine mass flow rate

V is the cavern volume

$$\frac{d(MU)}{dt} = \dot{m}_{in}H_{in} - \dot{m}_{out}H_{out} - h_{amb}A_{cavern}(T - T_{amb}) \qquad (2.5)$$

Where,

$(d(MU))/dt$ is the cavern air internal energy rate of increase

M is the cavern air mass

H_{in} is the incoming air specific enthalpy

H_{out} is the outgoing air specific enthalpy

h_{amb} is the heat transfer coefficient between the air and cavern wall

A_{cavern} is the heat transfer area between the air and the cavern wall

T is the air temperature

T_{amb} is the wall temperature of the cavern

2.1.4 Existing installations of CAES systems

Huntorf near Bremen in West Germany is host to the first ever CAES plant built in 1978 primarily to provide black-start services. It is currently being used as a peak shaving unit and as a supplement to other storage facilities on the electrical power system to compensate for the generation gap due to the slow response of conventional power generation plants [8].

The unit has a dual solution mined salt cavern of approximately 150,000 m^3 each and located approximately 600 m underground. A maximum pressure of 10 MPa is produced via 60 MW compressors and has a capacity of 290 MW which could last for 4 hours. The starting reliability is rated at 99% with an availability of 90% [24].

Another existing CAES installation which has been in operation since 1991 is the McIntosh 110 MW plant built in southwestern Alabama on the McIntosh salt dome. It uses a salt cavern of approximately 560,000 m^3 designed to operate between 45 and 74 bar for 26 hours [8]. The operational aspects of the plant are similar to those of the Huntorf plant. The distinguishing features of the McIntosh plant as compared to the Huntorf plant is that the fuel consumption is reduced by approximately 22% at full load due to the inclusion of a heat recuperator as well as a dual-fuel combustor which is capable of burning natural gas and fuel oil [8]. The McIntosh plant achieves 91.2% and 92.1% average starting reliabilities with 96.8% and 99.5% average running reliabilities for the generation and compression cycles respectively [8].

2.2 Battery energy storage

The storing of electrical energy in the form of chemical energy in batteries is one of the most established methods of electrical energy storage. Electrochemical cells made from an electrolyte material with an attached positive and negative electrode is the heart of the battery. Batteries provide a rapid response for both charge and discharge and can respond rapidly in the order of 20 milliseconds to load changes [6]. An electrochemical reaction at the electrodes generates a flow of electric current through an external circuit during discharge of the battery. The discharge rate is dependent on the chemical reaction rates which determines the amount of available energy. The battery can be recharged through a reversible process by applying an external power source to the electrodes [25].

The use of batteries for large scale applications which includes renewable energy systems has led to the development of newer battery technologies which offer increased energy storage densities, higher reliability, lower cost and with greater cycling capabilities [26]. Table 2-1 shows a comparison of battery attributes for selected battery technologies. Battery systems due to being modular, quiet and non-polluting, are able to be installed near load centers, however, the choice of battery technology is a defining criteria. The round-trip efficiency which is dependent on the frequency of cycling and the electrochemistry used, is in the 60-80% range [6]. Batteries used in power systems offer a wide range of applications which include spinning reserve, power factor correction, load leveling and stabilizing as well as load frequency control [26].

Table 2-1 – Comparison of key battery attributes [24]

Attributes	Lead Acid	Li Ion	NaS	Ni-Cd	Zn-Br
Depth of Discharge	75%	80%	100%	100%	100%
Cost	Low	Very High	High and auxiliary heating systems needed	High	High

Attributes	Lead Acid	Li Ion	NaS	Ni-Cd	Zn-Br
Lifespan (Cycles)	1000	3000	2500	3000	2000
Efficiency	72-78%	100%	89%	72-78%	75%
Self-discharge	Average	Negligible	Negligible	High	Negligible
Maturity of Technology	Mature	Non-Mature	Mature	Mature	Non-Mature

Existing applications of battery energy storage systems include a 10 MW (40 MWh), 4 hour discharge plant built at the 12 kV substation facility in Chino, California [6] and a 1.2 MW, 1.2 MWh (1:1 power-energy ratio) for Metlakatla Power and Light (MP&L) in Alaska [27]. The Alaskan application saved MP&L around US$6.6 million over a period of 11 years as well as nearly eliminating the use of fossil fuels [27].

2.2.1 Lithium-Ion batteries

A flow of current is generated in a lithium-ion battery when lithium ions flow between the anode and cathode [28]. Plug-in hybrid electric vehicles is the latest technology to use lithium-ion batteries with more common usage found in power electronic devices. Lithium-ion batteries have the highest power density of all batteries on the commercial market on a per-unit-of-volume basis of between 500 W/kg to 2,000 W/kg and energy densities ranging from 80 Wh/kg to 150 Wh/kg [16].

A long life span together with a low self-discharge, high energy density and no requirement for scheduled cycling, are the main advantages of lithium-ion batteries. When compared to other battery technologies, they are proven to be more expensive with prices likely to increase as limited lithium-ion resources are depleted [29]. Lithium-ion batteries have a very high efficiency of almost 100% and is therefore primarily used on laptops and other portable electrical equipment [24].

2.2.2 Nickel-Metal Hydride batteries

Nickel-Metal Hydride batteries are being used as back-up power sources for telecommunication services with optical fiber cables. Each terminal of the optical fiber network requires a power source due to the inability for electric power to be supplied through optical fiber cables. Electric power is supplied at the optical network terminals together with converting of optical signals. The batteries used as a back-up need to be able to supply power for several hours [30].

Nickel-Metal Hydride batteries make use of the pulse charging method which prevents over-charging. For fiber optic network application, the Nickel-Metal Hydride battery is assembled from 6 cells and rated at 2,000 mAh with a weight of 0.55 lb [30]. It is able to operate at temperatures ranging from -10 °C to +55 °C with a projected life span of 7.5 years at 30 °C [30].

2.2.3 Nickel-Cadmium batteries

Nickel-Cadmium batteries have very good performance at high and low temperature operation and offers a better life cycle time than lead-acid. They can store up to 27 MW of power which make them very useful for power system applications [24]. Nickel-Cadmium batteries have an efficiency of between 72-78% with a high self-discharging rate of 5-20% of charge lost per month [24]. They have a typical maximum energy density of 50 Wh/kg and a lifetime at deep discharge levels between 1,500 and 3,000 cycles [16]. They are however more expensive than traditional lead-acid batteries and contain toxic components which makes disposal environmentally challenging [31]. Benefits of Nickel-Cadmium batteries include low life cycle cost, low maintenance, resistance to abuse, environmentally safe and long life with high reliability [32]. Nickel-Cadmium batteries were used to provide spinning reserve for a transmission project in Alaska and have also been applied in a variety of backup power applications. A 26 MW battery rated for 15 minutes was used in this project and is the largest utility application in North America [33]. It is comprised of 3,440 cells in a string of four batteries with a total voltage of 5,200 V [24].

2.2.4 Sodium-Sulfur batteries

Sodium-sulfur batteries store and release electrical energy through an electrochemical reaction between the sulfur at the positive electrode and sodium at the negative electrode. Advantages of sodium-sulfur batteries include low material costs, good temperature stability, high coulombic efficiency, long cycle life and a high energy density almost triple that of lead-acid batteries [28]. They are however only suitable for large-scale stationary applications as a result of sodium being highly corrosive [16].

Sodium-sulfur batteries have a lifespan of 2,500 cycles for a 100% depth of discharge at a temperature of 300 °C which therefore requires energy thereby decreasing the overall system efficiency and negatively impacting the cost [24]. They can be applied in DC distribution systems due to the high efficiency of 85% for DC conversion [28]. Applications using sodium-sulfur include renewable integration, peak shaving, emergency power and power quality management [24]. The batteries are built in modules rated in kW that allows for MW battery systems to be built by combining the kW modules [28].

Sodium-Sulfur batteries are a relatively mature technology with over 55 installations globally in 2003 [31]. Northern Japan is host to the largest single Sodium-Sulfur battery installation. It is a 34 MW, 245 MWh system which is used for wind power stabilization of a 51 MW wind farm. The battery installation allows for the wind farm to be 100% dispatchable during on-peak periods [33]. The United States makes use of 9 MW Sodium-Sulfur battery installations for backup power, firming wind capacity and for peak shaving [33].

2.2.5 Lithium Titanate batteries

Lithium-Titanate batteries use manganese in the cathode and titanate anodes which allows for good performance at lower temperatures, fast-charge capability and a very stable design. They have a relatively long life and are able to be discharged to 0% [33].

2.2.6 Zinc-Bromine batteries

Zinc-bromine batteries operate by circulating reactants through the battery with the use of a pump system. The non-destructive charging and discharging of energy through the electrochemical reaction allows a depth of discharge of up to 100%. The battery has a life span is rating of 2,500 cycles and is more environmentally friendly in comparison with lead-acid batteries due to the use of less toxic electrolytes [28]. Zinc-bromine batteries have negligible self-discharge with an efficiency of 75% and have high power and energy density [24]. Three 60 cell battery stacks are connected in parallel to make up a 50 kWh module with the advantage of being able to replace individual stacks instead of the entire module. Each module is rated to discharge at 150 A for four hours at an average voltage of 96 V [28].

2.2.7 Lead-Acid batteries

Lead-acid batteries is the most developed form of battery energy storage system technology most commonly known for its application in automobiles and as backup power in uninterruptable power supplies [28]. The power output is non-linear which therefore allows for the use in applications such as switching components and control systems power quality management. Lead-acid batteries have very low energy density of around 30 Wh/kg with power density around 180 W/kg [34]. They also have a short operational life of 4-5 years/750 cycles with their life cycle dependent on discharge rate, usage and the number of deep discharge cycles [28]. Lead-acid batteries also have a high maintenance requirement, capacity drop at low temperatures and hazards associated with lead and sulphuric acid during production and disposal [31].

Life-cycle and performance of lead-acid batteries is improved through the use of advanced materials and technologies which allows these advanced lead-acid batteries to be used for distribution and transmission grid level support [28].

The low cost of lead-acid batteries is regarded as their main benefit. A depth of discharge of 75% can be tolerated with an efficiency of 72-78%. Lead-acid batteries is currently the most matured battery technology [24].

There is currently two UPS installations in East Asia that utilize Valve Regulated Lead Acid (VRLA) batteries. These batteries are rated at 2.8 MW and 4.2 MW and provide protection until such time that the back-up generators are brought on line. The installations utilize 1,165 VRLA cells rated at 2 V and discharge to 1,900 V (1.65 V/cell) in 5 minutes [30].

2.3 Thermal energy storage (TES)

The earth is seen as a source of renewable energy whereby geothermal energy is extracted from the earth at great depth as demonstrated by the occurrence of volcanic eruptions and hot springs. The earth can also be used for the storage of heat or cold energy in subsoil sand layers referred to as aquifers or in soil/rock using boreholes [35]. There are three main components to this method of storage namely the useful energy potential, the storage medium and the energy flow mechanism. The useful energy potential can be sourced from solar thermal, industrial waste heat and winter cold, however, the integration with the energy storage medium together with the transportation of the waste energy can be a challenge [35]. TES technology can be expected to have a roundtrip efficiency of up to 60% with the use of a heat pump and is estimated to have favorable economies of scale [36]. The performance of a solar-assisted heat pump system (SAHPS) based on geothermal energy storage was studied and verified that the whole energy efficiency of the coupled system is improved [37]. This system also considerably reduces fossil fuel usage and CO_2, SO_x and NO_x emissions to the atmosphere [38]. Rapidly increasing applications of ground source heat pump (GSHP) systems in China led to the idea of solar-ground coupled heat pump systems (SGCHPS) being widely accepted and recognized as one of the most energy efficient, cost effective and cleanest systems for space heating and cooling [39]. SGCHPS systems are used mainly for hospitals, hotels, shopping centers and offices due to the higher initial cost [38].

2.3.1 Aquiferous low-temperature TES

The process of cooling or icing of water during low demand (off-peak) hours and storage for use at a later stage during high demand (peak time) to meet the cooling needs is known as aquiferous low-temperature thermal energy storage [24]. The temperature difference between the warm return water from the heat exchanger and the chilled/iced water stored in the tank determines the amount of cooling energy stored. This form of

thermal energy storage is primarily suited to lowering the peak industrial and commercial cooling loads during the daytime [24]. It is primarily applicable to large commercial buildings for heating and cooling purposes [40] which therefore allows for smaller chillers to be used thereby substantially lowering the air conditioning operating costs with particular benefit to peak demand charges [24].

An aquiferous thermal energy storage (ATES) system has two groups of wells connected to the heating, ventilation and cooling (HVAC) system with groundwater extracted from the wells by submersible pumps. The condenser of the HVAC system is cooled using groundwater from the cold well while the waste heat is stored in the aquifer through the warm well and can be recovered when required [40].

The first application of an integrated ATES with an HVAC system was in Mersin, a city near the Mediterranean coast in Turkey. The ATES system when compared to the conventional HVAC system used 60% less electrical energy during the cooling mode [40]. A feasibility study of such a system for a hospital in Adana, Turkey showed the savings in energy which ultimately contributed to environmental benefits by decreasing CO_2 emissions by 2,100 tons/year, SO_x by 7 tons/year and NO_x by 8 tons/year [40].

2.3.2 Cryogenic energy storage (CES)

CES is a form of electrical energy storage system which is considered a green option due to no direct emissions through the use of air and nitrogen which is abundantly available in the atmosphere [41]. Ambient air is filtered to remove impurities during the storage process while also removing water and carbon dioxide to prevent freezing [42]. Cryogen in the form of liquid nitrogen or liquid air produced from the process can be used commercially or for refrigeration purposes [41] and can be generated in a few different ways namely renewable generated electricity, off-peak power or mechanically from hydro or wind turbines [24]. At times of peak power requirements electricity is generated using heated cryogen to drive a cryogenic heat engine by boiling the liquid using the heat from the surrounding environment. The CES system is also able to use waste heat from the flue gas of a power plant [24]. CES has many uses including powering vehicles, providing direct cooling and refrigeration and for air conditioning units. It has no effect on the environment, has a long storage period, capital cost per unit energy is low and it has a relatively high density in the order of 100-200 Wh/kg [24]. The one drawback of CES is

that it has a relatively low efficiency of 40~50% due to the large amount of energy required to compress the gases [41]. Highview Power Storage's (HPS) 80 MW biomass power plant in Slough, UK has successfully implemented CES. The CES unit is capable of storing 2.5 MWh of energy via a 60 ton liquid nitrogen tank with a maximum output of 300 kW [43]. CES offers the following benefits [42]:

- Proven technology which has been around for any years is used;
- CES regulations already exist;
- Tanks are less costly due to low pressure storage;
- Air is non-toxic and does not explode;
- Liquid air has four times the energy density of compressed air.

2.3.3 Molten salt storage and room temperature ionic liquids (RTILs)

RTILs can be stored without decomposition at temperatures of 100s of degrees and have therefore been proposed for storage of energy. They are organic salts with a melting temperature below 25 °C and with negligible vapor pressure in the relevant temperature range [24]. Testing of the two-tank molten salt storage system using molten salt as the heat transfer fluid was done in the "Solar Two" Central Receiver Solar Power Plant demonstration project in California [24].

Molten-salt storage which is one of the concentrating solar power (CSP) storage methods, is the only storage currently in use commercially. Thermal storage systems offer a very high annual storage efficiency of up to 99% for commercial plants [44]. Heat losses through the tank walls are minimized through insulation while the heat exchange process between mediums such as salt to steam for towers, accounts for the other heat losses. Conversion losses however do not affect the efficiency of the thermal storage system due to the energy being stored as heat prior to conversion to electricity through the Rankine cycle [44].

Solar salt is used together with molten-salt power towers due to its high upper stability temperature limit of 600 °C which allows for the use of high-efficiency Rankine cycle turbines [44]. A steady flow of power can be produced dependent on the storage of

sufficient energy in the hot salt tank which is made possible due to the energy generation system being completely independent of the energy collection system [44].

Trough and tower storage plants are two methods of transferring heat to the molten-salt. Trough plants use parabolic trough mirrors to heat oil to its thermal limit °C through CSP and feeds the oil directly to the oil-to-steam heat exchanger resulting in power being produced immediately. The remaining oil is passed through an oil-to-salt heat exchanger to heat the molten-salt for storage to be used to produce power on demand [44]. Tower plants use molten-salt as the heat transfer fluid and the storage medium. Molten-salt at the top of the tower is heated by CSP from a field of heliostat mirrors. The heated molten-salt is stored at the bottom of the tower where it is passed through a heat exchanger to create superheated steam to turn the turbine to generate electricity.

Molten-salt power tower storage systems have several advantages which include lower salt requirements, simplified piping schemes, improved winter performance, higher steam cycle efficiency and elimination of heat transfer oil and associated heat exchangers [44]. Investigations into the improvement of molten-salts thermal properties and the development of single tank storage solutions are currently being investigated.

The Gemasolar plant was the first commercial power tower to operate with molten-salt storage and using water as the cooling medium. The key statistics for the Gemasolar plant are listed in Table 2-2:

Table 2-2 – Key statistics for Gemasolar plant [44]

Characteristic	**Quantity**
Number of heliostats	2 650
Total reflective area (m^2)	306 658
Tower height (m)	140
Receiver power (MW_t)	120
Turbine power, gross (MW_e)	19.9

Characteristic	Quantity
Turbine power, net (MW_e)	17
Storage size (hours of operation without solar radiation)	15
Storage tank dimensions (height x diameter, m)	10.5 x 23
Mass of salt (tons)	8 500
Annual net electricity generation (MWh/year)	110 000
Capacity factor	74%

The Thémis station in France uses molten salts for storage of 40,000 kWh of thermal energy economically and to simplify the solar panel regulation [22]. Other commercial installations of molten-salt CSP storage include the Andasol-1 trough plant near Guadix in the province of Granada, Spain with 7.5 h of molten-salt storage. This has grown to a total of eight plants each with 7.5 h of molten storage [44].

2.3.4 Phase change materials (PCMs)

PCMs are latent heat storage materials with the transfer of thermal energy occurring when a material changes phases from either solid to liquid or liquid to solid. This energy storage technology uses materials that have a phase change at a temperature matching the thermal input source [24]. A heat transfer fluid is used to transfer the heat between the thermal accumulator and the exterior environment [22]. Higher energy storage densities are possible due to the heat generated during this phase change as compared to non-phase change high temperature materials. More heat per unit volume to the order of 5-14 times is stored by PCMs compared to sensible storage materials such as water, masonry or rock [45]. Sensible heat storage although relatively inexpensive, has a low energy density and variable discharging temperature. PCMs enable higher storage capacities and target-oriented discharging temperatures [46]. Sodium hydroxide has a specific thermal storage capacity of 1,332 MJ/m^3 between temperatures of 120-360 °C and is therefore considered to be a good storage fluid [22]. PCMs are classified as organic, inorganic and eutectic. A heat transfer mean from the source to PCM is required due to the phase

change. This can be accomplished by the embedding of PCM in a matrix made of another solid material with high heat conduction as well as encapsulation of small amounts of PCM [24]. Most PCMs have low thermal conductivity, long cycling lives and are non-toxic [47]. These properties result in slow charge and discharge rates during the phase change coupled with small volume changes [48]. PCM storage still needs to be developed further.

2.4 Hydrogen energy storage

Hydrogen is seen as an energy carrier rather than an energy storage device due to it being a substance that can store energy by being charged. It must be removed or separated from water or from compounds containing hydrocarbons by electrolysis or reforming processes, however, the use of a renewable energy source, fossil fuels or nuclear energy is required for these reforming processes [6]. Several basic components as depicted in Figure 2-2, make up the hydrogen-based storage system. These include an electrolyzer system which uses the method of electrolysis of water to produce hydrogen, a hydrogen storage system in the form of a steel tank or geologic storage and finally a fuel cell or internal combustion engine to convert the hydrogen back into electricity. The use of a fuel-cell is preferred due to its higher conversion efficiency. Depending on the operating pressure and efficiency of an electrolyzer-fuel cell combination or the efficiency of a reversible fuel cell device, the round trip efficiency ranges from 60-85% [6].

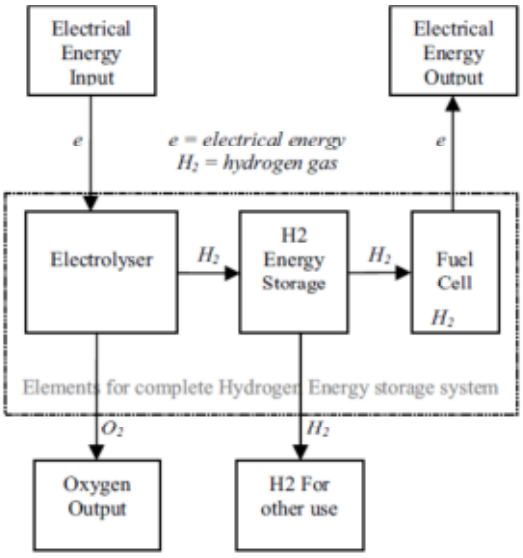

Figure 2-2 - Basic elements of a hydrogen energy system [25]

There are five methods of storing hydrogen in different states. These are compression of gas, liquefaction, physisorption, metal hydrides and complex hydrides, with the method of compressed gas storage being the most appropriate. This method is primarily for standby applications where space is not a limitation [49]. Large quantities of renewable energy such as wind power and photovoltaic power are also able to be stored and transported using the carbon-hydride energy storage system (CHES). The electric power generated through the use of renewable energies is converted into hydrogen energy which is then further converted into methylcyclohexane (MCH) which is an organic hydride used as the energy storage medium. This allows excess renewable energy to be stored for long periods of time to be used at times when demand exceeds supply [50].

Hydrogen as a fuel and energy carrier has many advantages including being storable, lightweight, non-toxic, transportable and depending on its storage form, a high energy density. Further advantages include producing non-toxic exhaust emissions (depending on the oxidant used), usage in all sectors of the economy and can be generated from various energy sources with various means of production [49]. Disadvantages include safety issues (combustibility of hydrogen) and difficulty of being stored with a high energy density [49]. The first full scale application of wind/hydrogen was in July 2004 at Utsira in Norway and is powered by two 600kW wind turbines operating at wind speeds in the range of 2.5-25 m/s. A 48 kW, 10 Nm^3/h electrolyzer is used to produce hydrogen which is stored compressed in a 2,400 Nm^3 container. When wind energy is in short supply, the stored hydrogen is used to produce power by a 10 kW fuel cell and a 55 kW hydrogen internal combustion engine [49]. Another application is a 350 kW solar hydrogen demonstration plant in Saudi Arabia which has been in operation since 1993 and produces 463 m^3 of hydrogen at normal pressure [51].

2.5 Superconducting magnetic energy storage

Superconducting magnetic energy storage (SMES) is a unique diurnal energy storage technique in that there is no conversion from one form of energy such as mechanical, thermal or chemical, to electrical energy [52]. The electrical energy is rather stored directly as a circulating current in the magnetic field of a large superconductive coil which allows a direct electrical current to flow through it with virtually no loss [53]. A power converter module is used to convert the direct current to alternating current for delivery to the power

system. SMES devices are specified according to the inductively stored energy and the rated power. These can be represented as follows [26]:

$$E = \frac{1}{2}LI^2 \qquad (2.6)$$

$$P = \frac{dE}{dt} = LI\frac{dI}{dt} = VI \qquad (2.7)$$

Where,

E is the inductively stored energy in Joules

L is the coil inductance

I is the coil DC current

P is the rated power in Watts

V is the voltage across the coil

The SMES coil is required to operate at cryogenic temperatures (-150 °C to -273 °C) in order to remain in a state of superconductivity [53]. Cryogenic refrigerators in the form of helium or nitrogen liquid vessels is therefore an integral subsystem of the SMES together with solid-state power conditioning devices, climate controls, safety devices, monitors, controls and utility and user interface equipment as depicted in Figure 2-3.

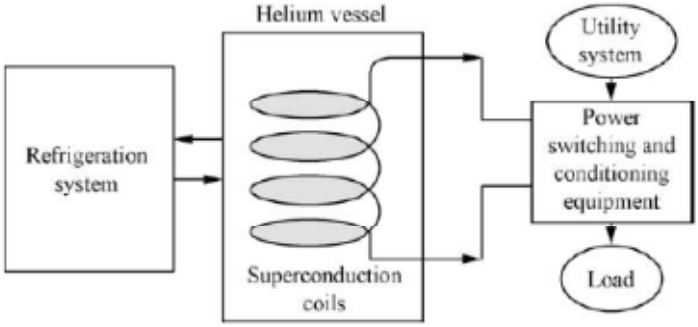

Figure 2-3 - SMES system [24]

The SMES system is able to provide a rapid response at efficiencies of 95-98% or more for both cycles of charge and discharge [22] with the availability of energy independent of the discharge rating [54]. The change-over from charging to discharging can be done within 17 milliseconds [6]. Utility applications include load leveling, frequency support during loss of generation, transient and dynamic stability enhancement, dynamic voltage support (VAR compensation), power quality improvement and increasing transmission line capacity therefore enhancing overall reliability of power systems [55]. Typical ratings are 1~10 MW with a storage time of seconds while the larger SMES systems are in the range of 10~100 MW with a storage time of minutes [24].

There are several advantages of SMES systems. These include the following [53]:

- Power in large amounts can be released within a fraction of a cycle with full recharge taking a few minutes making it very efficient and economical.
- Performance does not degrade over the life-span of the system including controllability and reliability.
- Highly mobile due to being compact and self-contained.
- No hazardous chemicals and no production of flammable gases.
- Approximate life-span of at least 20 years.

One of the biggest technical challenges that need to be considered during the system design is the potential for the production of large magnetic fields which is due to the fact that the SMES system cryostats become rapidly pressurized when the coils become non-superconducting [53]. This requires careful component design and stay out zones. In the case of coil failure, the quick release of stored energy is vital to prevent the coil from being damaged. Releasing the stored energy in to the power system might shock the system resulting in damage to other equipment connected to the power system. Pre-cooling of the system can take as long as four months to cool the superconducting coil from room temperature to operating temperature [53]. This reduces the availability of the SMES system. SMES systems have low energy density with large parasitic energy losses, and is expensive [31].

The first three-phase converter SMES system was tested at the Los Alamos National Laboratory (LANL) in 1974 [6]. In 1976, the Bonneville Power Authority together with LANL

designed and constructed a 30 MJ, 10 MW SMES unit [6]. The European Organization for Nuclear Research, CERN, is home to one of the largest superconducting magnets that was constructed for the liquid-hydrogen bubble chamber with a stored energy of approximately 0.2 MWh [56].

2.6 Ocean renewable energy storage (ORES)

The offshore environment can be used for economical utility-scale energy storage while at the same time being unobtrusive and safe [33]. Ocean renewable energy storage is a system of storing energy in concrete spheres deep underwater. A secondary application of the sphere is to act as an anchor for floating wind turbines (FWTs) [33]. Figure 2-4 represents the ORES charging and discharging process. Energy is stored by pumping water out of the spheres and when required, flow of water is allowed back in to the sphere through a turbine thereby generating electricity. When excess power from renewable energy sources such as an ocean current turbine, wave energy harvester or wind turbine is available and the spheres are required to be charged, the excess power is used to operate the pump/turbine to pump water out of the sphere. Storage is found to be economically feasible at depths ranging from 200 m to 1,500 m with cost per megawatt hour of storage dropping until 1,500 m [33]. The storage capacity is maximized for a given volume by placing the sphere in deeper locations.

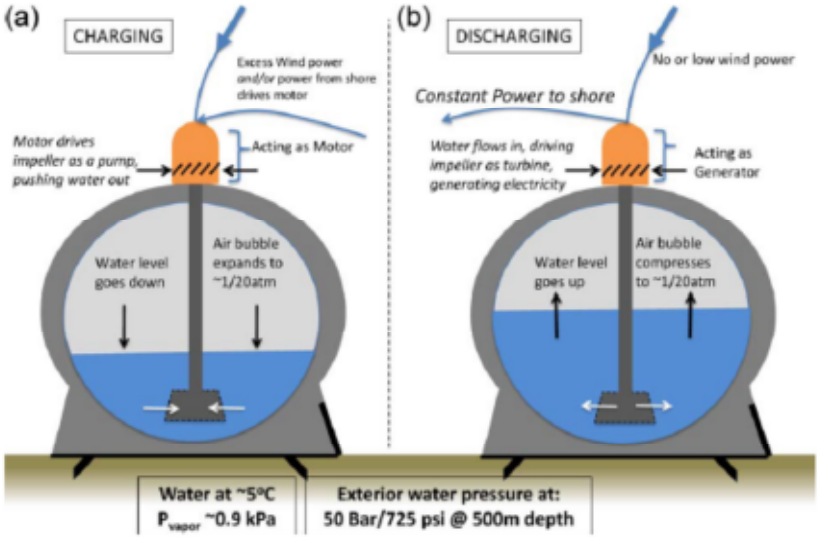

Figure 2-4 - ORES concept for charging and discharging [33]

The storage cylinder total charge capacity (in megawatt hours) can be related to the inner volume of the sphere, depth and efficiency of the pump/turbine unit. This relationship can be represented by the following equation [33]:

$$C_{\max} = \frac{\rho_{sw} \cdot \eta_{turb} . d . g . V_{inner}}{3.69x10^9} \qquad (2.8)$$

Where,

ρ_{sw} is the seawater density (1,025 kg/m^3)

η_{turb} is the efficiency of the turbine typically (85%)

g is the gravitational acceleration of 9.81 m/s^2

d is the depth of the sphere in meters

V_{inner} is the sphere interior volume

3.69x10^9 is the conversion from Joules to Megawatt hours.

The major challenge associated with this technology involves finding a suitable location. Large areas with excellent wind resources are required, along with suitable bottom topography conditions and a reasonable distance from the shore and load center. Other challenges include corrosion and clogging from sediment ingestion during turbine operation and effects on nearby marine life during pumping and turbine operation [33].

The ORES system will have a round trip efficiency between 65-70% with a turbine efficiency of 80-85% [33]. The life-span is estimated at up to 40 years based on offshore platform applications.

2.7 Flywheel energy storage

Flywheel energy storage is an electromechanical storage system whereby kinetic energy is stored in a rotor that spins at extremely high velocities. The momentum of the rotating rotor is responsible for the stored energy [53]. A decelerating torque is applied to slow

down the flywheel thereby retrieving the stored energy which is returned as kinetic energy to the electrical motor operating as a generator [16]. The flywheel energy storage scheme consists of a rotor complete with suspension system, a motor/generator system to couple energy to and from the rotor, and a containment enclosure [57]. The rotor spins on bearings in a vacuum to reduce friction and increase efficiency [36]. The friction loss of a 200 tons flywheel is estimated at 200 kW [22]. The flywheel can be classified according to speed as either low or high with speeds of up to 6,000 rpm and 50,000 rpm respectively [34]. Specific energy achieved for low speed flywheels is in the order of 5 Wh/kg while high speed flywheels can achieve specific energy of 100 Wh/kg [16]. A typical flywheel system is depicted in Figure 2-5. The stored kinetic energy is transformed into electrical energy and vice-versa, by the electrical machine driving the flywheel. The rotor design and control system technology has advanced over the years making flywheel energy storage a very useful means of storing energy. It is highly durable and capable of tens of thousands of cycles per year [6]. Development of the flywheel technology includes operation of the wheel in a vacuum and using a levitated magnetic bearing to reduce bearing heat loss [6].

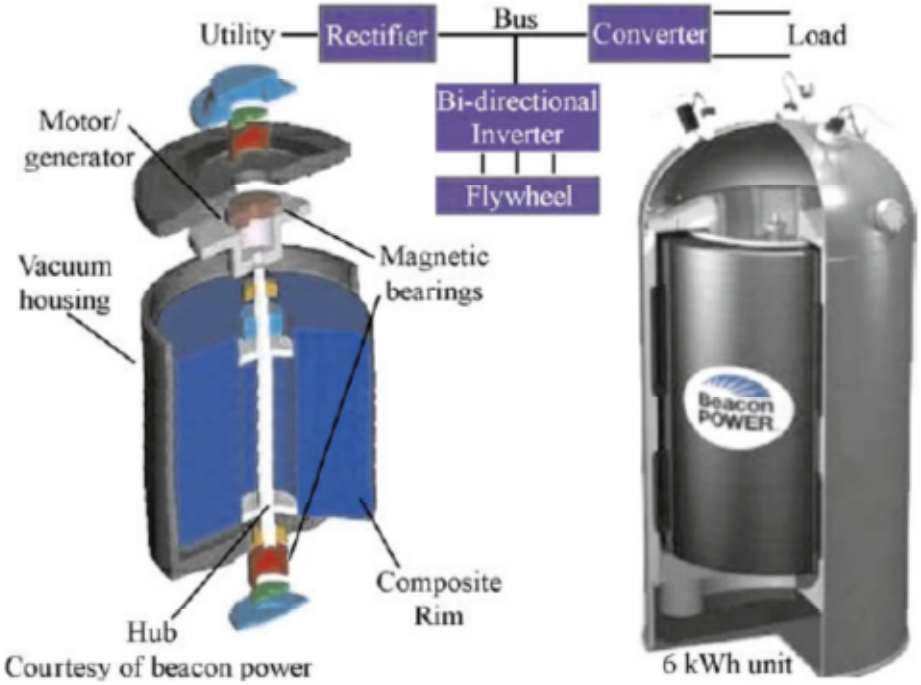

Figure 2-5 - Flywheel system [24]

The stored kinetic energy in the flywheel, with moment of inertia, and spinning at a particular speed, can be represented as [58]:

$$Ec = \frac{1}{2} I\omega^2 \qquad (2.9)$$

Where,

Ec is the stored kinetic energy in the flywheel

I is the moment of inertia

ω is the speed

The flywheel mass and geometry determines the moment of inertia of the flywheel [58]:

$$I = \int r^2 dm \qquad (2.10)$$

Where,

r is the distance of each differential mass element in relation to the spinning axis

dm is the differential mass element

Power quality is an area whereby flywheel energy storage is used to provide reliability and stability to the power system with its quick response to power system anomalies such as frequency deviations, voltage sags, voltage swells and temporary interruptions [6]. Other applications include a battery substitute in a UPS, delivering ac power to the UPS where the utility source has failed and in an engine-generator set whereby the flywheel provides energy to the generator due to the failure of the utility source until such time that the engine has started and reached operating speed [30]. Flywheel systems offer many advantages as outlined below [30]:

- Minimum operation and maintenance requirements resulting in exceptionally long service life and low life-cycle costs.

- Compact and self-contained which allows the flywheel system to be placed in space constrained areas.
- No hazardous chemicals nor is flammable gases produced.
- Much higher charging and discharging rate in comparison with lead-acid batteries.
- The flywheel system storage capacity is not affected by exposure to temperature extremes due to it being independent of temperature fluctuations.
- Available energy is measured accurately by measuring the speed and calculating the energy.
- Provide AC generator or DC converter output.

The one significant challenge with flywheel systems is containment issues due to rotating energy equipment. This challenge needs to be addressed with careful selection of sites, material selection, containment design and thorough testing and rating of equipment [36]. Other negative factors are the installed cost which is 1-1.4 times that of batteries as well as storage expansion not being easy [30], low energy density and large standby losses [31].

Flywheel energy storage has a life expectancy of around 20 years and with a round-trip efficiency which includes the electronics, flywheel drag, frequency of cycling and bearings, of 80-85%. The more common modular flywheel designs range in size from greater than 10 MW to around 250 kW for 10 to 15 minutes [6]. Stabilizing power supply and achieving a smoothing effect on the output from wind turbines is a potential application of flywheels [59]. A medium scale flywheel application is by New York's Power Authority. The application consists of ten 100 kW, 30 second flywheels for regenerative breaking and startup of subway transit cars [6]. Another flywheel application is in Stephentown, New York and started operation in 2011. It uses 200 flywheels for an output of 20 MW and a storage capacity of 5 MWh that allows it to provide maximum output for 15 minutes [6].

2.8 Supercapacitor energy storage

A supercapacitor is an electrochemical double layer capacitor which has a greater energy density and capacitance compared to conventional capacitors [18]. Energy is stored by using an electrolyte solution which is located between two solid conductors as depicted in Figure 2-6, rather than the more common arrangement of conventional capacitors which

make use of a solid dielectric between the electrodes. The electrodes of supercapacitors are often made from porous carbon as the conductor with an aqueous or non-aqueous electrolyte. Due to the surface area of activated carbons being very high in the order of 2,000 m^2 per gram as well as the distance between the plates being less than 1 nm result in large capcitances and stored energy [24].

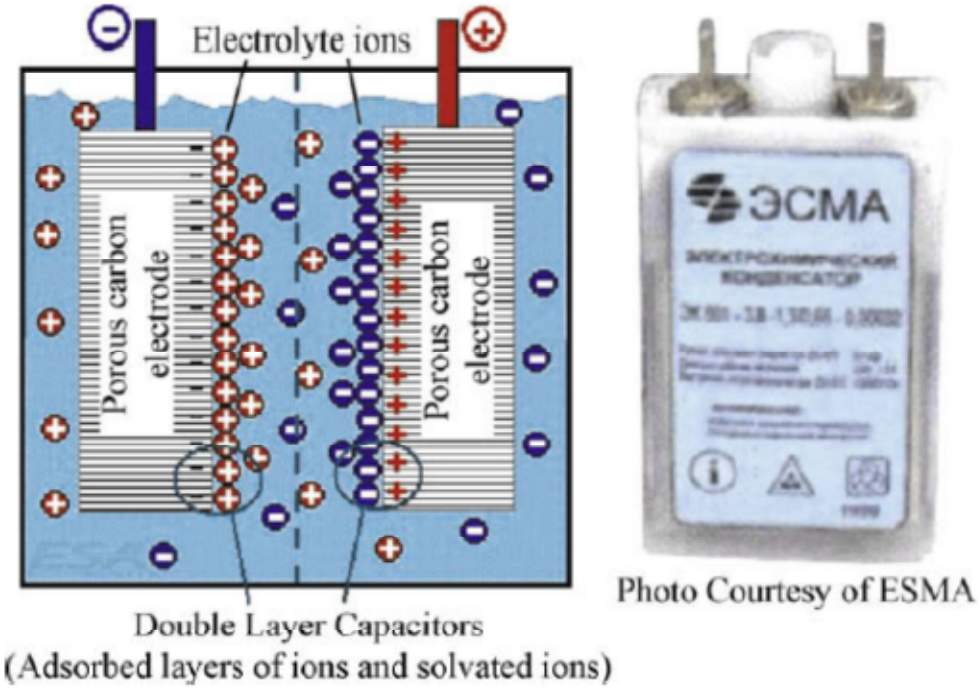

Figure 2-6 - Supercapacitor [24]

The supercapacitor energy storage system does not involve any chemical reactions which therefore allows charging and discharging to the order of hundreds of thousands of times. It is operates between a wide temperature range between -40 °C to +70 °C as a result of being highly temperature, shock and vibration resistant [60]. With the advances of using nano-tube technology to increase the surface area of the capacitor, the energy density of the supercapacitor is comparable to that of a lithium-ion battery. Supercapacitors are rated up to 2.7 V and are able to be combined for a maximum string voltage in the order of 1,500 V [6]. However, to be truly effective in a large scale energy storage system, they will need to be able to handle multiple kV.

The capacitance represents the relationship between the stored charge and the voltage between the plates. This relationship can be represented by the following equation [26]:

$$q = CV \qquad (2.11)$$

Where,

q is the charge stored

C is the the capacitance

V is the voltage

The permittivity of the dielectric, the area of the plates, and the distance between the plates, determines the capacitance. This is substantiated by the following equation [26]:

$$C = \frac{\varepsilon A}{d} \qquad (2.12)$$

Where,

ε is the dielectric permittivity

A is the area of the plates

d is the distance between the plates

The energy stored on the capacitor depends on the capacitance and on the square of the voltage, as represented by the following equation [26]:

$$E = \frac{1}{2} CV^2 \qquad (2.13)$$

Where,

E is the capacitor stored energy

The capacitor energy storage capability is proportional to the capacitance and the voltage stored on the capacitor. However, the voltage withstand strength of the dielectric limits the voltage stored [26]. Supercapacitors currently have a round trip efficiency of 84-95% [6]. Their very high cycle life of more than 500,000 cycles at 100% depth of discharge [16] coupled with the fact that they can be modular, quiet and non-polluting makes supercapacitors a very desirable energy storage device [6]. Their lifetime of up to 12 years [16] and high self-discharge rate of 14% of nominal energy per month are seen as limiting factors [34]. The cost of supercapacitors of 240,000 R/kWh is also seen as a significant issue [16]. They are currently being used for blade-pitch control devices for individual wind turbine generators which allows the rate at which power increases and decreases with changes in wind velocity to be controlled. This application is especially desirable for wind turbines connected to weak utility power grids to decrease voltage and power fluctuations [61, 62]. Supercapacitors are also used for short-term storage in power converters and are most applicable for high peak power, low-energy situations. Supercapacitors can also provide support during momentary interruptions and voltage sags by assisting in extended availability of power [26].

2.9 Pumped hydroelectric energy storage (PHES)

Pumped Hydroelectric Energy Storage (PHES) is the most wide spread energy storage technology in use today with over 200 installations worldwide [18]. The total combined generation capacity of these installations is over 90 GW and contributes to approximately 3% of the world's generating capacity [6]. The European Union, USA and Japan have as of 2009 contributed 36 GW, 21.8 GW and 24.5 GW respectively to the total worldwide installed capacity of PHES [63].

PHES is a storage technology whereby the potential of water raised against gravity is the stored energy in itself. A mass of 1 ton of water falling 100 m generates 0.272 kWh [22]. Energy is taken from the grid and returned at a later time when it is needed. Water is pumped from a lower reservoir (afterbay) to a higher reservoir (forebay) through a turbine and stored in the higher reservoir as bulk potential energy. When the energy is required in the form of electrical energy to meet peak load demand, the water is released from the upper reservoir through the turbine to the lower reservoir [15]. Water is pumped back to the upper reservoir during off-peak periods. A schematic diagram of a PHES scheme is

depicted in Figure 2-7. A large amount of energy can be produced and sustained for significant periods (days) of time with the size of the reservoir directly impacting the storage capacity [6].

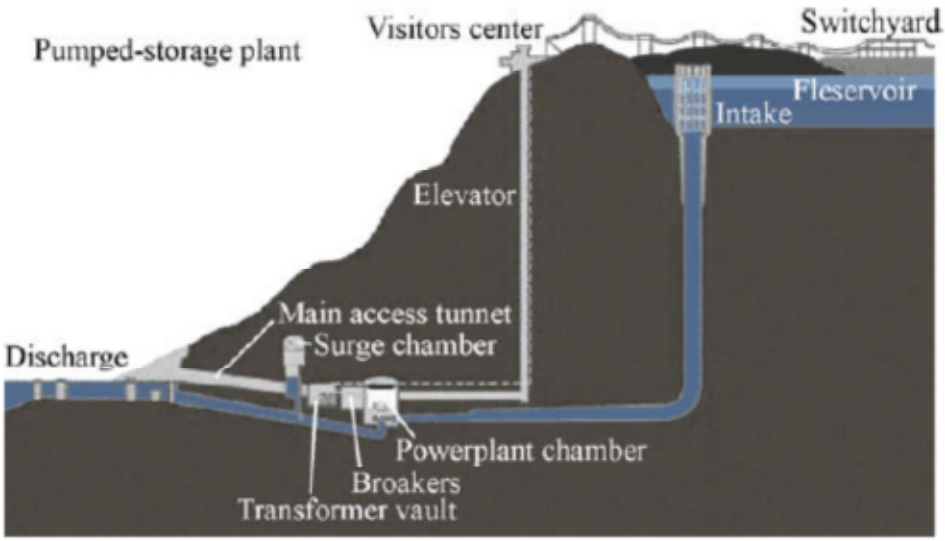

Figure 2-7 – Schematic diagram of a PHES [24]

PHES plants can be designed to be brought online rapidly i.e. between 1 and 2.4 seconds, as a source of assured reserve capacity with the ability to react almost instantaneously based on load requirements [8]. Its ability to respond to peak load fluctuations assists with more uniform and efficient loading on the base load fossil-fueled units operating in conjunction with the PHES plant [8]. The use of a combined wind and small PHES system has also been proposed for the storage of wind generated power in off-peak (low demand) periods and improve the controllability of the wind generated power [64, 65, 66].

2.9.1 Cost of PHES

PHES systems have the lowest investment risk with regards to the lowest levelized cost of delivered energy relative to the cost per kilowatt-hour of electricity produced, which is comparable to combined cycle gas turbines [15]. The cost of PHES depends primarily on the site which includes elevation difference, length of water conduits, operating drawdown of reserves, size of reservoirs and size of the plant. PHES plants are costly to build and are known to take a considerable amount of time to plan and to build. An example of this is

a PHES plant in the Alps which is rated for 1.06 GW of power and 8.5 GWh of energy storage capacity [6]. This plant took a total of 37 years to plan and build [67]. The low operating cost of PHES plants consisting of pumping energy and operation and maintenance is the major cost advantage when compared to other energy storage technologies.

2.9.2 PHES site requirements

The major drawback of PHES technology is the significant amount of land with suitable topography required to accommodate both the upper and lower reservoirs as well as ensuring an elevation or head between the two reservoirs [22]. Alternative designs for the lower reservoir or afterbay include oceans and lakes [8]. The availability of water resources is also another challenge and requires suitable alternatives to natural water resources to be considered such as the coupling of a PHES facility with an agricultural water supply as well as the possibility of utilizing the water produced from the gas and oil extraction industry [8]. The opposition from environmental groups citing deforestation, biodiversity, fisheries and water resources as major concerns needs to be overcome [14]. A considerable increase in GHG emissions can result from the development of hydroelectric reservoirs [68] with atmospheric carbon increasing due to the clearing of biomass from the land prior to construction of the reservoirs [69]. The proximity to existing transmission infrastructure and load centers also needs to be given serious consideration.

One of the ways to overcome the environmental issues and which has proven to be technically feasible, is to locate the reservoirs underground [6]. This concept is known as Underground Pumped Hydroelectric Energy Storage (UGPHES) which will be discussed later in more detail.

2.9.3 PHES performance and modelling

Elevation change (head) and water are the two fundamental resources required by PHES facilities [8]. The availability of power and energy of a PHES facility can be determined by the availability of water and the potential elevation change. This can be represented by the following equation [8]:

$$PE = mgH \qquad (2.14)$$

Where,

PE represents the potential energy in Joules

m is the mass [volume (m^3).density 1000 kg/m^3]

g is the gravitational acceleration of 9.81 m/s^2

H is the hydraulic head height in meters (m).

The output power can be presented as:

$$P = Q\ x\ H\ x\ \rho\ x\ g\ x\ \eta \qquad (2.15)$$

Where,

P is the power generated (W)

Q is the fluid flow (m^3/s)

H is the hydraulic head height (m)

ρ is the fluid density (kg/m^3) = 1000 (kg/m^3) for water

g is the gravitational acceleration (m/s^2) or 9.81 (m/s^2)

η is the efficiency

The head and the flow have an inversely proportional relationship whereby the water utilization can be minimized with a larger head. Similarly, if the flow is maximized the head can be reduced [8] as shown in Figure 2-8.

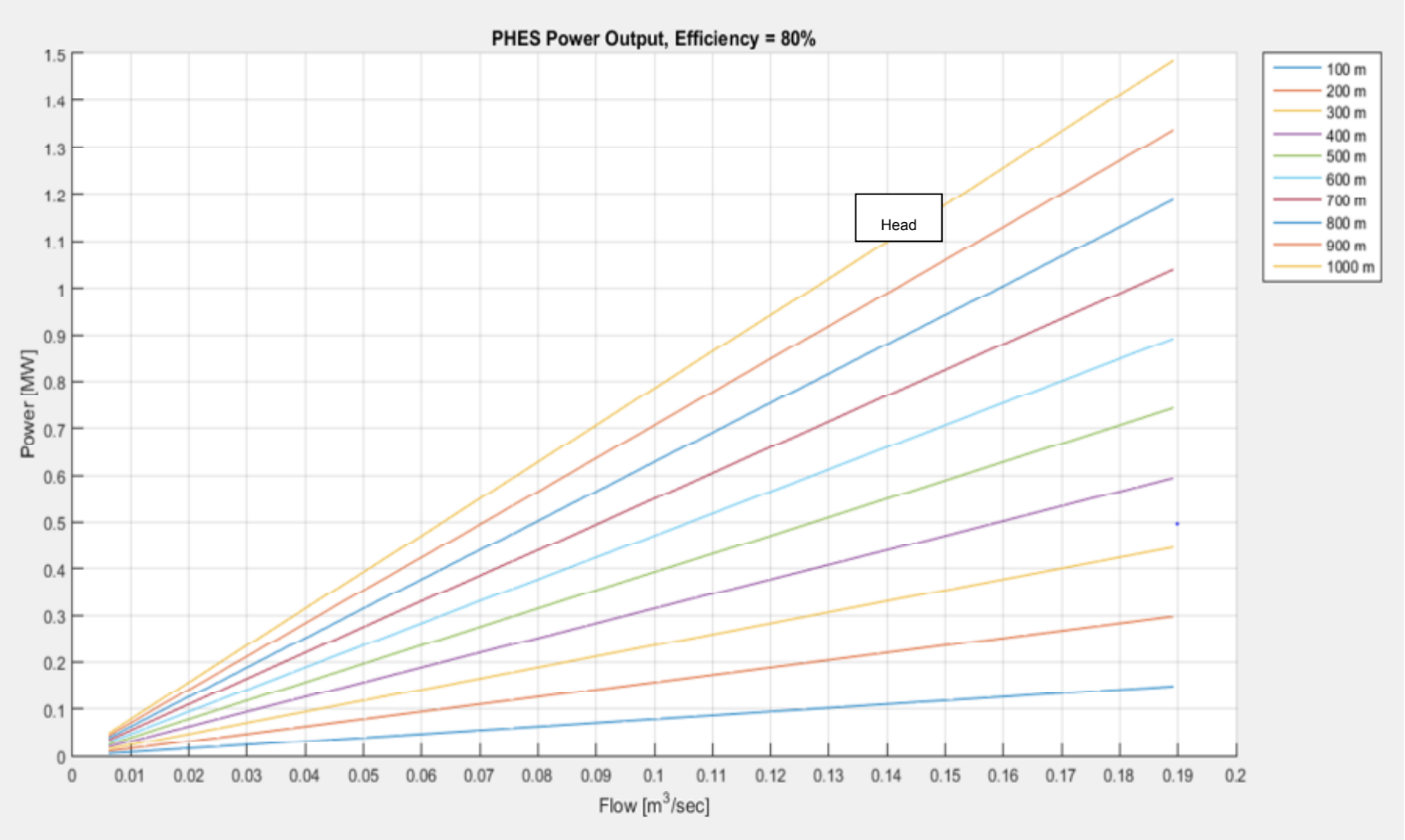

Figure 2-8 – PHES power output vs flow and head height with 80% efficiency

An assessment of the total energy available in the raised volume of water in the form of potential energy will allow for a controlled dispatch of the stored energy by varying the power of the specific system [8]. PHES facilities have a turnaround efficiency ranging from 70-80% with newer variable speed PHES plants operating at an efficiency of between 70-100% [6]. The efficiency is dependent on design characteristics such as the plant size, penstock (main water conduit between the forebay and the turbo machinery) diameter, hydro-turbines used and the height between the upper and lower reservoir [6]. The loss of efficiency is due to a number of factors which include efficiency losses in the motor generator and pump turbine, rolling resistance and turbulence in the penstock, and tail race (water conduit between the afterbay and turbo machinery) whereby some energy is retained by the water as it flows into the tail race [8].

Equation (2.15) considers a steady or laminar flow of water whereby Q remains constant considering an average (mean) flow velocity. The average velocity is the total flow rate divided by the cross-sectional area and is represented in units of length per time.

$$V = \frac{Q}{A} \qquad (2.16)$$

$$Q = V\ x\ A \qquad (2.17)$$

Where,

V is the average velocity (m/s)

Q is the fluid flow (m^3/s)

A is the cross-sectional area in square meters (m^2)

Substituting (2.17) into (2.15) introduces the average velocity component into the equation:

$$P = V\ x\ A\ x\ H\ x\ \rho\ x\ g\ x\ \eta \qquad (2.18)$$

For most surface water systems as in the case of the upper reservoir of a PHES system, the flow is considered to be turbulent [70]. The continuous mixing of low flow velocity with higher flow velocity, leads to the turbulent velocities being closer to the mean velocity [71].

The Reynolds number is used to classify flow as either turbulent or laminar and is represented as follows [71]:

$$Re = \frac{4\ x\ V\ x\ R}{v} \qquad (2.19)$$

Where,

Re is the Reynolds number (unitless)

V is the average velocity (m/s)

R is the hydraulic radius (m)

v represents the kinematic viscosity (m^2/s)

Using the Reynolds number, the velocity V can be represented as follows:

$$V = \frac{Re\ x\ v}{4R} \qquad (2.20)$$

Substituting equation (2.20) into equation (2.18), the power output represented as a function of the Reynolds number is as follows:

$$P = \left(\frac{Re\ x\ v}{4R}\right) x\ A\ x\ H\ x\ \rho\ x\ g\ x\ \eta \qquad (2.21)$$

From equation (2.21) it is evident that a larger Reynolds number results in a greater power output provided that the hydraulic radius remains constant.

Fluctuations in velocity are created due to turbulent eddies. For turbulent flow, the velocity includes both a mean and a turbulent component. This can be decomposed, known as the Reynold's decomposition, to represent the flow as follows [72]:

$$u(t) = \overline{u} + u'(t) \qquad (2.22)$$

$$u'(t) = u(t) - \overline{u} \qquad (2.23)$$

Where,

$u'(t)$ is the turbulent fluctuation (m/s)

$\overline{u}$ is the mean velocity (m/s)

The mean velocity can be evaluated through integration as follows [70]:

$$\overline{u} = \int_{t}^{t+T} u(t)dt \qquad (2.24)$$

With turbulent velocity represented as a function of time $\frac{dV}{dt}$, introducing this into equation (2.18) results in the following equation showing the power output also as a function of time:

$$\frac{dP}{dt} = \frac{dV}{dt}\ x\ A\ x\ H\ x\ \rho\ x\ g\ x\ \eta \qquad (2.25)$$

Figure 2-9 shows the power output as a function of changing velocity for an efficiency of 80%:

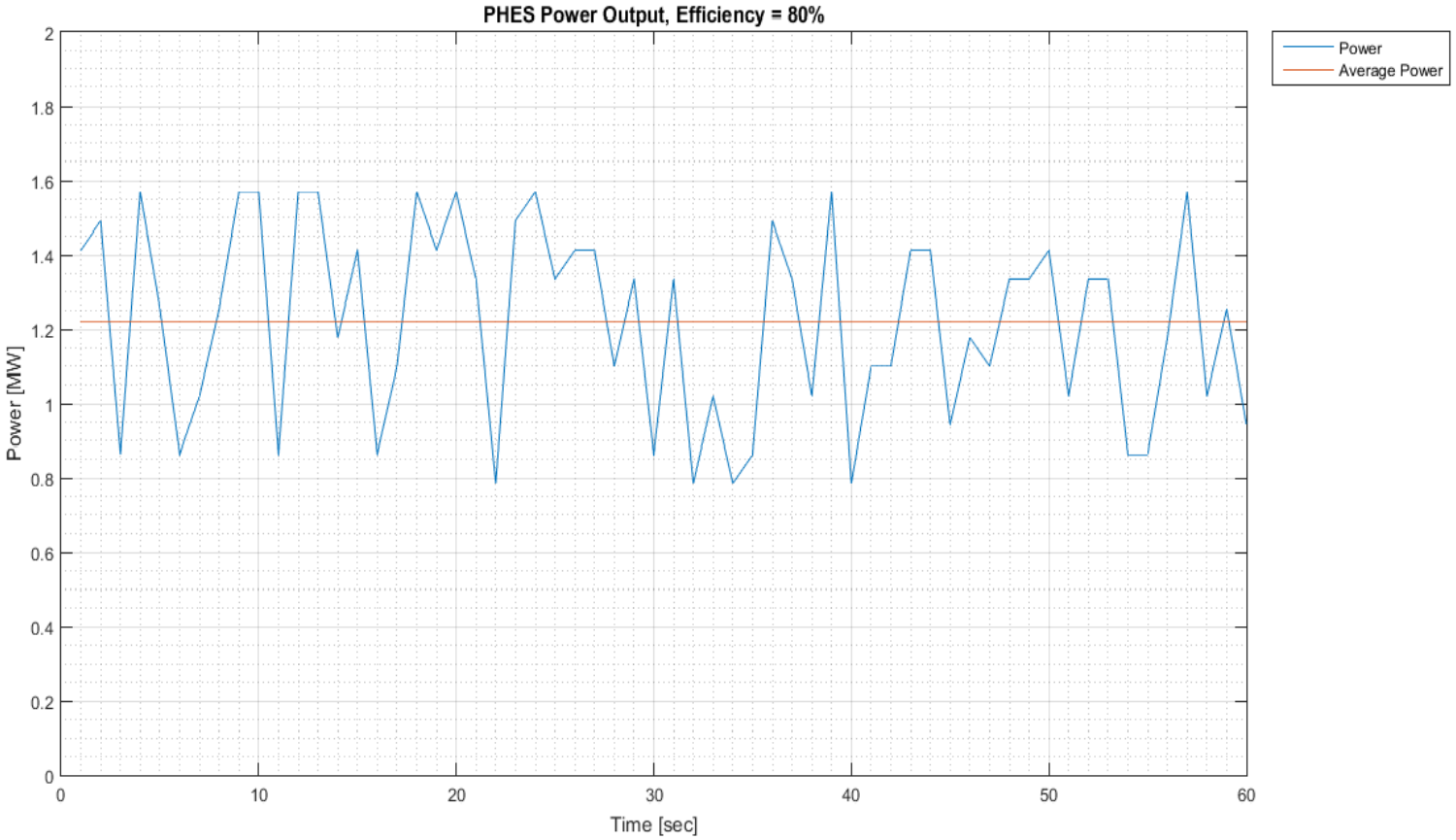

Figure 2-9 – PHES output for turbulent velocity

2.9.4 Existing installations of PHES systems

The Drakensberg pumped storage scheme built in 1981, is located in the Northern Drakensberg mountains of South Africa and is one of the largest pumped storage schemes in the world. This scheme makes use of four dams with the electricity generation equipment located between the Driekloof Dam and the Kilburn Dam. Electricity storage is in the form of 27,000,000 m^3 of water which translates to 27.6 GWh of electricity [4]. During times of peak electricity demand, water is released from the Driekloof Dam to the Kilburn Dam through four 250 MW turbine generators. Water is pumped back to the Driekloof Dam during times of low electricity demand [4].

The Ingula pumped storage scheme which is also located in the Drakensberg of South Africa, is still under construction since 2005 with expected completion in 2015 [5]. The lower Braamhoek Dam is 4.6 km away from the upper Bedford Dam and connected to an underground power station by the use of tunnels. The headrace tunnel is 2 km long with the tailrace at 2.5 km. The power station will house four 333 MW reversible pump turbines [5].

Other installations include Lac des Dix, Switzerland (2,009 MW), Guangzhou, China (2,400 MW), Kanagawa, Japan (2,700 MW) and Bath County, USA (2,710 MW) [73].

CHAPTER THREE

UNDERGROUND PUMPED HYDROELECTRIC ENERGY STORAGE (UGPHES)

Underground Pumped Hydroelectric Energy Storage (UGPHES) is a very similar energy storage concept to PHES with the major difference being that the lower reservoir (afterbay) is in an underground cavern system. The underground reservoir must have the capability of storing water without compromising the structural integrity or water quality. The upper reservoir (forebay) is constructed in the same manner as the conventional PHES scheme and is usually located directly above the lower reservoir as shown in Figure 3-1. Water conduits and powerstations are also located below ground with variations in the location of the powerstations allowing for two classifications of UGPHES namely single-stage and double-stage [74].

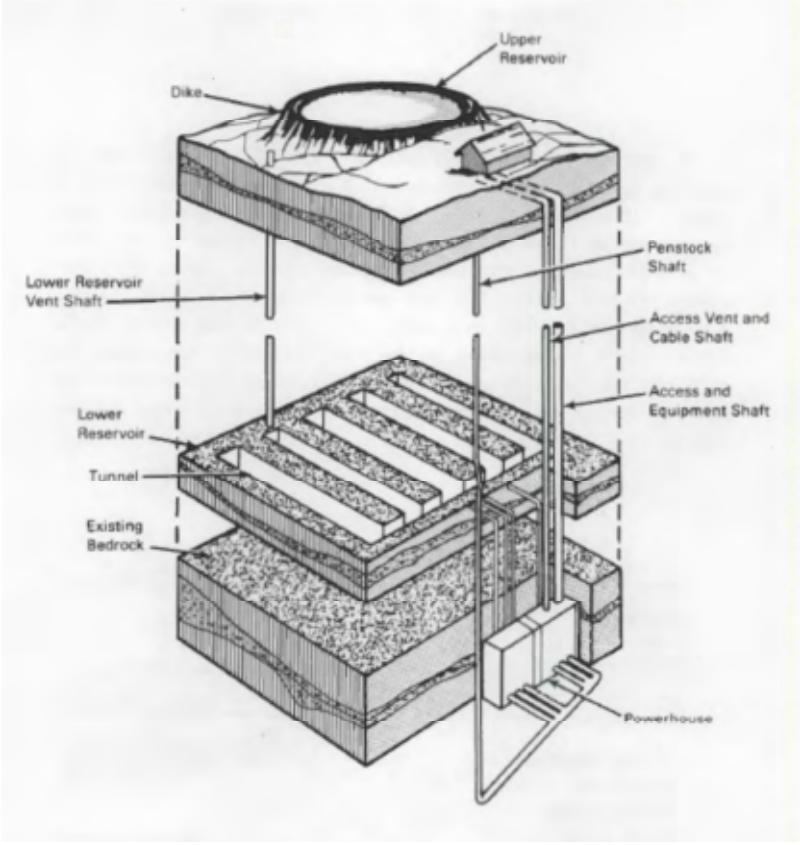

Figure 3-1 – Three dimensional concept of a UGPHES plant [75]

The single-stage UGPHES scheme is a system whereby there is a single vertical drop or hydroelectric head and a single underground powerstation between the upper and lower reservoir. The hydroelectric head is limited either by the head at which reversible pump/turbine units can operate or by geologic conditions [76].

In a double-stage UGPHES scheme there are two vertical drops or hydroelectric head and two underground powerstations between the upper and lower reservoir. A small reservoir between the two powerstations located at the level of the upper powerstation is used for equalizing the flow between the two powerstations [76]. With the lower reservoir being the largest cost item of UGPHES, the double-stage scheme is usually less costly than the single-stage scheme [75]. With the inverse relationship between the head and reservoir volume, double-staging effectively increases the head thereby reducing lower reservoir volume requirements and ultimately resulting in a nearly proportional cost saving. Additional costs are incurred due to the deeper shafts, equalizing reservoir and the second powerstation, however these are much less than the cost saving in the lower volume reservoirs [75].

3.1 Cost of UGPHES

There is no doubting the technical feasibility and advantages associated with UGPHES schemes, however the exorbitant costs of implementing such a scheme has seen none constructed thus far [6]. Considering an aquifer UGPHES system, the cost depends on whether there is an existing surface reservoir, transmissivity of the aquifer and depth to water [8]. The present regulatory and economic climates coupled with the relatively low cost of natural gas to fuel turbines for peaking power and the prospective payback periods (time consuming for planning and construction and pricey) which are too long to attract investors makes UGPHES an unattractive option at this point in time [77].

3.2 UGPHES site requirements

The site requirements or elements essential for a UGPHES scheme include surface conditions for a suitable and dependable reservoir, adequate water supply for initial reservoir filling and make-up, satisfactory underground structures or rock at required depths for the underground reservoirs and powerstations [75].

A regional geologic analysis of sites deemed suitable for the location of a UGPHES scheme followed by an in-depth detailed analysis of particular areas is required prior to the selection of a site. Good rock conditions is imperative for the lower reservoir with granite at the required depth being the most suitable. Limestone of low solubility as well as other hard and massive igneous and metamorphic rocks are also found to be suitable [78]. One of the methods used to attain a large underground cavern is through a process whereby underground salt is dissolved over several plant cycles [8]. The lower reservoir is not simply a single large cavern but rather a network of extruded narrow caverns which improves the structural integrity of the reservoir [79]. The use of underground aquifers as the lower reservoir is also an option which will later be discussed in depth.

The upper reservoir of an UGPHES scheme can be located off a stream which will also require a pipeline and pumping station. Excavated, embankment or a combination are the main types of upper reservoir design [8]. In the case whereby the upper reservoir is required to be excavated, the cost of excavating and lining the reservoir coupled with the challenge of maintaining the water quality are causes for concern [80]. The high energy content in the water due to the high head makes the water supply requirement for UGPHES comparatively small.

The environmental challenges facing UGPHES are a lot more manageable as compared to those affecting PHES. The most frequent issues that arise is the disposal of spoil generated from the excavation of the lower reservoir and the gradual temperature increase of cycled water [77]. The spoil from the excavation of the lower reservoir could be used in the construction of the upper reservoir while the gradual water temperature increase is not seen as a serious problem [77].

3.3 UGPHES performance and modelling

The power output of a UGPHES installation may be represented by the basic laminal fluid power equation which can also be used to illustrate the inverse relationship between the head and flow [8]:

$$P = Q\ x\ H\ x\ \rho\ x\ g\ x\ \eta \qquad (3.1)$$

Where,

P is the power generated (W)

Q is the fluid flow (m^3/s)

H is the hydraulic head height (m)

ρ is the water density (kg/m^3) = 1,000 (kg/m^3) for water

g is the gravitational acceleration (m/s^2) or 9.81 (m/s^2)

η is the efficiency

The components of the electrical system including the motor generator have relatively high efficiencies with the pump or turbine having the greatest impact on the system efficiency [81, 82]. The power output can be maximized by maximizing the head and the flow. In instances where the head is limited due to the characteristics of the installation, the flow rate can be looked at as an opportunity to maximize the power output. The flow and reservoir volume affect the energy capacity however the required duration of power generation constrains these parameters [8].

The hydraulic head, electrical system efficiency and flow capacity are the most important parameters for optimization of the system design. When considering an aquifer system, the measured flow that can be re-injected into the aquifer is of interest. In modelling the performance of an aquifer system, it is approximated that the re-injection flow capacity is the same as the yield capacity of the well under steady state flow conditions [3]. A cone of depression around the well is created at the point where the pump is located when drawing water because of the finite transmissivity (the rate which groundwater flows horizontally through an aquifer) of the aquifer material. The location of the pump in the well and the hydraulic conductivity of the material create the limits for the well yield [3].

A mound of injection resulting from the hydraulic conductivity of the aquifer material occurs when water is injected into the well as shown in Figure 3-2. The hydraulic head and transmissivities of the aquifer determine the injection flow rate however, the location of the turbine or pump also has an effect on the injection flow rate [8].

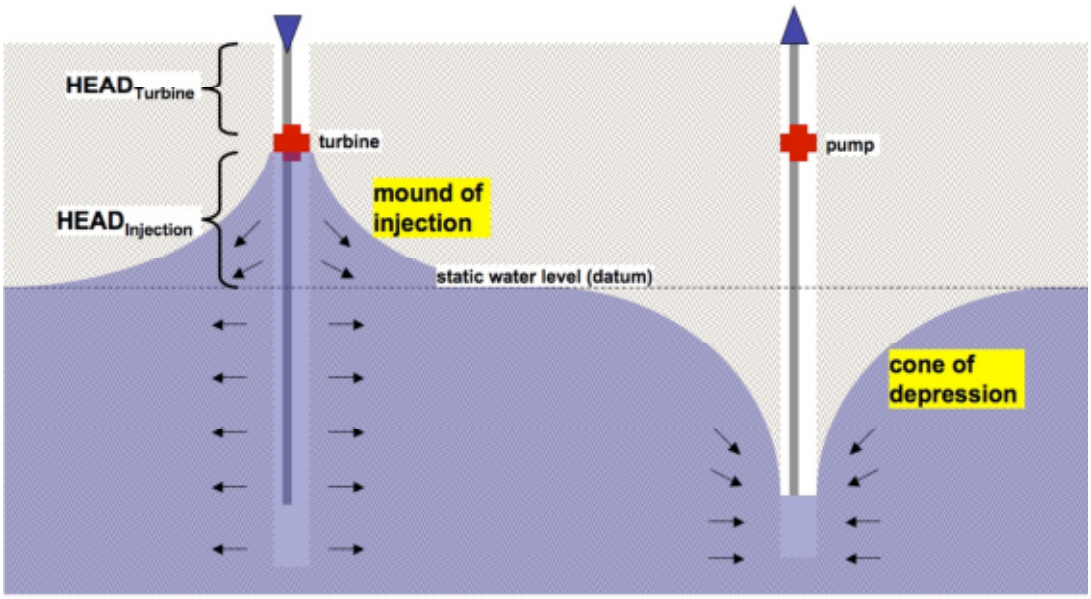

Figure 3-2 - Mound of injection and cone of depression [3]

Water flow in a confined aquifer can be represented by the groundwater equation which is represented as follows [83]:

$$\frac{S}{T} \cdot \frac{\partial h}{\partial t} = \frac{1}{r} \cdot \frac{\partial}{\partial r} \cdot \left(r \cdot \frac{\partial h}{\partial r} \right) \qquad (3.2)$$

Where,

S is the storage coefficient

T represents the transmissivity (m^2/s)

h is the hydraulic head (m)

r is the radius from well

∂h is the drawdown ($h_{initial}$ – h (m))

Equation (3.2) can be correlated to the height of an injection mound operating in an unconfined aquifer. Assuming that the pumping occurs over a long period of time, the equation representing drawdown over time is as follows [8]:

$$drawdown\ (head) = \frac{2.3 \cdot Q}{4 \cdot \pi \cdot T} \cdot \log\left(\frac{2.25 \cdot T \cdot t}{r^2 \cdot S} \right) \qquad (3.3)$$

Where, Q is the water flow (m^3/s)

It can be determined from equation (3.3) that the transmissivity is an important parameter to be considered when determining the drawdown during design of the power output of the system. An inversely proportional relationship exists between the drawdown, transmissivity and flow; drawdown decreases as the transmissivity and flow increases as shown in Figure 3-3.

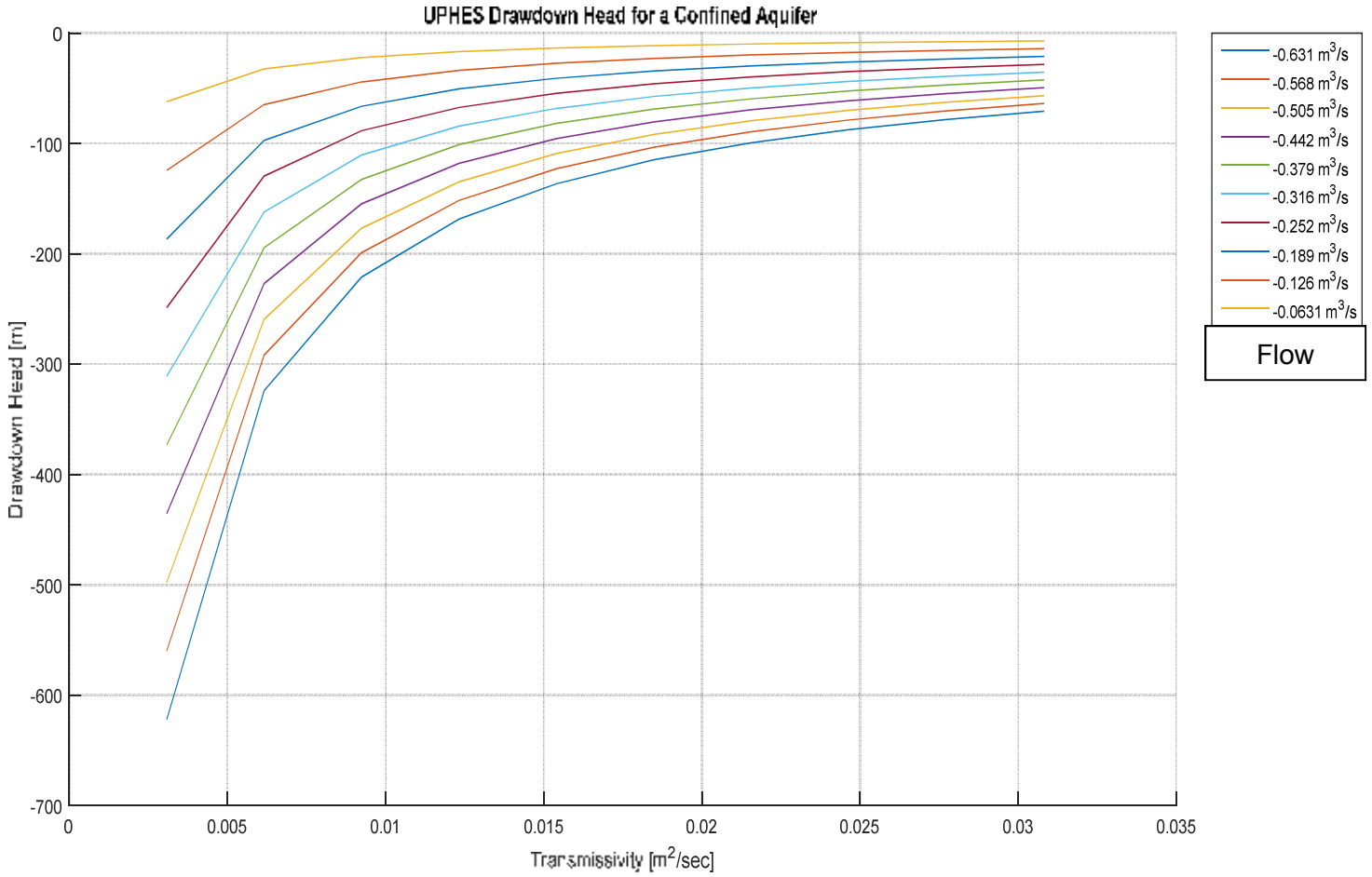

Figure 3-3 – UGPHES drawdown head with variable transmissivity and flow for a confined aquifer

In an aquifer with low transmissivity, the mound of injection can become too high thereby severely limiting the drawdown which can in effect negate the turbine's ability to produce power from injection flow [3]. Therefore, the aquifer transmissivity must be as large as possible in order to reduce the mound of injection which in effect increases the hydraulic head for power generation through the turbine. The major design parameters of the aquifer UGPHES system is therefore the aquifer transmissivity, injection mound height and the depth to water [8]. In making use of large underground caverns as the lower reservoir, the issue of transmissivity and injection mound height is not a cause for concern.

The situation with regards to the transmissivity and injection mound as described above, can be represented as a simple electrical circuit as shown in Figure 3-4.

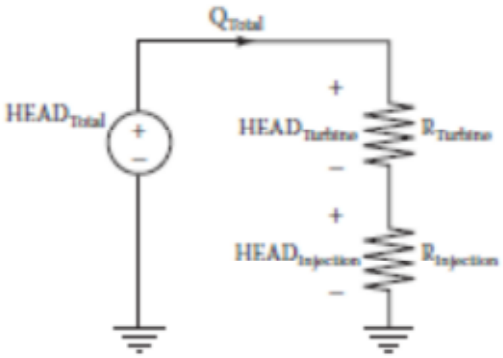

Figure 3-4 – Electrical circuit model for hydraulic head [8]

The parameters associated with this is a voltage source which represents the total hydraulic head potential ($HEAD_{Total}$), resistances representing the "head drop" for the turbine (resistance to water flow in the pipe and the turbine - $R_{Turbine}$) and the aquifer transmissivity ($R_{Injection}$), and the current (Q_{Total}) which represents the flow of water. With the $HEAD_{Total}$ held constant, a reduction in $R_{Injection}$ will result in an increase in $R_{Turbine}$ while keeping Q_{Total} constant but increasing the turbine power output. These relationships are governed by the linear behavior of an electric circuit as per Ohm's Law as follows [3]:

$$HEAD_{Total} = HEAD_{Turbine} + HEAD_{Injection} \qquad (3.4)$$

$$HEAD_{Turbine} = Q_{Total} * R_{Turbine} \qquad (3.5)$$

$$HEAD_{Injection} = Q_{Total} * R_{Injection} \quad (3.6)$$

$$Power_{Turbine} = Q_{Total} * HEAD_{Turbine} \quad (3.7)$$

The flow (current) through the circuit is proportional to the transmissivity (resistance) in the circuit. The resistance and conductance in the circuit can be represented by [3]:

$$R = \frac{l}{\sigma . A} \quad (3.8)$$

$$G = \frac{1}{R} = \frac{\sigma . A}{l} \quad (3.9)$$

Where,

R is the resistance (Ω)

G is the conductance (S)

l is the length (m)

σ is the conductivity (S/m)

A represents the area (m^2)

The aquifer transmissivity can be represented by [83]:

$$T = \frac{k . A}{r} \quad (3.10)$$

$$T = k . b \quad (3.11)$$

$$T = \frac{\kappa . \gamma . b}{\mu} \quad (3.12)$$

Where,

T is the transmissivity (m^2/s)

k is the hydraulic conductivity (m/s)

A is the area (m^2)

r is the radius (m)

b is aquifer thickness (m)

κ is intrinsic permeability (m^2)

γ is the specific weight of water (1,000 kg/m^3 at 4 °C)

μ is the dynamic viscosity of water (0.00089 Pa/s)

3.3.1 Water hammer effects on a confined aquifer well system

Water hammer is a phenomenon whereby an abrupt or sudden change to the flow in a confined system resulting in transient events, can lead to large pressure fluctuations. It is an important phenomenon that needs to be considered due to the extreme variations in pressure whereby a dramatic rise in pressure resulting from a high pressure wave can result in damage to the well while a negative wave can result in pressures which can be extremely low thereby creating the possibility of intrusion of contaminants. Transient events can also result in the abnormal operation of pumps [84]. Transient flow in a closed conduit which in this case is the well system can be described by the equations of momentum and continuity.

For the momentum equation, consider x as the top of the well (upper reservoir), Q represents the flow, and the pressure head plus the elevation head is H. $x + \Delta x$ is considered the bottom of the well (lower reservoir) resulting in a flow at this position of $(Q + \frac{\partial Q}{\partial x}\Delta x)$, the piezometric head is $(H + \frac{\partial H}{\partial x}\Delta x)$ where $\frac{\partial Q}{\partial x}$ and $\frac{\partial H}{\partial x}$ are the partitial derivatives of Q and H with respect to x and are considered to increase in the positive x direction [84].

F_1 and F_2 which are the pressure forces, together with the wall shear force due to friction S, and the body force are the forces that act on the fluid element. The shear force is represented by the following equation [84]:

$$S = \frac{\gamma}{8g} f V^2 \pi D \Delta x \qquad (3.13)$$

Where,

S is the shear force

g is the gravitational acceleration

f is the Darcy-Weisbach friction factor

V is the average fluid velocity in the well

D is the well diameter

γ is the specific weight of water

Δx is the length of the well

$\gamma/8gfV^2$ is the wall shear stress τ_0

$\pi D\Delta x$ is the area that the shear is acting on

$\partial A/\partial x\Delta x\gamma A$ can be neglected due to it being negligible compared to $\partial H/\partial x\Delta x\gamma A$ [85].

The pressure and the weight components are accounted for by the piezometric head $(H = \frac{p}{\gamma} + z)$. F_1 and F_2 is represented as follows [84]:

$$F_1 = (H - z)\gamma A \qquad (3.14)$$

$$F_2 = \left(H + \frac{\partial H}{\partial x}\Delta x - z\right)\gamma A \qquad (3.15)$$

Where the fluid element area on either side is represented by A.

Summing the forces in the direction of flow [84]:

$$F = F_1 - F_2 - S \qquad (3.16)$$

Substituting equations (3.13), (3.14) and (3.15) into equation (3.16):

$$F = \left((H - z)\gamma A\right) - \left(\left(H + \frac{\partial H}{\partial x}\Delta x - z\right)\gamma A\right) - \frac{\gamma}{8g} f V^2 \pi D\Delta x \qquad (3.17)$$

Equation (3.17) can be simplified to:

$$F = -\gamma A\frac{\partial H}{\partial x}\Delta x - \frac{\gamma}{8g} f V^2\, \pi D\Delta x \qquad (3.18)$$

Newton's second law of motion [86, 87]:

$$F = m\frac{dV}{dt} \qquad (3.19)$$

Where,

m is the mass of the fluid element

dV/dt is the acceleration of the fluid element

The fluid element mass can be represented as [84]:

$$Mass = \frac{\gamma}{g} A\Delta x \qquad (3.20)$$

Substituting equations (3.19) and (3.20) into equation (3.18) and dividing by mass:

$$\frac{dV}{dt} = -g\frac{\partial H}{\partial x} - \frac{fV^2}{2D} \qquad (3.21)$$

The partial derivative of velocity gives the total derivative dV/dt [84]:

$$\frac{dV}{dt} = \frac{\partial V}{\partial t} + \frac{dx}{dt}\frac{\partial V}{\partial x} \qquad (3.22)$$

Replacing $dx/dt = V$ [84]:

$$\frac{dV}{dt} = \frac{\partial V}{\partial t} + V\frac{\partial V}{\partial x} \qquad (3.23)$$

$V\partial V/\partial x$ may be neglected since the velocity change term due to position being negligible compared to the velocity change with time term [85]. Neglecting $V\partial V/\partial x$ and substituting into equation (3.21):

$$\frac{\partial V}{\partial t} + g\frac{\partial H}{\partial x} + \frac{fV^2}{2D} = 0 \qquad (3.24)$$

Equation (3.24) represents the momentum equation for water hammer used for one dimensional pipe flow expressed as a function of velocity and piezometric head [84]:

The continuity equation considers the continuity of the flow in the well, the well wall extension and expansion due to well wall elasticity and compressibility of the fluid. The

moving, deforming control volume is represented by the continuity equation as follows [86, 87]:

$$\int_{C.V} \frac{\partial \rho}{\partial t} d\forall + \int_{C.S} \rho \vec{V}_b \, d\vec{A} + \int_{C.S} \rho \vec{V}_r \, \vec{n} d\vec{A} = 0 \qquad (3.25)$$

Where,

$C.V.$ is the control volume

$C.S.$ is the control surface

ρ is the fluid density

$d\forall$ is the elemental volume

$\vec{V}_b$ is the boundary velocity of $C.V.$

$\vec{V}_r$ is the relative velocity of the fluid with respect to the control volume boundary velocity

$\vec{V}$ is the actual fluid velocity

$\vec{n}$ is the outward drawn normal for the area dA

A is the well cross-sectional area

Equation (3.25) can be rewritten as [86, 87]:

$$\frac{d}{\partial t} \int_{C.V.} \rho d\forall + \int_{C.S.} \rho V_{rn} \, dA = 0 \qquad (3.26)$$

Where,

$V_{rn} = V_r \cos\theta$ and θ is the angle between $\vec{V}_r$ and $\vec{n}$

Writing equation (3.25) in differential form [87]:

$$\frac{\partial \rho}{\partial t}(AdL) + \rho \frac{\delta \forall}{\delta t} + \frac{\partial}{\partial x}(\rho V) dLA = 0 \qquad (3.27)$$

Where,

A is the cross-sectional area of the well

$\delta\forall$ is the incremental volume due to well expansion

dL is the elemental well length

$V = V_{rn}$ is the water velocity

$\delta\forall$ can be written as [88]:

$$\delta\forall = AdL\left(\frac{1-v^2}{E}\right)\left(\frac{\delta pd}{e}\right) \qquad (3.28)$$

Where,

v is the Poisson ratio

E is the Young's modulus of elasticity

δp is the pressure increment

d is the pipe inner diameter

e is the pipe wall thickness

Substituting equation (3.28) into equation (3.27):

$$\frac{\partial\rho}{\partial t}(AdL) + \rho AdL\left(\frac{1-v^2}{E}\right)\frac{dp}{dt}\frac{d}{e} + \frac{\partial}{\partial x}(\rho V)dLA = 0 \qquad (3.29)$$

Equation (3.29) reduces to [84]:

$$\frac{1}{\rho}\frac{\partial\rho}{\partial t} + \left(\frac{1-v^2}{E}\right)\frac{dp}{dt}\frac{d}{e} + \frac{\partial V}{\partial x} + \frac{V}{\rho}\frac{\partial\rho}{\partial x} = 0 \qquad (3.30)$$

Replacing the following in equation (3.30) [84]:

$$\frac{1}{\rho}\left[\frac{\partial\rho}{\partial t} + \frac{\partial\rho}{\partial x}V\right] = \frac{1}{\rho}\frac{d\rho}{dt} \qquad (3.31)$$

Where,

$$V = \frac{dx}{dt} \qquad (3.32)$$

And,

$$\frac{d\rho}{dt} = \frac{\rho}{K}\frac{dp}{dt} \qquad (3.33)$$

Where,

K represents the bulk modulus of the fluid

Therefore [84],

$$\frac{dp}{dt}\left[\frac{1}{K} + \left(\frac{1-v^2}{E}\right)\frac{d}{e}\right] + \frac{\partial V}{\partial x} = 0 \qquad (3.34)$$

Substituting,

$$\frac{1}{\rho c^2} = \left[\frac{1}{K} + \left(\frac{1-v^2}{E}\right)\frac{d}{e}\right] = \frac{1}{K}\left[1 + \frac{Kc_1 d}{Ee}\right] \qquad (3.35)$$

Where,

c is the wavespeed and $c_1 = (1 - v^2)$

Results in:

$$\left[\frac{\partial p}{\partial t} + \frac{\partial p}{\partial x}V\right] + \rho c^2 \frac{\partial V}{\partial x} = 0 \qquad (3.36)$$

Dividing equation (3.36) by γ yields the continuity equation [84]:

$$\left[\frac{\partial H}{\partial t} + \frac{\partial H}{\partial x}V\right] + \frac{c^2}{g}\frac{\partial V}{\partial x} = 0 \qquad (3.37)$$

3.4 Existing installations of UGPHES systems

There is to date no existing UGPHES installation in operation. There are however two UGPHES projects that are at various stages of development. The Elmhurst Quarry Pumped Storage Project (EQPS) which is located in the City of Elmhurst, DuPage County, Illinois, USA, is a UGPHES project that will utilize an abandoned mine and quarry for both the upper and lower reservoir. It is in close proximity to existing electrical transmission and a large load center, has renewable energy opportunities, low environmental impacts and has flood control capabilities [89]. The power generated will be used during peak demand

periods whereby water will gravity flow from an above-ground reservoir, through the pump-turbine and into the lower underground reservoir in the form of abandoned mine caverns. Off-peak power will be used to return the water to the upper reservoir. The initial design capacity will have a storage potential estimated at 708.5 GWh and rated between 50 MW and 250 MW [89].

The Riverbank Wiscasset Energy Centre (RWEC) to be located in Wiscasset, Lincoln County, Maine, USA, is the site for a proposed UGPHES facility of 1,000 MW. Water will be diverted down vertical shafts of 2,000 ft, through four 250 MW pump turbines and stored in underground caverns [89]. The water will be pumped back to the upper reservoir using low-cost off-peak power. The facility will be located in close proximity to existing electric transmission lines and an industrial substation. There is also a proposed UGPHES project for Estonia – Muuga port whereby the sea will be used as the upper reservoir and the lower reservoir will be located underground [77]. Seawater which will be drawn from the Baltic Sea will be used due to its marginal salt content of only 4-6%. The following technical parameters are proposed for the project [77]:

- 450 MW of maximum storage / input power;
- 500 MW of maximum generation / output power;
- Three reversible pump-turbines rated 1 x 100 MW and 2 x 175 MW;
- One additional turbine of 50 MW;
- Maximum flow rate during pumping or generating of 120 m^3/s;
- 500 m of water head;
- Lower reservoir volume of 5,200,000 m^3;
- Roundtrip efficiency of 75% (generating 88% and pumping 85%);

The use of this UGPHES installation will be for a hybrid installation with wind power as the renewable energy source [77].

3.5 Technological adaptation of UGPHES

An adaptation of UGPHES technology is by a company known as Gravity Power, LLC. They have developed the Gravity Power Module (GPM) shown in Figure 3-5, which makes use of a very large piston that is suspended in a deep water filled shaft and a return pipe

connecting to a pump-turbine mounted at ground level. Leakage around the piston which is comprised of reinforced rock or concrete, is prevented by using sliding seals [90]. The shaft is filled with water only once at startup and then sealed with no further requirements for water. Electricity is produced when the piston drops thus forcing water down the storage shaft. The water is pushed up the return pipe and through the turbine to produce electricity. The storage of energy is the process in reverse whereby water is forced by the pump (motor/generator spinning in reverse) back down the return pipe and into the shaft causing the piston to lift [90].

The GPM system is highly efficient with low pump-turbine losses and minimal friction, and is able to store hundreds of megawatt-hours per shaft [90]. The cost of the GPM module is primarily dependent on the cost of construction of the shaft which requires less excavation per storage capacity. The overall cost is significantly lower than that for conventional UGPHES [90]. Aside from the cost advantage, there are many other advantages associated with the GPM which include modularity (small footprint and unobtrusive operation), low cost per megawatt-hour, high efficiency, long lifetime, environmental compatibility leading to fast permitting and rapid construction resulting in a short time from project start to revenue [90].

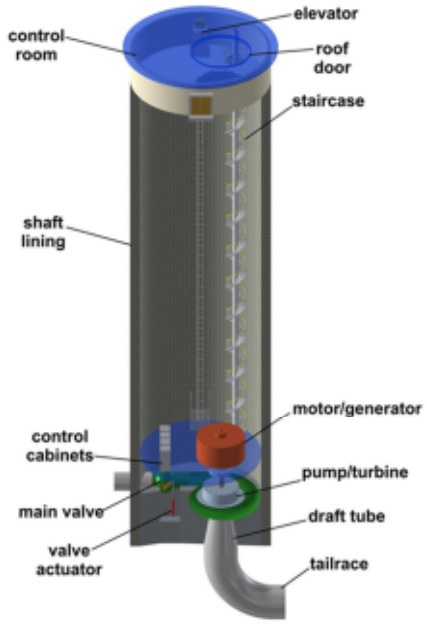

Figure 3-5 - Gravity Power Module [90]

CHAPTER 4

AQUIFER UNDERGROUND PUMPED HYDROELECTRIC ENERGY STORAGE

An aquifer or groundwater UGPHES as shown in Figure 4-1 is a system whereby an integrated pump-turbine unit located below the surface of the aquifer water level is used to either pump water to the surface reservoir or to generate electricity when water is released from the surface reservoir back in to the aquifer [3].

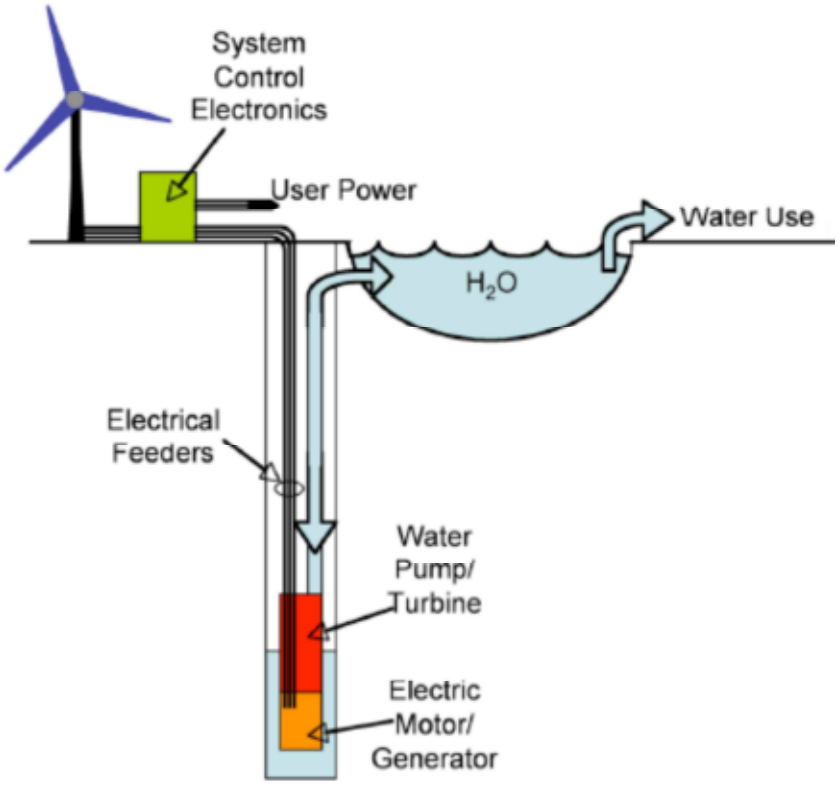

Figure 4-1 – Aquifer UGPHES system concept illustration [8]

The weight of the water in the surface reservoir is stored as gravitational potential energy with respect to the aquifer. The volume of the surface reservoir and head height is directly proportional to the energy storage needs required by the application as shown in Figure 4-2. This also dictates the positioning of the integrated pump-turbine unit whereby for large

UGPHES installations, it is located below the lower reservoir in an effort to avoid water hammering issues [3].

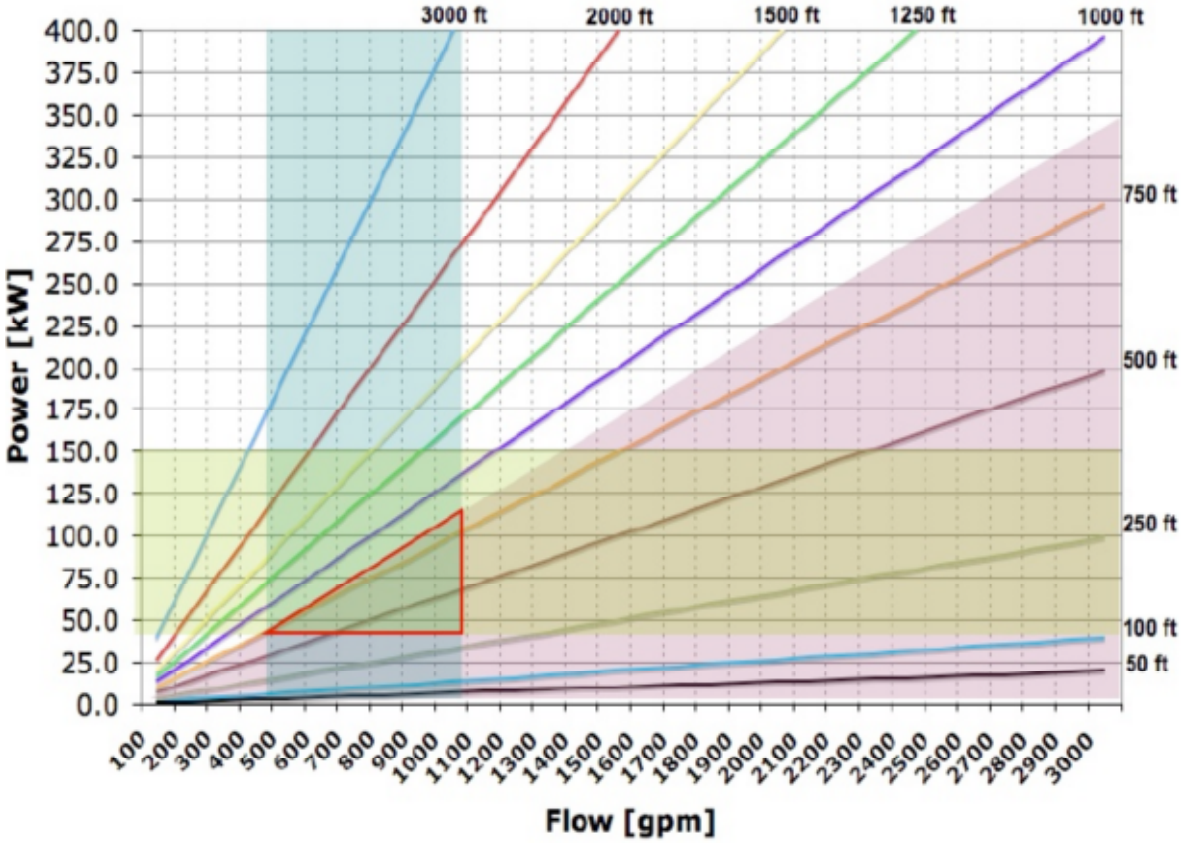

Figure 4-2 – Relationship of flow and head to power output and expected ranges [8]

A primary requirement of the aquifer UGPHES system is a deep well to the groundwater. The well is constructed to meet flow demands by the using an adequately sized water tube together with a conduit for the electrical feeders. The size and construction of the well directly impacts the size of the integrated pump-turbine assembly that can be installed and the water flow capacity [3]. This ultimately impacts the sizing of the system for maximum power. Where an unconfined aquifer is not deep enough, a well may be dug to interface with deeper confined aquifers [3]. Water flow capacity can be maximized through well modifications such as radial or horizontal as shown in Figure 4-3 and Figure 4-4 respectively.

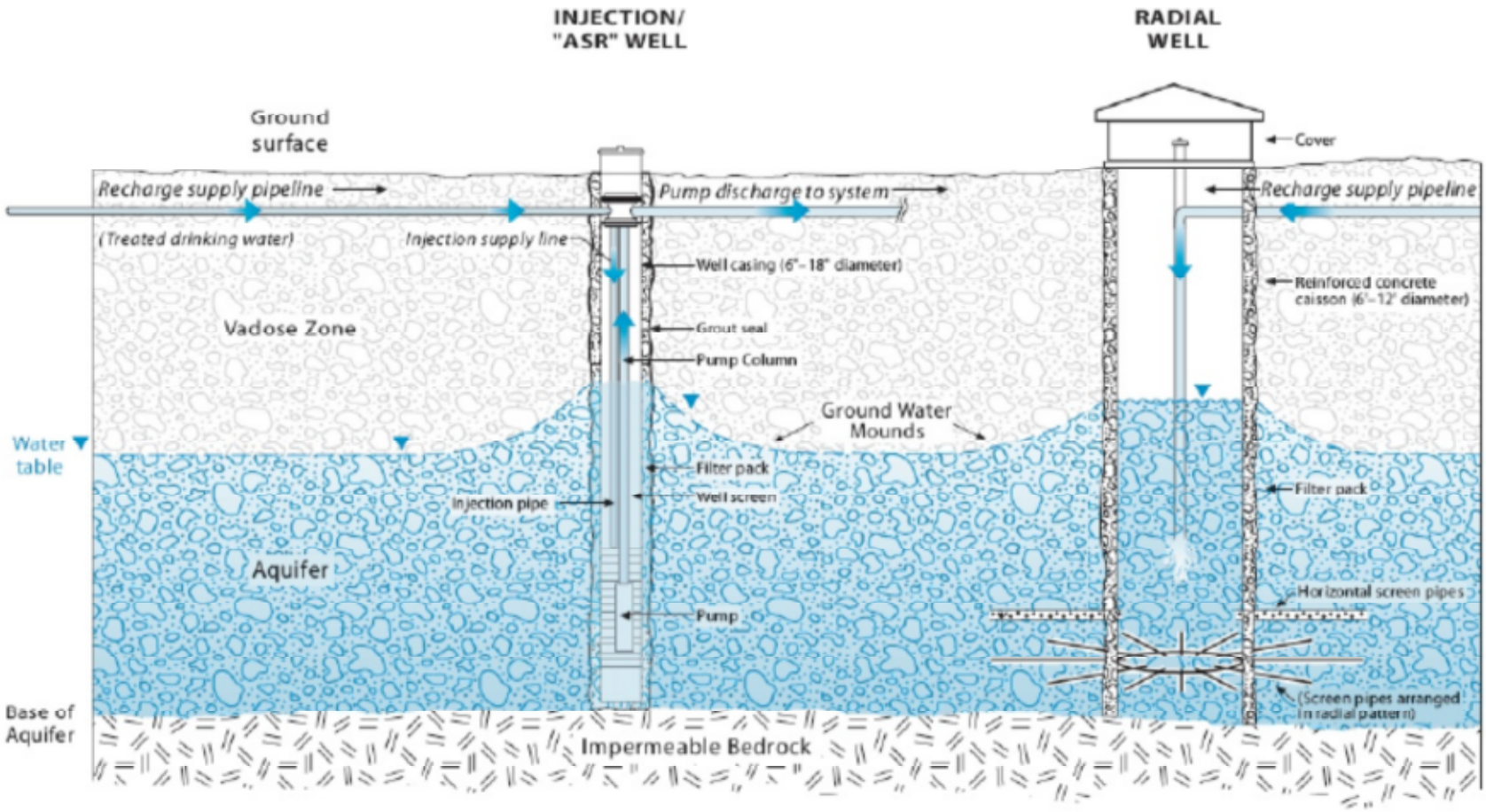

Figure 4-3 – Direct injection radial unconfined aquifer well concept [91]

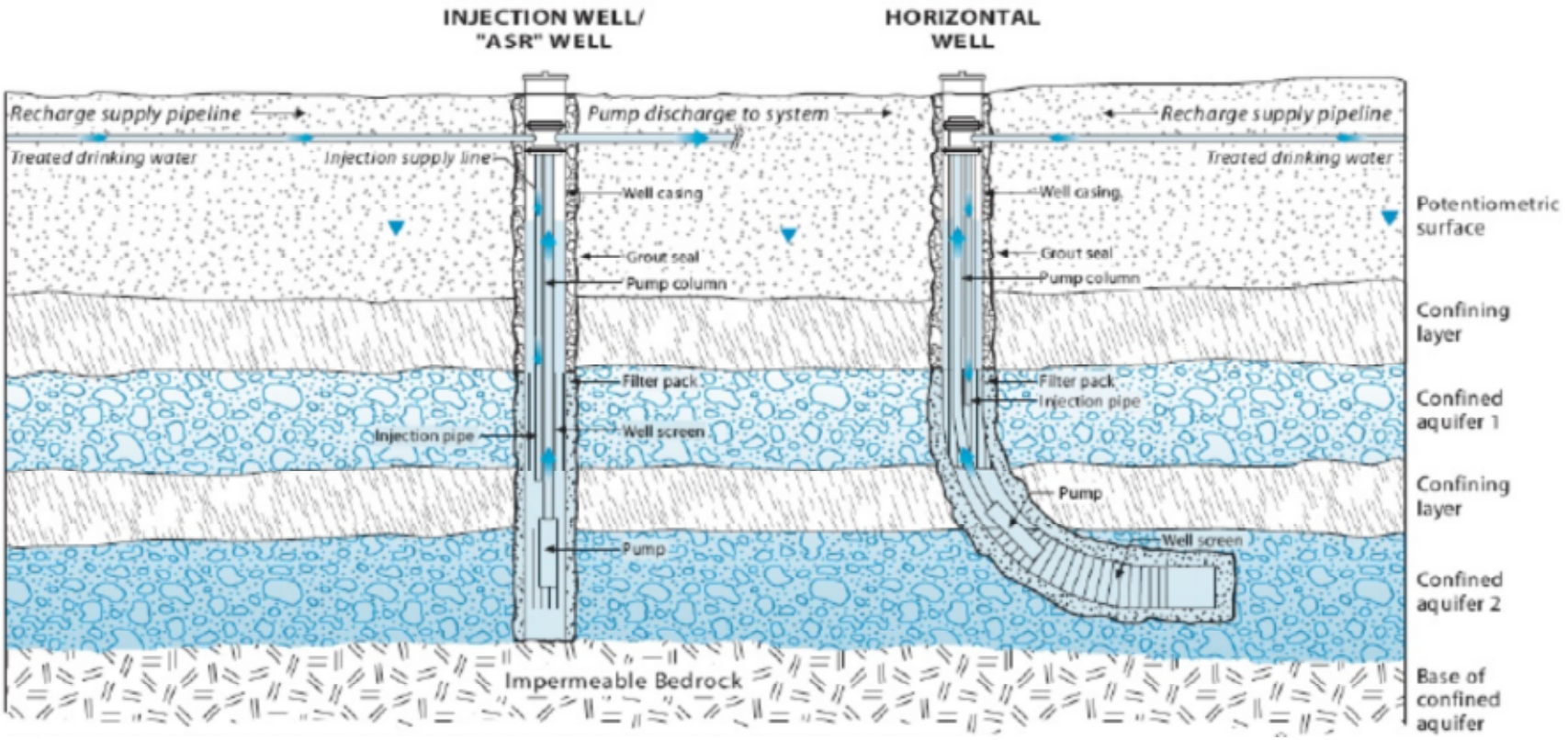

Figure 4-4 – Direct injection horizontal confined aquifer well concept [91]

4.1 Aquifers in South Africa

South Africa is underlain over 80% by relatively low-yielding, shallow, weathered and/or fractured rock aquifer systems. However, in the northern and southern parts of the country consisting of dolomitic and quartzitic aquifer systems, along with primary aquifers along the coastline, groundwater is able to be abstracted at relatively high rates [92]. Figure 4-5 shows the distribution of significant secondary and primary aquifer systems in South Africa. Aquifer consumption in South Africa contributes only around 15% of the total volume of water consumed in the country [93].

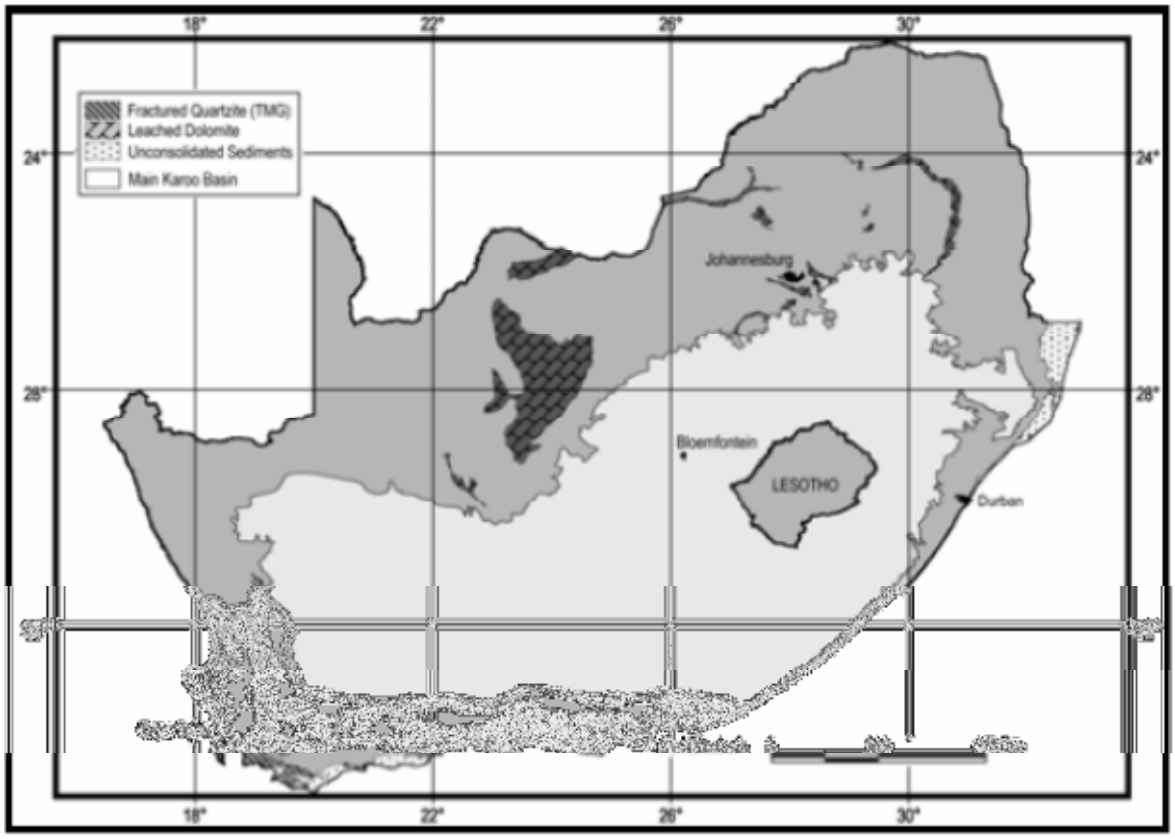

Figure 4-5 – Distribution of significant secondary and primary aquifer systems in South Africa [94]

Figure 4-6 shows the distribution of aquifer storage systems in South Africa which indicates approximately 235,500 Mm^3 of storage.

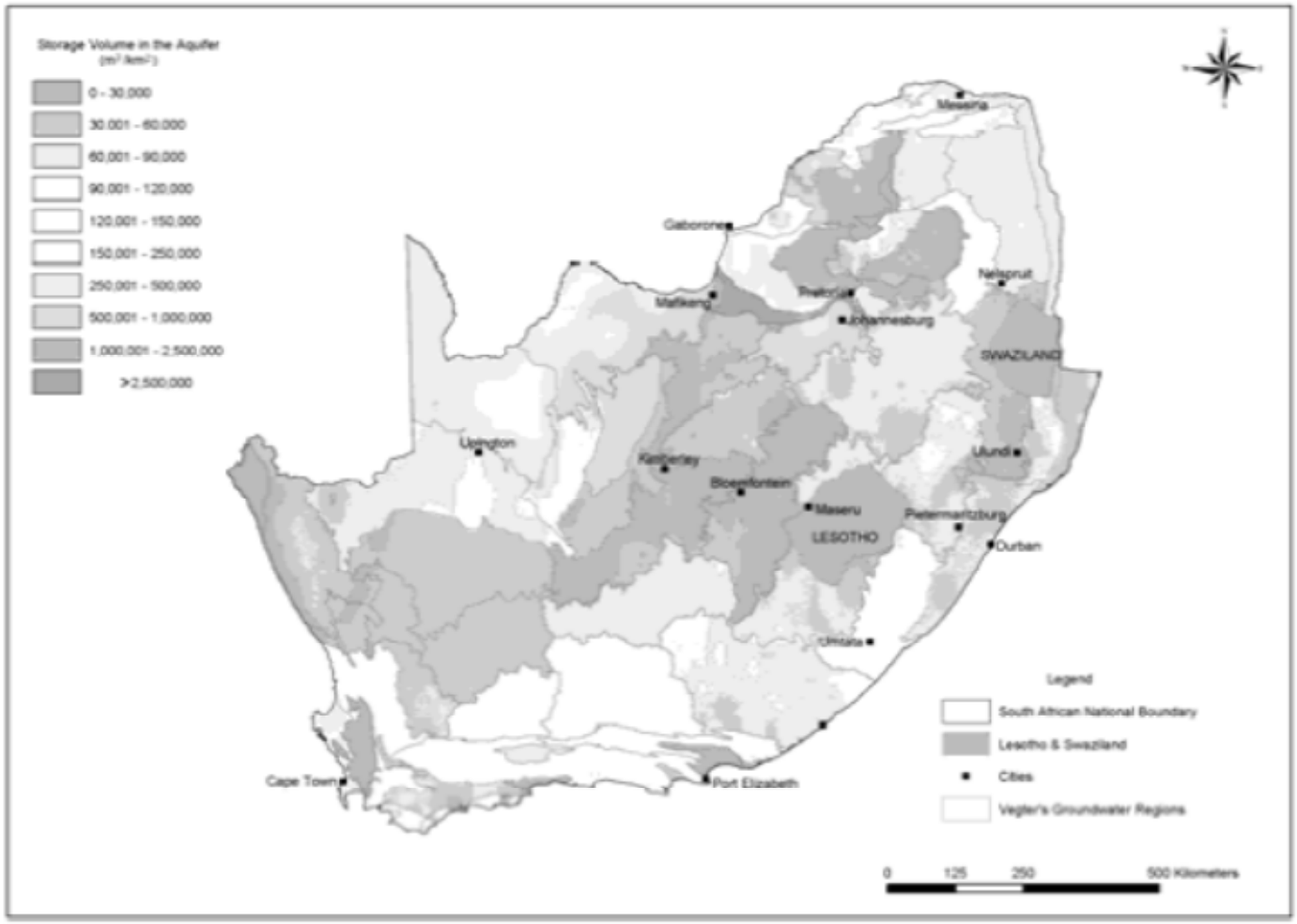

Figure 4-6 – Estimated total volume (m^3/km^2) of groundwater stored in South African aquifers [94]

The South African mean annual groundwater recharge volume from rainfall is 30,520 Mm^3 which is estimated using various empirical rainfall versus recharge relationships and the chloride-mass-balance [92]. The abstraction of the maximum volume (m^3) of groundwater per unit area per annum without continued long term declining water levels, is known as the Groundwater Resource Potential (GRP). For South Africa, this ranges from a maximum of 47,727 Mm^3/a to as low as 7,536 Mm^3/a [92]. The Average Groundwater Resource Potential map is shown in Figure 4-7. The Average Groundwater Exploitation Potential (AGEP) which utilizes the total volume of groundwater available for abstraction under normal rainfall conditions is recommended for water resource planning purposes. This is estimated at 19,073 Mm^3/a which declines to 16,253 Mm^3/a during drought conditions in South Africa [92].

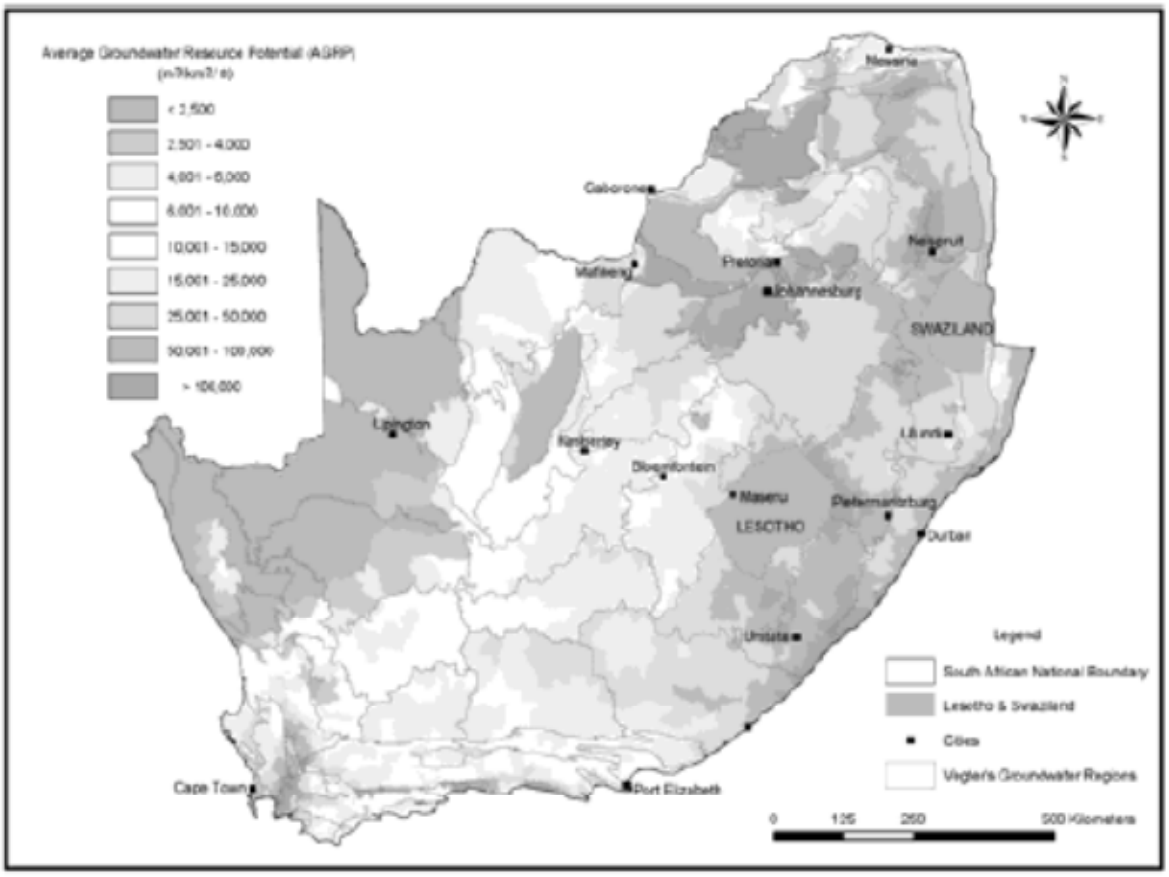

Figure 4-7 – Average groundwater resource potential for South Africa [94]

The Department of Water Affairs (DWA) South Africa, has developed a series of aquifer maps based on aquifer classification, vulnerability and susceptibility, to provide the appropriate information to national water resource managers and planners. These maps are a vital source of information that can be used for identification of aquifers suitable for implementation in a UGPHES scheme. It is evident from Table 4-1 that an aquifer classified as a major aquifer system is the most suited for UGPHES application although other important factors including the head height will also need to be considered.

South Africa has developed three aquifer maps namely aquifer classification, aquifer vulnerability and aquifer susceptibility to assist with the Reconstruction and Development Programme (RDP) in South Africa of which the role of groundwater resources is of high importance [95]. The aquifer classification map in Appendix A, indicates the aquifer classification system of South Africa. The aquifer vulnerability map in Appendix B indicates the tendency or likelihood of contamination of the aquifer, while the aquifer susceptibility map in Appendix C includes both the aquifer vulnerability and aquifer classification, while also indicating the relative ease with which a groundwater body can be potentially contaminated.

The South African aquifers are classified as tabulated below:

Table 4-1 – Aquifer system management classification [95]

Aquifer Type	Description
Sole Source Aquifer System	An aquifer for which there is no available alternative source and which is used to supply 50% or more of domestic water for a given area.
Major Aquifer System	Able to support large abstractions with high water quality. Highly permeable formations with probable presence of fracturing.
Minor Aquifer System	Variable water quality with limited extent. Potentially fractured rocks with formations of variable permeability.
Non-Aquifer System	Negligible permeability regarded as not containing groundwater that can be in exploited. Water quality may not be good enough for use.

Aquifer Type	Description
Special Aquifer System	Classified as special following due process by the Ministry of Water Affairs.

The maps indicate an abundance of aquifer systems in South Africa with certain potential to develop selected aquifer systems for UGPHES schemes. These selected aquifer systems are discussed further in an effort to identify key knowledge gaps and to ascertain the extent and suitability of the aquifers for the implementation of UGPHES schemes.

4.1.1 The South African Transvaal aquifer (SATVLA)

The SATVLA is one of the world's largest subterranean sedimentary aquifers with an area approximated from the Geosciences map of 500 km by 250 km and incorporating the area from Springs and Brakapan east of Johannesburg; to Lenasia south of the city; Zuurbekom, Carltonville and Magaliesberg on the West Rand; Kuruman in the Northern Cape and even as far as parts of Botswana as shown in Figure 4-8 [96, 97].

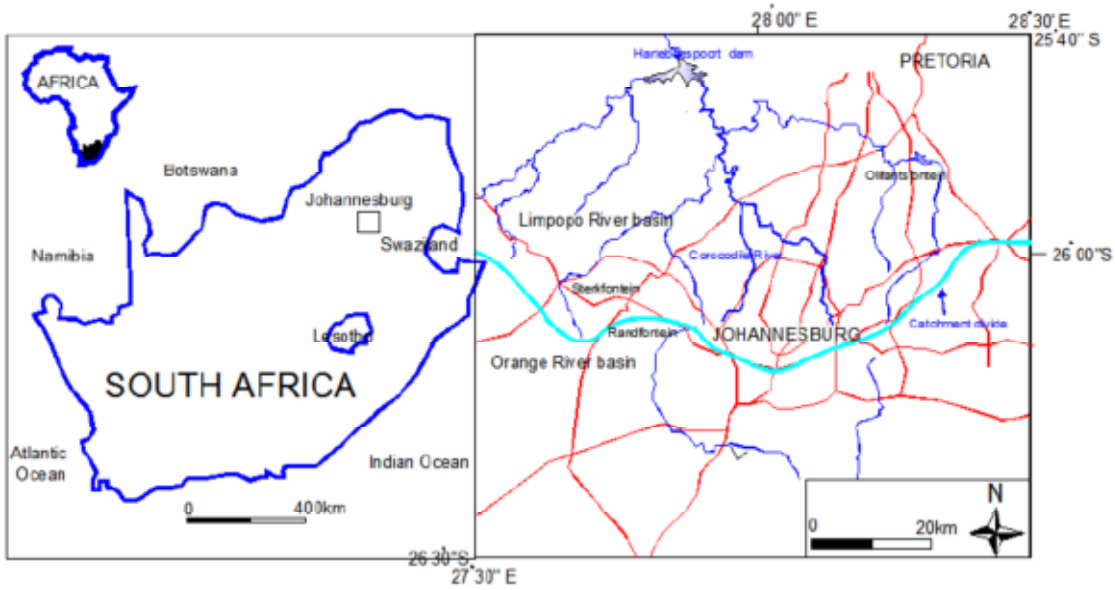

Figure 4-8 – Location map of the SATVLA area, Johannesburg at the north central part of the country (east-west solid line is water divide between Limpopo and Orange Rivers, blue lines represent streams and red lines represent roads) [96]

The area also includes the Bushveld Igneous Complex (BIC) shown in Figure 4-9 which is the world's largest known layered intrusion with an estimated area of 182,000 km^2 and hosts many billions of Terra litres of subterranean groundwater [97].

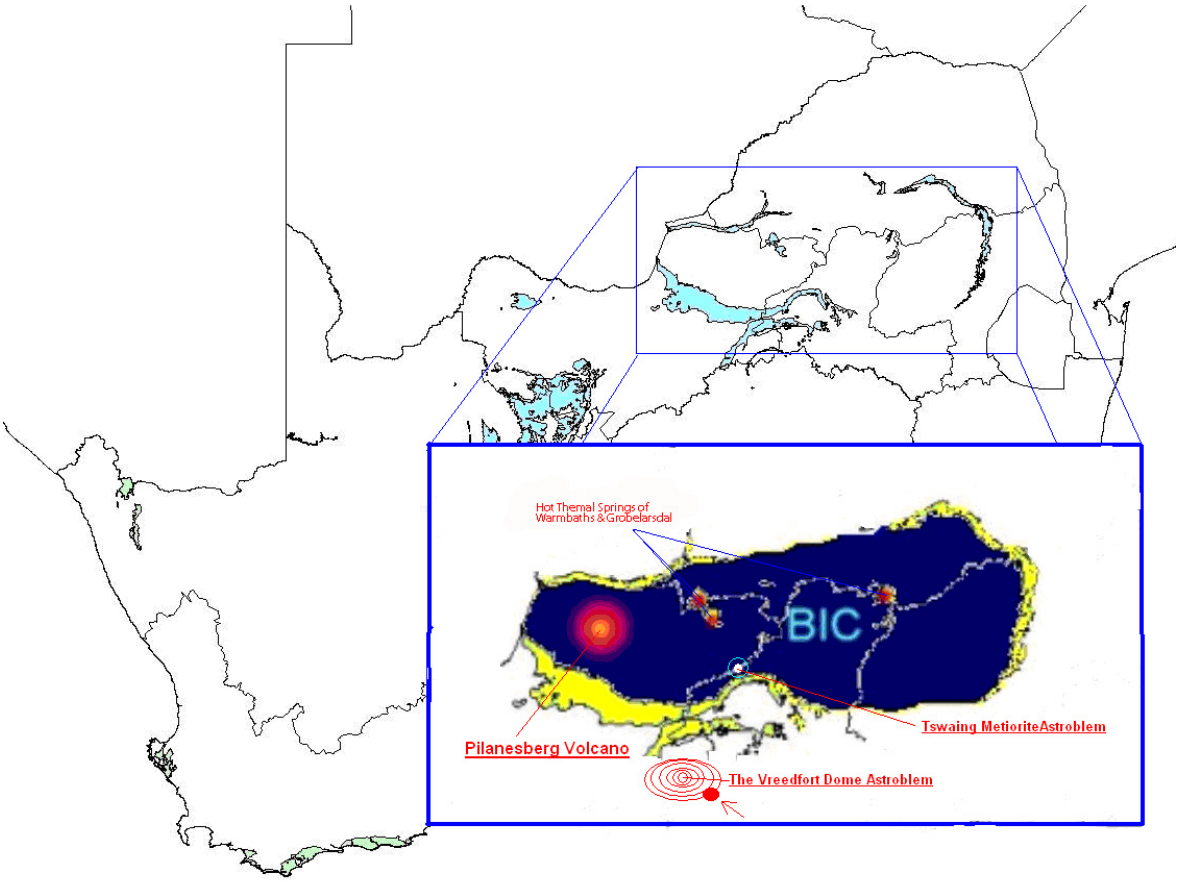

Figure 4-9 – Location map of the Bushveld Igneous Complex – [97]

The mean annual rainfall in the SATVLA area is between 600 to 700 mm/year [98] and is an extremely important contribution to the groundwater recharge. The dolomitic aquifers have been identified as highly productive aquifers in the region [99, 100]. Mining in the area pumped out 110 ML/day of groundwater until 2008 [101] which has not affected the shallow groundwater. Recharge of the shallow aquifer is increased considerably due to surface discharge of pumped water to dams, reservoirs and local streams [102].

The SATVLA area holds much promise for the development of UGPHES schemes from an aquifer vastness, availability of groundwater and groundwater recharge perspective.

Further investigations will have to be carried out to ascertain depth to groundwater related to the head of the UGPHES scheme which is a vitally important parameter in determining the power output.

4.1.2 The Karoo aquifer system

The main Karoo basin shown in Figure 4-10 covers an area of approximately 500,000 km^2 [103]. The upper shallow aquifer system (less than 300 m deep) of the Karoo is relatively well understood due to detailed research over the years and groundwater exploration while deeper formations (greater than 300 m to greater than 4,000 m deep) and associated groundwater occurrences are relatively unknown. The occurrence of a continuous aquiferous zone from the shallow aquifer zone to the deep formations is considered highly unlikely [104].

The existence of undetected deep aquifers is a strong possibility which can only be confirmed by exploration drilling. Deep (up to 4,692 m) exploration drilling in the 1960s and 1970s did indicate isolated occurrences of deep, saline groundwater in the Karoo formations and fresher underground water from the underlying Witteberg Group [105]. The Karoo area has only two known hot springs that are estimated to be more than a 1,000 m deep [26].

The key knowledge gaps for the Karoo aquifer system is the presence or otherwise of deep aquifers, the hydraulic interconnectivity between the shallow aquifer and deeper formations, and the existence of upward migration of deep groundwater [104].

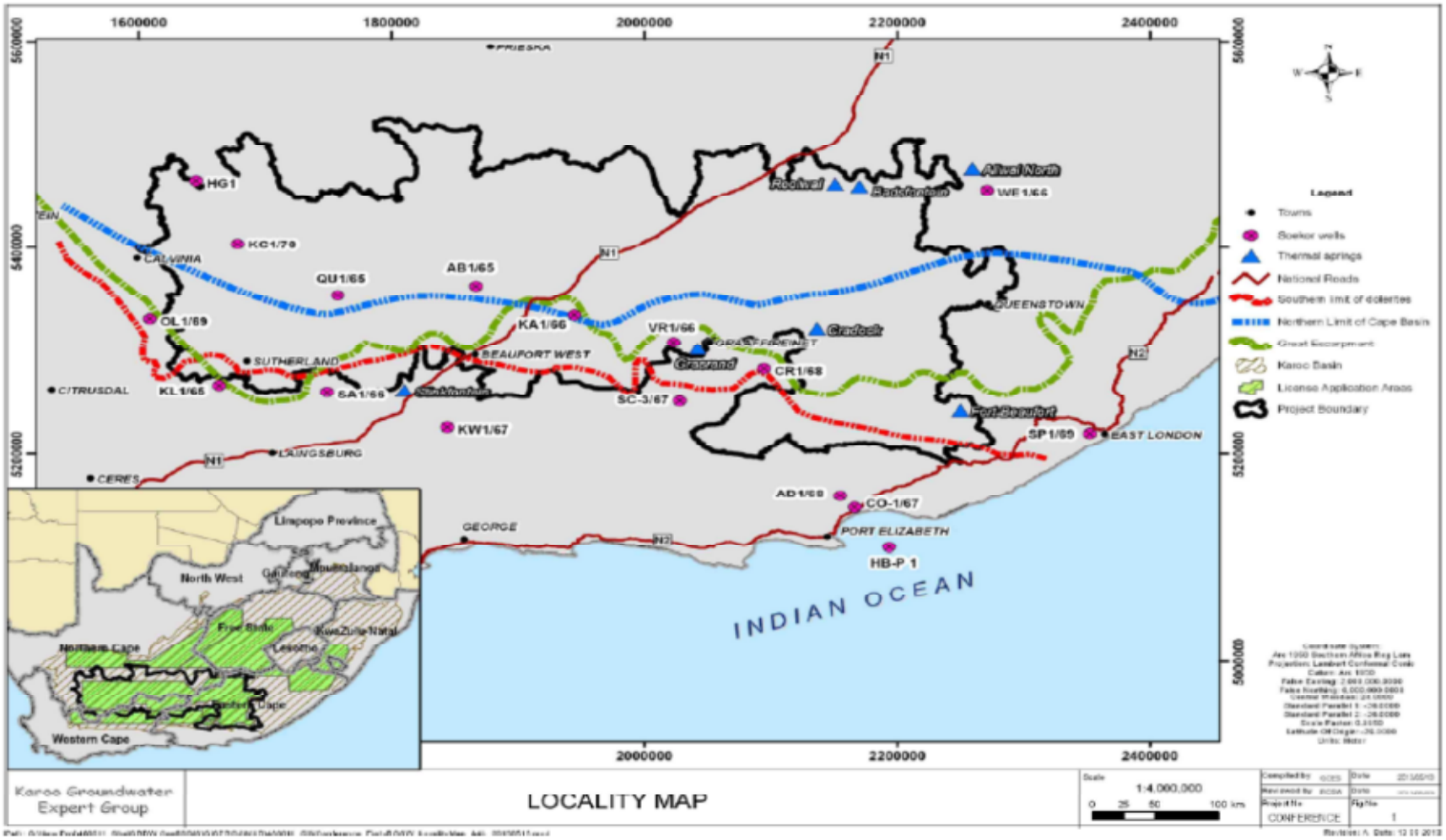

Figure 4-10 – The Karoo aquifer system and other key regional features [104]

4.2 Aquifer under seabed

Deep Water Research (DWR) which is a marine research company from Cape Town in South Africa, has identified the possibility of fresh water aquifers occurring in significant volumes off the coast of South Africa, more specifically approximately 60 km off Port Elizabeth which they claim could be very long term and consistent. Years of oil and gas exploration in the area revealed the possible existence of fresh water aquifers at least a kilometer beneath the seabed where a potentially abundant supply of fresh water was intersected by an exploration well off Port Elizabeth [106]. DWR has reached an agreement with oil and water exploration and sea spring water companies, to explore sites on the south, east and west coasts of South Africa including Namibia for the existence of aquifers under the seabed.

While this looks very promising from a water supply perspective for potable water and human consumption, the adaptation of an onshore aquifer system for use as a UGPHES scheme will surely be challenging if at all possible. This is an area that will surely require future extensive research from a technical, financial and viability perspective.

4.2 Aquifers in Namibia

The Cuvelai-Etosha Basin (CEB) in central-northern Namibia, represents the largest aquifer system in Namibia known as the Ohangwena II that extends into Southern Angola covering an area of approximately 100,000 km^2. It is part of the much larger Kalahari basin which covers parts of Angola, Namibia, Zambia, Botswana and South Africa and is estimated to be able to supply the north of Namibia for 400 years at current rates of consumption [107, 9]. The Ohangwena II aquifer however, is still in the process of being investigated in terms of its sustainable capacity as well as the sustainable management of the transboundary resource. A project known as Groundwater Management in the North of Namibia (GMNN), is currently underway that will ultimately provide the relevant information and procedures required towards sustainable management and utilization of the aquifer [108].

The CEB which is the most densely populated area in Namibia and hosting approximately half the country's population, relies on an inefficient open canal and pipeline network from Angola to provide drinking water supply for most of the population in the CEB. There is no

doubting the potential of such a vast aquifer to be used for UGPHES scheme/s, however utilizing the Ohangwena II vast aquifer for anything other than a sustainable resource for human consumption and other basic social needs will certainly be a challenge in itself considering the fact that Namibia is the most arid African nation south of the Sahara [107]. Appendix D shows a map of groundwater and aquifers in Namibia.

Namibia's electrical generating capacity is currently severely constrained. This is due in part to the fact that South Africa supplies nearly half of Namibia's electricity [109]. Namibia is currently actively embarking on ways to increase the electricity generation capacity in the country through the investigation of solar photovoltaic, wind, hydro and gas technologies. However, utilizing the Ohangwena II vast aquifer for a UGPHES scheme can benefit both Namibia and South Africa in the long term. The GMNN project will provide important technical details which can be used to further investigate the aquifer's suitability for implementation of a UGPHES scheme from a technical, economic and political perspective.

4.3 Transboundary aquifers shared by South Africa

Transboundary groundwater or shared aquifer resources refers to a volume of groundwater shared between two or more countries. Approximately 5,116 km of land border and seven aquifers is shared between South Africa and Namibia, Botswana, Zimbabwe, Mozambique, Swaziland and Lesotho as shown in Figure 4-11 [2]. The seven transboundary aquifers shared with South Africa have been identified for further investigation with only one of the seven consisting of only shallow and local aquifers [110].

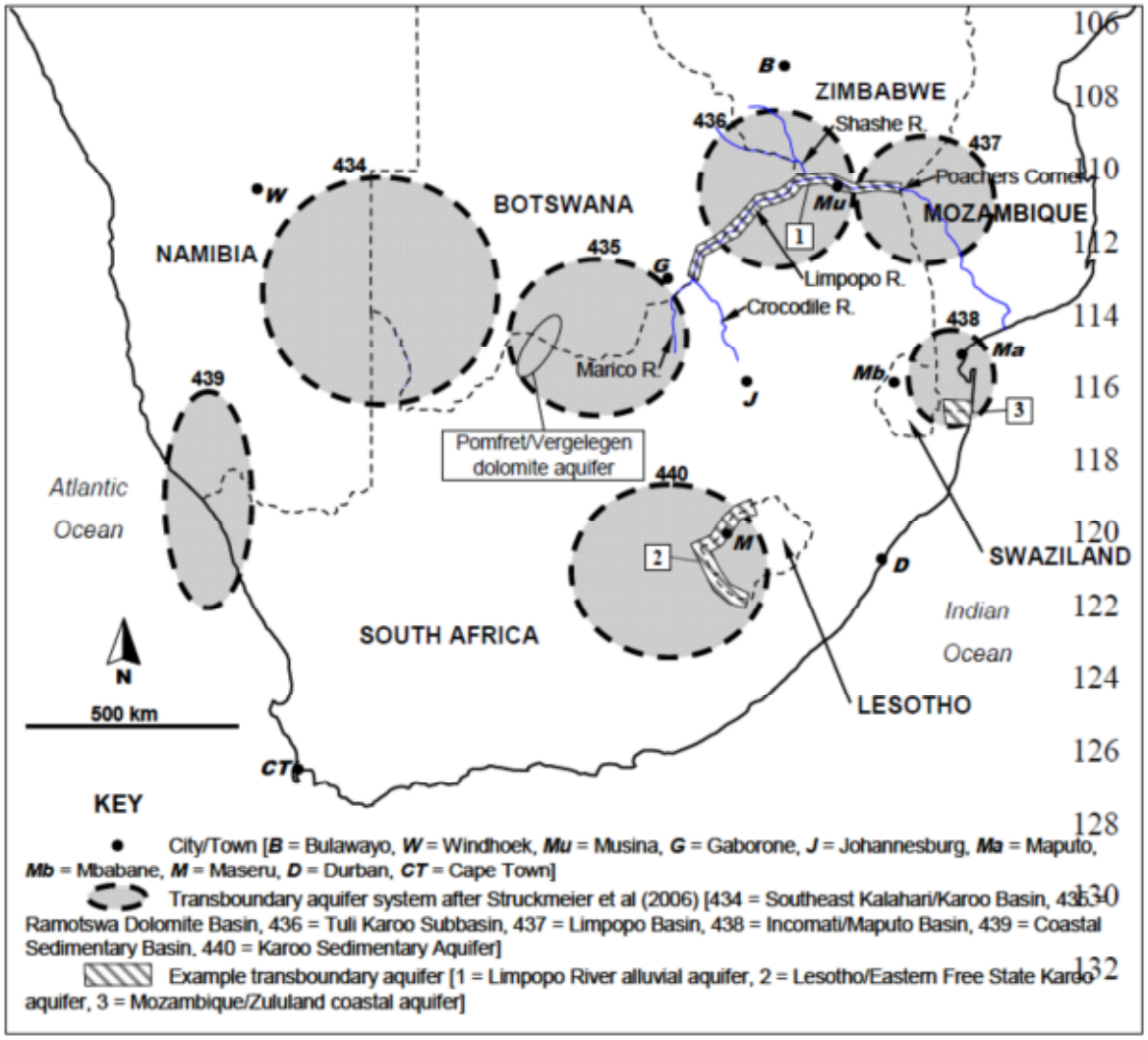

Figure 4-11 – Map of seven transboundary aquifer systems shared with South Africa [110]

Whilst this is encouraging from an electrical perspective through the development of UGPHES schemes and cross boundary wheeling of electricity, the actual management of transboundary groundwater may be a challenge. Further consideration needs to be given to the nature of the aquifer itself in terms of its hydraulic properties which includes transmissivity.

4.4.1 Limpopo river alluvial aquifer

The northern border between Botswana, Mozambique, Zimbabwe and South Africa is created by the Limpopo River as shown in Figure 4-11. The irregular adjoining floodplain

resulting from unconsolidated alluvial deposits that fill the river channel constitutes an international transboundary aquifer [2, 111]. The aquifer is currently tapped by using wellpoint systems, hand-dug wells, infiltration galleries and boreholes generally located on the river bank [112]. The town of Musina meets its municipal water demand by tapping off the Limpopo river through the use of boreholes and wellpoints while agricultural use by neighboring countries from this aquifer is negligible. Resource-poor farmers consider this aquifer as a valuable source of water that allows during dry periods for meeting and sustaining irrigation demands [2].

It must be noted that there is no evidence of the potential of this aquifer being fully explored. Deeper exploratory wells need to be drilled in an effort to understand the full extent of the aquifer and its potential to be adapted for use in a UGPHES scheme.

4.4.2 Lesotho/Eastern Free State Karoo aquifer

The boundaries between western Lesotho and south-eastern South Africa are created by the Caledon, Senqu, Mohokare/Clarens and Makhaleng rivers. The aquifer characteristics for this area comprise of the Burgersdorp Formation, Molteno Formation and the Elliot Formation [2].

The Burgersdorp Formation is a semi-confined to confined aquifer able to support borehole yields <0.5 l/s and with a mean transmissivity of 20 m^2/d [113, 105]. Many boreholes have been dug in this formation and used for the supply of water to small rural communities and farms [2].

The Molteno Formation is classified as a semi-confined aquifer with an average transmissivity of 20 m^2/d and is regarded as the best aquifer in this region. The borehole yields from the Molteno Formation are >3 l/s while there is also spring discharges as high as 0.5l/s [113, 105].

The Elliot Formation is an aquifer that is classified as poor due to its compact nature. The underlying Molteno Formation and aquifer are often in hydraulic continuity. The borehole yields are only 0.9 l/s and transmissivity is 5 m^2/d [113, 105].

The low borehole yields and low transmissivities of the transboundary aquifers between Lesotho and South Africa makes this area unfavorable for the application of UGPHES technology. It must be noted as with the Limpopo River Alluvial Aquifer, that there is no evidence of the potential of this aquifer being fully explored with the drilling of deeper exploratory wells [2]. Deeper drilling could yield aquifers with improved transmissivities and well yields suitable for implementation in a UGPHES scheme.

4.4.3 Mozambique/Zululand Coastal aquifer

The Zululand coastal plain extends approximately 250 km south of the Mozambique and South Africa border along the northeast coast of South Africa, and approximately 1,000 km north towards and into Mozambique. Groundwater recharge figures for this area ranges between 5% and 18% across the plain [114]. Land use for this area which is sparsely populated, is limited to subsistence farming, nature conservation, irrigation farming using surface water and limited commercial forestry. The South African side of the boundary has a confirmed north-south groundwater divide which continues north towards and into Mozambique with the flow separated towards the coast (east) and the Pongola River (west) [2].

A primary aquifer with shallow groundwater levels underlies the entire plain giving rise to fresh water lakes which are used to support the water requirements of the majority of the local population. The aquifer capacity is estimated to be able to support a population >500,000 with the Uloa Formation being the most productive aquifer with transmissivity >1,000 m^2/d and borehole yields up to 30 l/s [2]. Limited information is available for the aquifer on the Mozambique side of the border however it is expected to be similar to that on the South African side [2].

It is envisaged that the demand for groundwater from this aquifer is unlikely to be significantly expanded in the future with little to no risk of competition for water between South Africa and Mozambique thereby negatively impacting the available water resources [110].

The vastness of this aquifer and excellent transmissivity presents a very promising opportunity for the development of a UGPHES scheme that could greatly contribute towards the dire need for generating capacity in South Africa. There are however many

parameters that will first need to be investigated to ascertain the viability of such a scheme in this area. One such parameter is the head height which is directly proportional to the power output. Due to the shallow groundwater levels, this could prove to be an obstacle.

4.4 Cost estimate of an aquifer UGPHES system

There is no existing installation of an aquifer UGPHES system hence the available associated costs are only an estimation. A cost estimation has however been done for a relatively small scale aquifer UGPHES system rated at 50 kW and providing 300 kWh of energy, to be implemented for use in an irrigation scheme. The cost estimation was done for two different sites each with existing wells, however the second site requires well modifications. The cost estimate was performed in 2001 hence a 15% escalation per annum is added in an effort to align the cost with current economies of scale. The cost for site1 is estimated at R40,815,077 and for site2 R46,652,534 [3]. It is clear that the costs are dependent on site characteristics which include the availability of a surface reservoir, the amount of possible well modification that may be required, transmissivity and depth to water [3].

CHAPTER FIVE

UGPHES SYSTEM USING EXISTING INFRASTRUCTURE

The ever increasing demand for energy storage coupled with the pressures of environmental concerns due to the required urban or suburban space development, has led to the use of subsurface space for the large scale storage of energy in the form of CAES and UGPHES technologies. These technologies which require the excavation of subsurface rock to depths of up to 1,500 m [80], are being developed in conjunction with the development of underground excavation technology which makes the use of subsurface space an attractive option for energy storage. A further consideration for subsurface space is the use of existing infrastructure in the form of abandoned mines and quarries [80].

5.1 Viability of using abandoned mines and quarries for UGPHES

The use of abandoned mines or quarries for UGPHES has enormous potential. Water is pumped from the bottom of the abandoned mine up to the surface in the case of excess electrical capacity and allowed to flow back through a turbine to the bottom of the mine when electricity is needed. There are numerous advantages associated with the use of abandoned mines or quarries [14]:

- Multiple extra sites for the installation of new energy storage facilities due to the vast number of abandoned mines and quarries;
- Faster and easier licensing procedures due to the mandatory recultivation process for the abandoned mines and quarries;
- Fewer environmental concerns due to already existing structures and hardly any intrusion to the landscape;
- Lower construction costs due to existing structures for the installation of at least the lower reservoir;
- Already existing grid connection points at high voltage level.

5.2 Challenges and possible solutions for using abandoned mines and quarries for UGPHES

While the numerous advantages of using abandoned mines and quarries are attractive, there are challenges and technical considerations including questions around the storage reservoirs, head, amount of stored energy, equipment sizing, feasibility of mining engineering, technical feasibility of the construction and ultimately the economic viability, which need to be considered for each unique situation of an abandoned mine or quarry [115]. The required size of the storage reservoirs is also of vital importance as it depends on the expected operation of the UGPHES system with many factors such as load profiles, operating policy, generation mix and supply-demand-balance having an effect on the required reservoir size [116].

5.3 Upper reservoir

The upper reservoir of a UGPHES scheme can be established on-surface where in the case of an abandoned mine, the area of the former mine which is potentially large may be used [115]. The establishing of the on-surface reservoir on a former mine may be realized without too much conflict from close settlement areas and environmentalists as it will contribute significantly to the rehabilitation of the former mining site which is currently a major issue in the South African mining industry [117, 118].

5.4 Lower reservoir

The use of existing cavities is dependent on the mining technique that was used during mining activities. In the case of coal mines, there are three global coal mining methods that are used namely Bord/Pillar, Longwall and Opencast [119].

The Bord/Pillar method shown in Figure 5-1 is the most important method of coal extraction in South Africa and is a form of mining whereby only a portion of the coal is extracted leaving behind the remaining coal that act as pillars to support the overlying rocks [120].

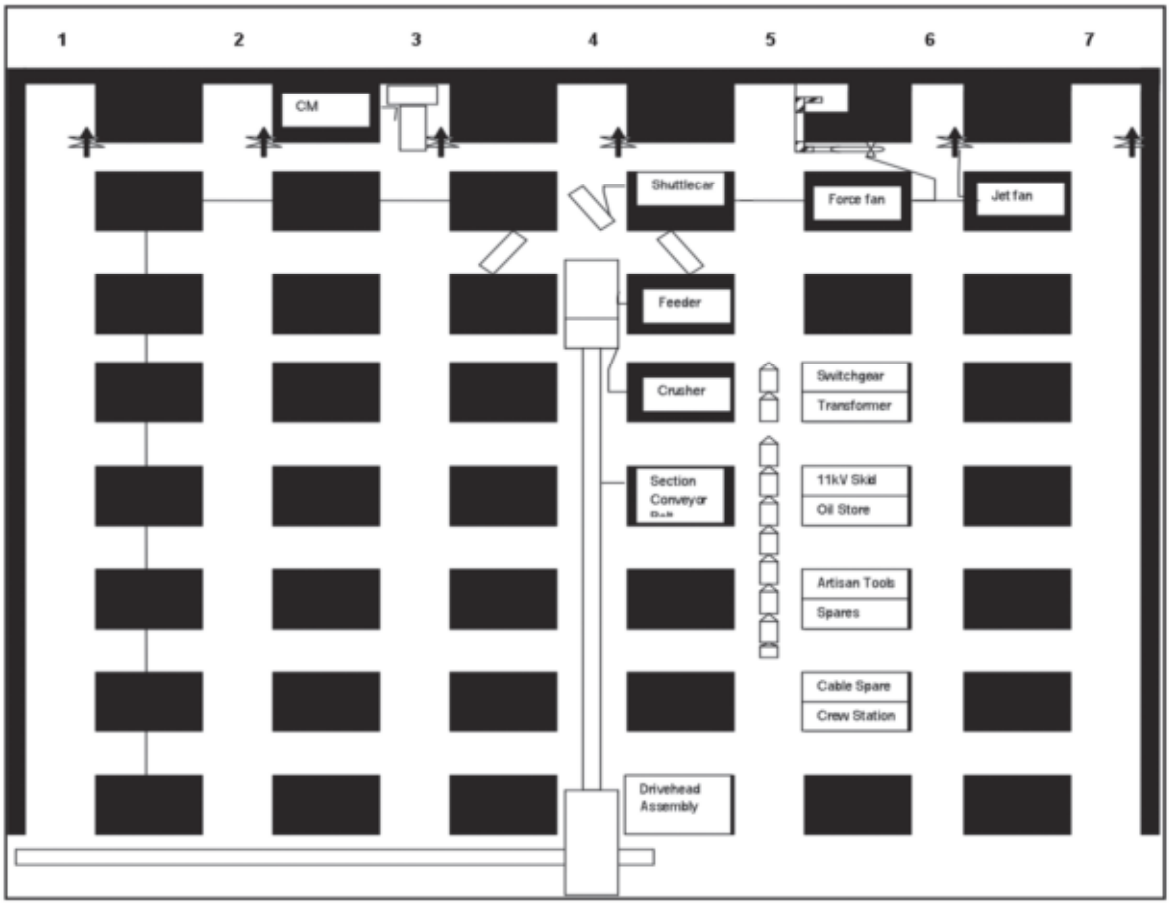

Figure 5-1 – Bord and pillar section plan view with associated equipment [121]

The Longwall method allows all the coal to be completely removed thereby allowing the roof of the mine to collapse into the void. It also creates additional void spaces which increases both inflow and seepage [119]. The method of Opencast mining allows the scraping and stockpiling of the soil cover. The rocks overlying the coal seam are blasted and removed thereby allowing the coal to be extracted. The broken rock is returned to the pit followed by landscaping of the site, returning of the soil and planting of grass. Groundwater aquifers are completely destroyed by Opencast mining thereby resulting in a single, massive aquifer in the mine void [119]. It is evident that the only coal mining technique that allows the original mine cavern to be reused is the Bord and Pillar method, although the cavern integrity would have to be thoroughly investigated to ensure adequate reinforcement and sealing.

The Longwall or Opencast mining method requires additional caverns to be excavated, using existing drifts or digging of new drifts. Drift grids which may be partly used after abandonment of mining operations can be quite extensive resulting in a potentially large storage volume [115]. During mining operations the grids are developed to various degrees and effort with the important segments of the grid secured to the highest degree of stiffness by cladding the walls with concrete and rib-shaped steel girders to carry the rock pressure above the tunnel to ensure the drift remains intact for a long period of time. The drift grid for each abandoned mine has to be investigated to ascertain the amount of drift kilometers there are in pits close to the water and to ensure a sufficient and steady downward slope to safeguard backflow of the stored water in pumping operation. While individual drift sections may be reused, new drifts will also have to be constructed [115].

5.5 Head and energy quantity

The head height of the abandoned mine is of vital importance as it contributes directly to the power output of a UGPHES scheme. The head height is also important for the selection of the pump and turbine combination with the Pelton turbine preferred to the Francis turbine for heads of more than 700 m [115]. The higher pressure of the Pelton turbine resulting from increasing heads may require slight modifications whereby the higher delivery heights have to be realized in several stages by using intermediate reservoirs. The pumps are therefore not seen as a limiting factor to the maximum possible head The head and water mass moved determine the amount of energy stored [115]. Table 5-1 shows the resulting energy capacity based on possible heads in relation to different masses of water. The gravity constant used is 9.81 m/s^2 and the turbine efficiency η = 95%.

Table 5-1 – Storage capacity in MWh for different heads and water masses [115]

Head [m]	**Water Mass [Mt]**					
	0.1	0.25	0.5	0.75	1	1.5
100	25.9	64.7	129.4	194.2	258.9	388.3

Head [m]	Water Mass [Mt]					
250	64.7	161.8	323.6	485.4	647.2	970.8
500	129.4	323.6	647.2	970.8	1294.4	1941.6
750	194.2	485.4	970.8	1456.2	1941.6	2912.3
1000	258.9	647.2	1294.4	1941.6	2588.8	3883.1
1250	323.6	809.0	1618.0	2427.0	3235.9	4853.9

It is evident that the water mass and head are directly proportional to the storage capacity. These are vital parameters when considering the use of an abandoned mine or quarry for a UGPHES scheme. Associated costs in achieving the storage capacity for each unique case of an abandoned mine or quarry will have to be evaluated to understand the viability of pursuing such an option.

5.6 Feasibility of mining engineering

Severe subsurface dangers associated with spontaneous combustion in the case of abandoned coal mines, droppings and mine collapse have mostly become controllable due to technical progress and improved security measures. However, in the case of an abandoned mine to be used for an UGPHES scheme, new challenges associated with slope, tunnel water tightness and stability have been brought to the fore [115].

A continuous downward slope to the deepest point in the cavern is required by the drift to be flooded to ensure water is collected before it is pumped back up to the surface. Existing drifts in abandoned mines previously used to collect leakage water will have to be individually investigated to ascertain the inclination of the drift and the suitability in line with the application for a UGPHES scheme. In the event that the inclination of the existing drifts do not suffice, new drifts will have to be constructed in an effort to realize the required slope [115].

Abandoned mines are susceptible to mine water ingress into the empty lower reservoir (cavern). This water needs to be pumped to the surface as it reduces the available pumping volume and ultimately reduces the plant efficiency with the added danger of infiltration of sediment into the system which poses a danger to the plant. The full development of drifts is a form of efficient counteraction as it minimizes the amount of intruding mine water and sediment [115]. Adequate drainage and a combination of cementitious and chemical grout will allow the construction of a grout curtain capable of cutting off a large percentage of mine water ingress [80].

The existing drift grids of abandoned mines are secured by long-wall supports which do not provide long term stability while other consideration of rock stresses which affect the cavern stability include gravitationally induced stresses, tectonic stresses and residual locked in stresses [80]. Occasional repair work will be required but this is considered technically and economically manageable [115].

5.7 Assembly and structure

The pressure pipes between the upper and lower reservoir are important components for a UGPHES plant with the added challenge of determining whether the existing drifts of abandoned mines are able to accommodate the pressure pipes. The design of pressure pits and adits is highly complex as it takes into account the inner pressure of the surrounded stones, flow characteristics, diameter of the pressure pipes to reduce frictional losses, choice of material and many other considerations [115].

Consideration needs to be given for the installation of the pumps and turbines to assess whether they are able to be assembled below ground and transport in the sub-surface machine and generator house. The disassembling of bulky components with reassembly underground is an option for consideration however this will result in additional costs [115].

5.8 Cost of electricity generation for a UGPHES scheme

The total investment cost of a UGPHES installation is comprised of the initial installation cost IC_{ss} together with the operating and maintenance costs [122, 123]. IC_{ss} can be expressed as a function of two coefficients c_e (R/kWh) and c_p (R/kW) where c_e is related to

the type of system and storage capacity and c_p refers to the type of the storage system and the hydro-turbine's nominal power. The following equation is based on the assumption that the UGPHES system has efficiency η=100% [124, 125]:

$$IC_{ss} = c_e E_{ss} + c_p N_{ss} = E_h \left[\frac{c_e d_0 \varepsilon}{\eta_{ss} DOD_L} + \frac{c_p \zeta}{CF \eta_p} \frac{1}{1+SF} \right] \qquad (5.1)$$

Where,

E_{ss} is the energy storage capacity of the UGPHES system (kWh)

N_{ss} is the nominal output power of the UGPHES system (kWh)

E_h is the electrical network average hourly load per annum (kW)

d_0 is the energy autonomy period of the UGPHES system (h)

ε is the energy demand ratio covered directly by the UGPHES system

η_{ss} is the energy transformation efficiency of the UGPHES system (round-trip)

DOD_L is the maximum permitted depth of discharge of the UGPHES system

ζ is the peak load demand ratio covered by the UGPHES system

CF is the electrical network capacity factor

η_p is the power efficiency of the UGPHES system

SF is the electrical network safety factor

The input energy cost EC_{ss} for a time period of n years can be expressed as [125]:

$$EC_{ss} = \frac{E_{stor}}{\eta_{ss}} c_1 \sum_{j=1}^{j=n} \left(\frac{(1+x_1)}{(1+i)} \right)^j$$

$$= \varepsilon \frac{E_{tot}}{\eta_{ss}} c_1 \sum_{j=1}^{j=n} \left(\frac{(1+x_1)}{(1+i)} \right)^j$$

$$= \varepsilon \frac{E_{tot}}{\eta_{ss}} c_1 X_1 \qquad (5.2)$$

Where,

E_{tot} is the local electricity network annual energy demand (kWh)

c_1 is the specific input energy cost (R/kWh)

i is the capital cost of the local market

x_1 is the mean annual escalation rate of the input energy price

The maintenance and operation cost can be separated into the fixed maintenance cost FC_{ss} and the variable maintenance cost $VC_{ss.}$ FC_{ss} is therefore represented as [125]:

$$FC_{ss} = IC_{ss} m \sum_{j=1}^{j=n} \left(\frac{1+x_2}{1+i} \right)^j = IC_{ss} m X_2 \qquad (5.3)$$

Where,

m is the fraction of annual maintenance and operation cost to the total initial investment

x_2 is the mean annual maintenance and operation cost inflation rate

Including a fuel input for the pumping cycle of a UGPHES scheme from the lower reservoir to the upper reservoir, equation (5.3) is rewritten as [125]:

$$FC_{ss} = IC_{ss} m \sum_{j=1}^{j=n} \left(\frac{1+x_2}{1+i} \right)^j + c_f(E_{stor}) \sum_{j=1}^{j=n} \left(\frac{1+x_3}{1+i} \right)^j$$

$$= IC_{ss} m X_2 + c_f(\varepsilon E_{tot}) X_3 \qquad (5.4)$$

Where,

c_f is the specific energy cost of fuel used (R/kWh)

x_3 is the mean annual escalation rate of fuel input price

The variable maintenance and operation costs is mainly associated with the replacement of major parts k_0 of the installation which have a shorter lifetime n_k than the installation as a whole n_{ss} and can be expressed as [125]:

$$VC_{ss} = IC_{ss} \sum_{k=1}^{k=k_0} r_k \left\{ \sum_{l=0}^{l=l_k} \left(\frac{(1+g_k)(1-\rho_k)}{(1+i)} \right)^{ln_k} \right\} = IC_{ss} vc_{ss} \qquad (5.5)$$

Where,

r_k is the replacement cost coefficient for major parts to be replaced

l_k is the times of replacement for major parts being replaced

g_k is the mean annual change of cost for major parts to be replaced

ρ_k is the mean annual change of technological improvement for major components

n_k is the lifetime of energy storage system's major parts to be replaced

l_k may be expressed as [125]:

$$l_k = \left[\frac{n-1}{n_k} \right] \qquad (5.6)$$

The total cost C_{ss} related to the UGPHES installation and operation after n years may be estimated using the following equation [125]:

$$C_{ss} = IC_{ss}(1-\gamma) + EC_{ss} + FC_{ss} + VC_{ss}$$

$$C_{ss} = IC_{ss}\{(1-\gamma) + mX_2 + vc_{ss}\} + (\varepsilon E_{tot})\left\{ \frac{c_1}{\eta_{ss}} X_1 + c_f X_3 \right\} - \frac{Y_n}{(1+i)^n} \qquad (5.7)$$

Where,

γ is the ratio of any possible total investment cost subsidy

Y_n is the residual value of the UGPHES system (R)

Defining $\overline{v}_n$ as the non-dimensional value of Y_n [125]:

$$\overline{v}_n = \frac{Y_n / IC_{ss}}{(1+i)^n} \qquad (5.8)$$

The electricity generation cost (R/kWh) of the UGPHES system is given as [125]:

$$c_0 = \frac{C_{ss}}{E_{stor} \sum_{j=1}^{j=n} \left(\frac{1+x_4}{1+i}\right)^j} = \frac{C_{ss}}{\varepsilon E_{tot} X_4} \qquad (5.9)$$

Substituting equations (5.2), (5.4), (5.5), (5.7) and (5.8) into (5.9) [125]:

$$c_0 = \frac{IC_{ss}}{\varepsilon E_{tot}} \left(\frac{1-\gamma}{X_4} + m\frac{X_2}{X_4} + \frac{vc_{ss}}{X_4} - \frac{\overline{v}_n}{X_4} \right) + \frac{c_1}{\eta_{ss}} \frac{X_1}{X_4} + c_f \frac{X_3}{X_4} \qquad (5.10)$$

5.9 Cost assessment of UGPHES in an abandoned mine

The cost assessment discussed is for the use of abandoned coal mines for UGPHES in the Ruhr area of Germany. The costs are focused specifically on the energy storage costs as this relates to the amount of energy that can be stored in the conceivable tracks of the lower reservoir [115].

The realized head is an important factor in determining the costs as the storage capacity increases proportionately with the head while the costs rise slowly with increasing head [115, 13]. The costs of a greater pit drift which include pressure pipes and turbines able to withstand higher stresses with turbine assembly becoming more difficult with increasing depth, are deemed to be relatively small. Costs associated with having to extend tracks for the lower reservoir which include excavation and lining are not related to the head. Newly excavated and fully lined drifts are assumed at 150-300 kR/m [115]. The costs of the lower reservoir are dependent only on the extracted volume and are considered to be quite

substantial. The doubling of the storable amount of energy theoretically leads to a reduction in the specific costs by 50%. Benchmark values for the costs of the lower reservoir at a depth of 500 m is 3,405 R/kWh whereas for a depth of 1000 m this cost decreases to 1,695 R/kWh [115]. A graph with the unit cost shares for UGPHES in an abandoned mine with 1,000 m head is shown in Figure 5-2.

Other costs related to the construction of a UGPHES plant which include the cost of the plant components, extension of the upper reservoir or construction of subsurface caverns for machines and generators are quantifiable only in specific cases. For a rough cost estimate of these parameters, the costs for the construction of a conventional PHES plant can be used. Where the costs of the lower reservoir are not taken into consideration, the largest cost share of approximately 37% is attributed to the turbines, pumps, generators and transformers while roughly equal cost shares arise for the land, upper reservoir and engineering expenditures for planning and construction of the plant [115].

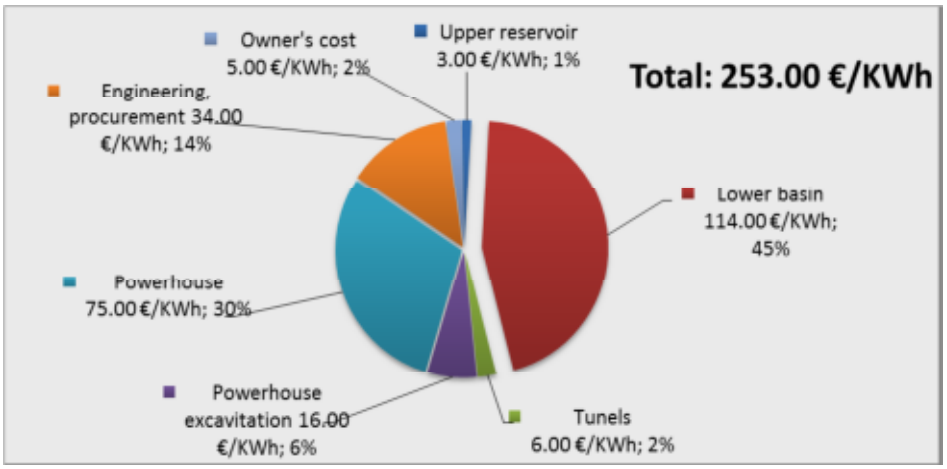

Figure 5-2 – Unit cost shares for UGPHES in an abandoned mine with 1,000 m head [115]

Assuming a head of 1,000 m, the following comparisons between the costs for a conventional PHES and a UGPHES using an abandoned mine can be assumed [115]:

- The upper reservoir costs are markedly lower for a UGPHES using an abandoned mine as fewer storage facilities are required to be constructed. In South Africa, rehabilitation of the mining site by the plant operator has become mandatory [117].

This is an opportunity for the low-cost construction of a lake or a reservoir independently of the UGPHES plant project.

- Modest real estate costs can be expected for the case of a UGPHES using an abandoned mine as the largest part of the UGPHES would be erected on the mine site or subsurface.
- With the construction of the lower reservoir in an abandoned mine currently not proven and tested, the planning and development costs are expected to contribute significantly to the overall costs thus rendering this aspect of the construction of a UGPHES in an abandoned mine more expensive than for a conventional PHES plant. This could however change in the future as the UGPHES technology in abandoned mines is developed further. The specific costs associated with the lower reservoir for an abandoned mine is assumed to be higher as compared to the conventional PHES. This is highly dependent on the condition of the existing cavern in terms of rock quality, location of portals, tunnels and other facility operations [80] and whether it is favorable for use as is or whether additional work will need to be done to allow it to be used for a UGPHES plant. The construction of a UGPHES plant with lower head will lead to higher specific costs as compared to a higher head as excavation costs will roughly remain the same while the storable amount of energy for a higher head will increase as shown in Figure 5-3.

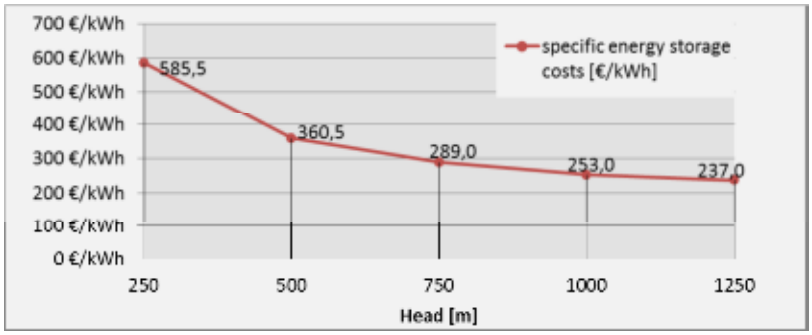

Figure 5-3 – Specific energy storage costs for different heads [115]

- The powerhouse costs which include the turbines, generators, pumps and transformers are assumed to cost more for the UGPHES plant. This can be attributed to the space saving disassembly and reassembly of components for the purposes of transportation subsurface.

- Considerably higher specific costs can be expected for the machine and generator cavern in the case of the UGPHES plant in an abandoned mine resulting from unfavorable conditions of the existing cavern. Where existing caverns can be used, the costs reduce accordingly.
- The construction costs for the pits and adits are assumed to be lower for the UGPHES in an abandoned mine as these can be reused with only minor additional development.

5.10 Abandoned mines in South Africa

The Department of Mineral Resources (DMR) of South Africa has identified approximately 6,000 abandoned and neglected mining sites which includes mine dumps across various parts of South Africa including the Northern Cape, Limpopo, Mpumalanga, Witwatersrand, Northern Namaqualand and Kwazulu-Natal [118]. Mine operators have previously abandoned mining operations with complete disregard for the management of the negative impacts on public health and safety and the environment. These include open shafts, unstable slopes on dumps and pits, collapse features, abandoned mine infrastructure, explosives, radioactivity, wind blown dust, water and soil contamination and in the case of coal mines, spontaneous combustion of coal and coal waste [118]. Another major concern associated with abandoned mines is the devastating impact on surface and groundwater resources. Mine-water challenges are not only at local mine level but also at regional level with over 10,000 km^2 of hydraulically interlinked coal mines and over 300 km of interlinked gold mines [126]. The DMR has put together a strategy to deal with the abandoned mines in an effort to rehabilitate the mines to a level where they can be used for other development activities where possible [117]. One such activity that needs to be explored is the use of the rehabilitated mines for implementation of UGPHES schemes.

Surface water refers to any place where the accumulation of surface water can occur and which is in direct contact or close to mine residue areas including unlined return water dams, open canals, storm water storage systems and natural and anthropic mine depressions [118]. In the case of the abandoned mines, this results in the surface water becoming heavily polluted with soluble heavy metals and chemical reactions leading to high salinity and acidity. This also results from water flowing from the mine dumps or decanting from underground by a process known as ground water rebound [127].

The dewatering of mine workings in underground or deep open pit mining often results in pollution which could result in the localized depression of the water table and subsequently a decrease in groundwater availability. Groundwater does in many cases recover close to its pre-mining levels, however the groundwater is polluted due to chemical reactions in the mined out areas [117]. A major concern regarding abandoned coal and gold mines is the formation of acid mine drainage (AMD) which after filling the underground mine voids, dissolves salts and mobilizes metals from mine workings and residue deposits, sometimes decant on to the surface resulting in the pollution of surface water bodies [128]. The groundwater pollution also results from the ingress of polluted surface water to the underground aquifers. It is estimated that AMD from neglected and abandoned gold mines in the Witwatersrand area could reach levels of 350 million litres per day thereby posing a threat to the fresh water supply from the Vaal River and Limpopo River watersheds [129]. In 2002, AMD from an abandoned mine in the Krugersdorp area began pouring out on to the surface with some of the 15 million litres of spillage per day flowing into a stream close to the Cradle of Humankind World Heritage Site. The AMD has already dissolved a 16,000 m^3 void in the calcium carbonate rocks outside the protected site and was finally responsible for a fish kill within the site [129].

The DMR has implemented an action plan to deal with the abandoned mines to remedy the impact on the pollution of both surface and groundwater resources by the dewatering of mine voids, dewatering and treatment of acid mine water, surface water diversion and passive water treatment which is the preferred option as it is more cost effective [130]. The rehabilitation method is dependent on the identified end land use as shown in Figure 5-4.

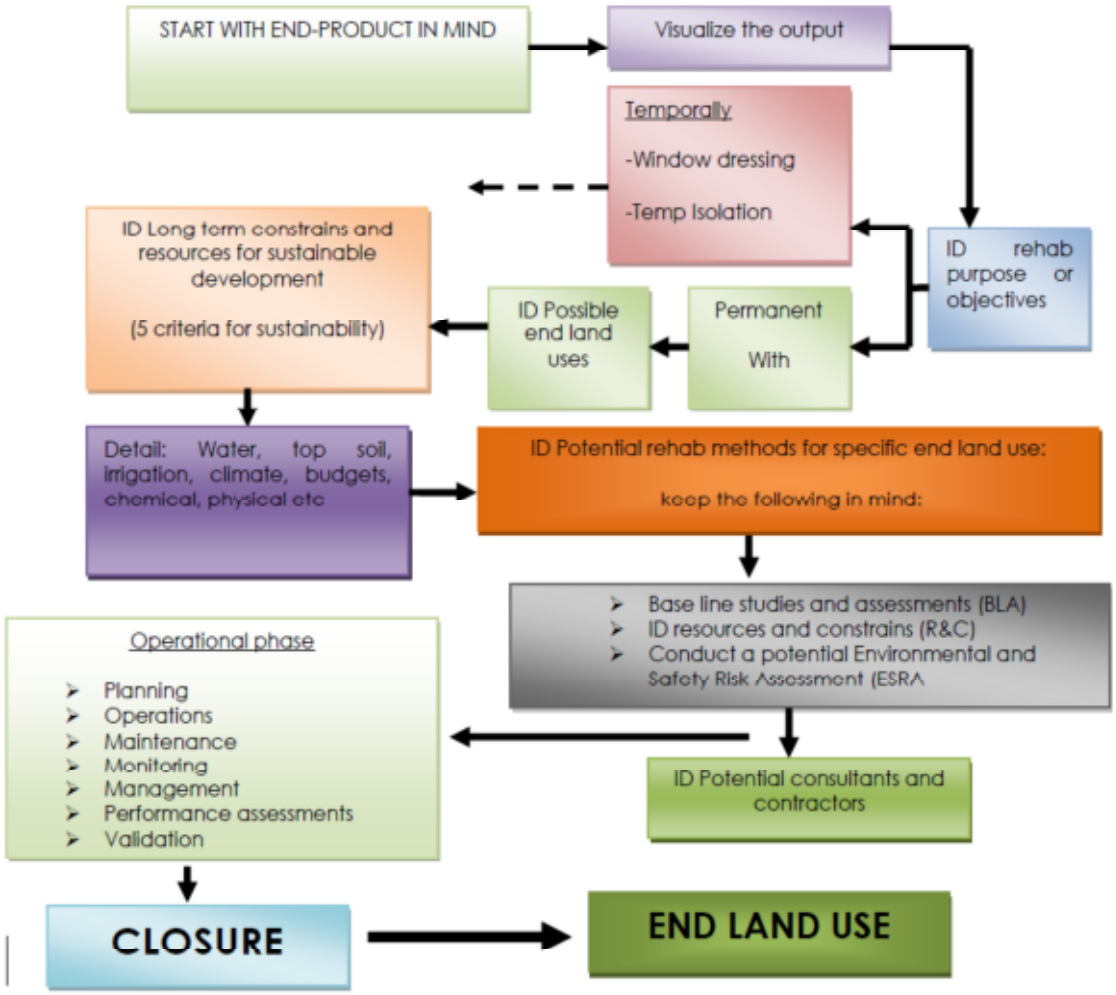

Figure 5-4 – South Africa's mine rehabilitation process [118]

The management of AMD associated with neglected and abandoned mines in South Africa is a major issue which will impact the development of UGPHES schemes due to the envisaged negative impacts of the polluted water on the UGPHES infrastructure especially with regards to the pump-turbine. The UGPHES technology will first have to be adopted as a viable energy storage option in South Africa and will require extensive research in to the technology. Further research will then be required to determine rehabilitation methodologies specifically for implementing UGPHES schemes as an End-Product at identified mine sites in South Africa.

5.11 Thermal extraction from mine water

While the flooding of abandoned mines is seen as a challenge, an interesting opportunity in the form of geothermal heating presents itself. Mine water from deep mines can potentially serve as a low grade geothermal source as shown in Figure 5-5, with the benefit being that it has a high heat capacity due to being intimately connected to the host rock thus providing good heat transfer as well as already decanting to the surface. Surface based heat pumps are also more cost-effective [131].

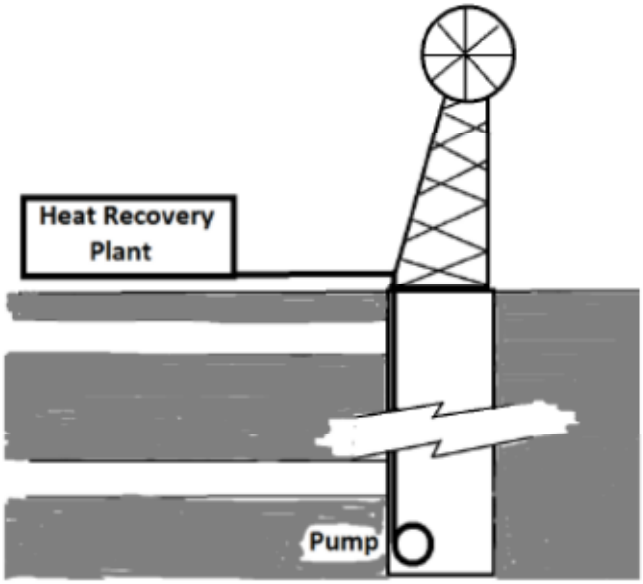

Figure 5-5 – Mine water heat extraction [131]

A single coal seam in Pennsylvania, West Virginia and Ohio discharges 380,000 L/min of mine water which is theoretically sufficient enough to heat and cool 20,000 homes [132]. The use of mine water for geothermal heat pump systems could reduce annual heating and cooling costs by 67% and 50% respectively over conventional methods [132].

5.12 Existing installations of UGPHES using abandoned mines or quarries

The Elmhurst Quarry Pumped Storage project as discussed in 3.10.4 is a development that will use an existing quarry and abandoned mine for a UGPHES scheme. The Mineville Pumped Storage Project (MPSP) has proposed the use of an underground mine located in

the Town of Moriah, New York. A draft license application has been made by the Moriah Hydro Corporation to the Federal Energy Regulatory Commission for the construction of a 260 MW UGPHES plant in the Old Bed, New Bed, Bonanza open pit and Harmony mines [133].

The existing mine cavities will house the upper and lower reservoirs with a concrete bulkhead separating and containing the upper reservoir within the mine. The upper reservoir will be formed underground between the existing +122 m and +305 m elevations of the mine with an approximate surface area of 50 acres and 732 acre-meter of volume. The lower reservoir will be formed between the existing -503 m and -320 m elevations of the mine with a surface area of approximately 50 acres and volume of 732 acre-meter. The vertical bored drop shafts will be 762 m long and 3 m in diameter [134].

The construction of the concrete powerhouse next to the mine approximately 625 m beneath the upper reservoir will be 21 m wide by 85 m long and 12 m high [134]. The project is proposing to use 20 pump-turbine/generator power trains each consisting of 5 reversible pump-turbines connected in series [133]. Each reversible pump-turbine will be directly coupled to a synchronous motor/generator rated at 2,600 kW and 3,450 hp in turbine mode and 2,790 hp in pump mode. The capacity of each parallel train will be 13,000 kW and a total installed capacity of 260,000 kW with all power trains operating in parallel [133].

The high and low pressure penstocks will be constructed from steel with a diameter of 4.5 m and embedded beneath the powerhouse floor. A new 115 kV substation will be constructed next to an existing 115 kV transmission line located a horizontal mile in proximity from the underground powerhouse [133].

5.13 UGPHES design for the abandoned Ohio limestone mine

The preliminary design for the proposed location of the powerhouse in the abandoned Ohio limestone mine UGPHES scheme provides insight into some of the design techniques for the development of a UGPHES scheme in an abandoned mine.

The abandoned Ohio limestone mine located approximately 671 m below the ground surface thus presenting the opportunity to develop a high head and with a volume of 9.6 million cubic meter was identified as an ideal location to be used for the implementation of a UGPHES system [135]. Figure 5-6 shows a vertical section of the mine containing strata and mining openings.

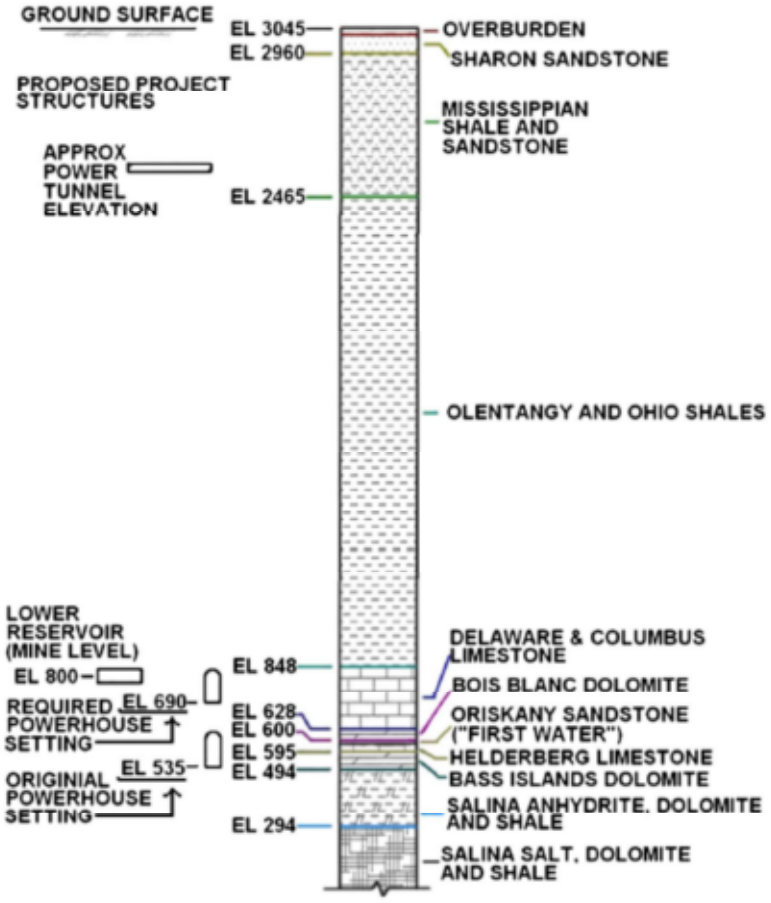

Figure 5-6 – A generalized stratigraphic section at the Ohio limestone mine [80]

The powerhouse was designed to be located 81 m below the bottom of the mine for the submergence of the pumps to avoid cavitation [80]. The proposed powerhouse location encountered brine water at high pressure which posed a problem. Two options were identified to mitigate this with the first option being to use a combination of grouting and drainage while the second option was to use pump-turbine equipment that did not require

such deep submergence. It was ultimately decided to avoid the brine water problem by raising the powerhouse sufficiently from the initially identified location [79].

Exploratory drilling was undertaken to ascertain the anticipated behavior of the mine due to further excavation as well as to ascertain the hydrogeology and and geology [80]. The two basic criteria that had to be met for the location of the powerhouse was to firstly ensure that the loading conditions emanating from the proposed excavations and the high pressure brine could be structurally stabilized. Secondly, the possibility of significant brine inflow had to be eliminated [79]. A number of failure mode analysis as shown in Figure 5-7, comprising of the finite element method (FEM), parallel FEM analysis, wedge and beam analyses and seepage analysis were performed to clearly establish the fluid flow conditions and rock stress in the rock strata for the safe location of the powerhouse [80].

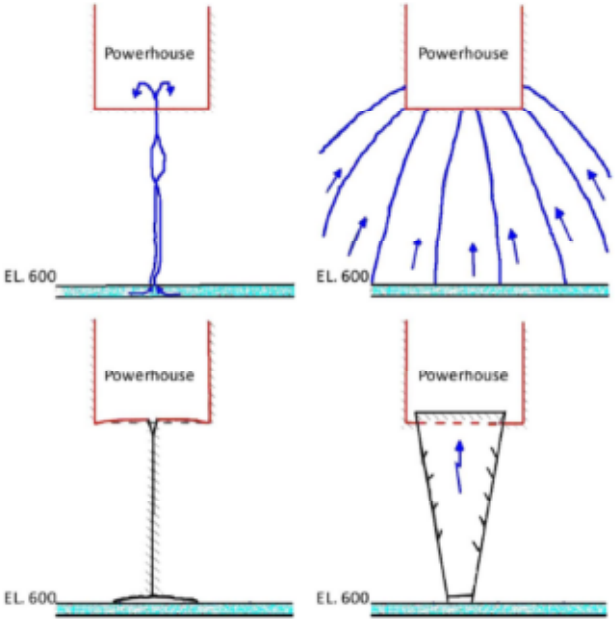

Figure 5-7 – Potential failure modes due to hydrofracture, excessive seepage, wedge failure and beam failure – clockwise from top [80]

The limit condition of the FEM analysis on the mine and powerhouse openings is for the highest stresses to be calculated in the mine at the point of failure. With the mine known to be stable it has a safety factor of one or greater. FEM analysis performed on the

powerhouse should show a powerhouse safety factor greater than that of the mine [79, 136].

The wedge analysis was performed to represent an extreme condition to assess the stability of a rock wedge formed by two inclined joints in the base of the powerhouse and a horizontal joint at the top of the Oriskany sandstone [80, 136]. The analysis showed that the powerhouse opening had to be lowered to within 12.2 m of the top of the Oriskany for wedge sliding to occur. The beam analysis was performed to determine the minimum depth of the rock below the powerhouse to prevent failure. The rock below the powerhouse was analyzed as a beam with the result showing that a beam thickness of 13.7 m would be sufficient to resist the loads imposed by the brine fluids at the Oriskany [79].

The seepage analysis was performed to ascertain the impact of the high pressure brine on potential seepage into the powerhouse. The calculated inflow was found to be 0.1 m^3/h which was regarded as negligible [79].

The above analysis showed that the setting of the powerhouse between the bottom of the powerhouse excavation and the top of the Oriskany stratum had to be at 27.4 m from a structural and seepage standpoint to be regarded as safe and stable with no risk of failure caused by the presence of fluids. It is interesting to note that this project did not go ahead for reasons other than the technical challenges [80].

CHAPTER 6

CONCLUSION

The bulk energy storage scheme known as Underground Pumped Hydroelectric Energy Storage (UGPHES) has been introduced and analyzed with an emphasis on its viability for implementation in South Africa to contribute to the currently constrained electricity supply. The use of aquifer systems and abandoned coal mines for the implementation of UGPHES systems has also been analyzed. Various design considerations which include the head of the installation, volume of the underground reservoir, structural integrity of abandoned mines, transmissivity of the aquifer system, water hammer, mound of injection and cone of depression, etc. are some of the critical factors that must be considered during system design as well as during scoping activities for the identification of suitable sites for the implementation of a UGPHES system.

A cost comparison with other bulk energy storage systems shows the UGPHES system to be very competitive especially in comparison with the conventional pumped hydroelectric energy storage. Using existing infrastructure in the form of abandoned mines for the lower reservoir, the mine quarry for the upper reservoir and existing wells, contribute to a reduction in capital costs. These costs however vary from site to site where considerable costs can be incurred should the abandoned mine need to be further excavated. South Africa has a large number of ownerless and derelict mines which can be considered for use in a UGPHES system. There is no doubting the potential of the abandoned mines considering the head, the storage volume, the use of the quarry as the upper reservoir and the abundance of groundwater. This will have a positive impact on the environment especially considering the problem of acid mine drainage (AMD).

The use of aquifers for UGPHES systems shows a lot of promise. South Africa alone has an abundance of groundwater which can be used for the implementation of UGPHES systems. Using transboundary aquifers also needs to be seriously considered as this will benefit both South Africa and the respective neighboring country as well as an overall contribution to the South African Power Pool (SAPP).

The UGPHES system certainly shows a lot potential, however this technology needs to be further investigated for implementation in South Africa. Future steps to be considered is

the identification of suitable pilot sites for both aquifers and abandoned mines, performing geological sampling tests, analyzing transmissivities, storativity values, field testing with a centrifugal pump/turbine to determine pump/turbine efficiencies and flow. The use of abandoned mines will also need to be included as part of South Africa's mine rehabilitation process.

REFERENCES

[1] Blyden, B.K., and Davidson, I.E., “Energizing Africa’s emerging economy,” Power and Energy Magazine, July-August 2005, Vol.3, Issue 4, pp.24-31, IEEE Power and Energy Society, ISSN:1540-7977, DOI:10.1109/MPAE.2005.1458227.

[2] Cobbing, J.E., Hobbs, P.J., Meyer, R., and Davies, J., “A critical overview of transboundary aquifers shared by South Africa,” Hydrogeology Journal, 2008, Vol.16, Issue 6, pp.1207-1214, DOI:10.1007/s10040-008-0285-2.

[3] Martin, G.D., “Aquifer Underground Pumped Hydroelectric Energy Storage,” MScEng Thesis, Department of Electrical and Computer Engineering, University of Colorado at Boulder, Colorado, USA, December 2007.

[4] Eskom. 2015. Drakensberg Pumped Storage Scheme. Johannesburg, SA. (http://www.eskom.co.za/AboutElectricity/FactsFigures/Documents/HY_0007DrakensbergPumpedStorageSchemeRev2.pdf).

[5] Eskom. 2015. Ingula Pumped Storage Scheme. Johannesburg, SA. (http://www.eskom.co.za/AboutElectricity/FactsFigures/Documents/HY_0003IngulaPumpedStorageSchemeRev10.pdf).

[6] Schainker, B.R., “Executive Overview: Energy Storage Options for a Sustainable Energy Future,” Power Engineering Society General Meeting, 2004, IEEE, Vol.2, 10 June 2004, Denver, CO, pp.2309-2314, ISBN:0-7803-8465-2, DOI:10.1109/PES.2004.1373298.

[7] Davidson, I.E., and Mwale, S.J.T., “Power deficits and outage planning in South Africa,” Conference: 2nd International Symposium on Energy Challenges and Mechanics, Vol.1, 19-21 August 2014, Aberdeen, Scotland, UK.

[8] Barnes, F.S., and Levine, J.G., Large Energy Storage Systems Handbook, Taylor & Francis Group, LLC, Florida, USA, 2011.

[9] McGrath, M., “Vast aquifer found in Namibia could last for centuries,” Science and Environment, BBC World Service, 20 July 2012, (http://www.bbc.com/news/science-environment-18875385).

[10] EPRI–DOE Handbook of Energy Storage for Transmission and Distribution Applications, EPRI, Palo Alto, CA, and the U.S. Department of Energy, Washington, DC:2003. 1001834.

[11] Raju, M. and Khaitan, S.K., “Modeling and simulation of compressed air storage in caverns: A case study of the Huntorf plant,” Journal of Applied Energy, January 2012, Vol. 89, Issue 1, pp.474-481, DOI:10.1016/j.apenergy.2011.08.019.

[12] De Samaniego Steta F, “Modelling of an advanced adiabatic compressed air energy storage (AA-CAES) unit and an optimal model-based operation strategy for its integration into power markets,” Master Thesis, EEH – Power Systems Laboratory, Swiss Federal Institute of Technology (ETH), Zurich, October 2010.

[13] Pickard, W.F., Shen, A.Q., and Hansing, N.J., “Parking the power: strategies and physical limitations for bulk energy storage in supply-demand matching on a grid whose input power is provided by intermittent sources,” Journal of Renewable and Sustainable Energy Reviews, October 2009, Vol. 13, Issue 8, pp.1934-45, DOI:10.1016/j.rser.2009.03.002.

[14] Weiss, T., and Schulz, D., “Using already existing artificial structures for energy storage in areas with high shares of renewable energies,” Innovative Smart Grid Technologies (ISGT Europe), 2012 3rd IEEE PES International Conference and Exhibition, IEEE, 14-17 October 2012, Berlin, pp.1-7, ISSN:2165-4816, E-ISBN:978-1-4673-2596-7, DOI:10.1109/ISGTEurope.2012.6465830.

[15] Rastler, D., “Electric energy storage technology options: a white paper primer on applications, costs and benefits,” EPRI, Palo Alto, CA, 2010, 1020676.

[16] Hadjipaschalis, I., Poullikkas, A., and Efthimiou, V., “Overview of current and future energy storage technologies for electric power applications,” Journal of Renewable

and Sustainable Energy Reviews, August-September 2009, Vol.13, Issues 6-7, pp.1513-1522, DOI:10.1016/j.rser.2008.09.028.

[17] Lim, S.D., Mazzoleni, A.P., Park, J., Ro, P.I. and Quinlan, B., "Conceptual Design of Ocean Compressed Air Energy Storage System," Oceans 2012, IEEE, 14-19 October 2012, Hampton Roads, VA, pp.1-8, ISBN:978-1-4673-0829-8, DOI:10.1109/OCEANS.2012.6404909.

[18] Evans, A., Strezov, V., and Evans, T.J., "Assessment of utility energy storage options for increased renewable energy penetration," Journal of Renewable and Sustainable Energy Reviews, August 2012, Vol.16, Issue 6, pp.4141-4147, DOI:10.1016/j.rser.2012.03.048.

[19] Zweibel, K., Mason, J., and Fthenakis, V., "A solar grand plan," Scientific American, Issue 298, January 2008, pp.64-73.

[20] "The economic impact of CAES on wind in Texas, Oklahoma and New Mexico," Ridge Energy Storage and Grid Services L.P., Final Report for Texas State Energy Conservation Office, 27 June 2005.

[21] Levine, J., Martin, G., Moutoux, R., and Barnes, F., "Large Scale Electrical Energy Storage in Colorado," CERI Research Report, 30 June 2007, (www.colorado.edu/engineering/energystorage).

[22] Ibrahim, H., Ilinca, A., and Perron, J., "Energy storage systems – characteristics and comparisons," Journal of Renewable and Sustainable Energy Reviews, June 2008, Vol.12, Issue 5, pp.1221-1250, DOI:10.1016/j.rser.2007.01.023.

[23] Taylor, J. and Halnes, A., "Analysis of Compressed Air Energy Storage," PCIC Europe 2010 Conference Record, IEEE, 15-17 June 2010, Oslo, pp.1-5, ISSN:2151-7665, E-ISBN:978-3-9523333-6-5.

[24] Chen, H., Cong, T.N., Yang, W., Tan, C., Li, Y. and Ding, Y., "Progress in Electrical Energy Storage System: A Critical Review," Journal of Progress in Natural Science, March 2009, Vol.19, Issue 3, pp.291-312, DOI:10.1016/j.pnsc.2008.07.014.

[25] Gazey, R., Dr. Ali, D. and Dr. Aklil, D., “Techno-economic assessment of energy storage systems for enabling projected increase of renewables onto electrical power grids,” Renewable Power Generation (RPG 2011), IET Conference, 6-8 September 2011, Edinburgh, pp.1-6, DOI:10.1049/cp.2011.0135.

[26] Ribeiro, P.F., Johnson, P.K., Crow, M.L., Arsoy, A. and Liu, Y., “Energy storage systems for advanced power applications,” Proceedings of the IEEE, Vol. 89, Issue 12, IEEE, December 2001, pp.1744-1756, ISSN:0018-9219, DOI:10.1109/5.975900.

[27] Manz, D., Piwko, R., and Miller, N., “The role of energy storage in the grid,” Power and Energy Magazine, IEEE, July-August 2012, Vol.10, Issue 4, pp.75-84, ISSN:1540-7977, DOI:10.1109/MPE.2012.2196337.

[28] Sparacino, A.R., Reed, G.F., Kerestes, R.J., Grainger, B.M. and Smith, Z.T., “Survey of battery energy storage systems and modeling techniques,” Power and Energy Society General Meeting, IEEE, 22-26 July 2012, San Diego, CA, pp.1-8, ISSN:1944-9925, E-ISBN:978-1-4673-2727-5, DOI:10.1109/PESGM.2012.6345071.

[29] Vazquez, S., Lukic, S.M., Galvan, E., Franquelo, L.G., and Carrasco, J.M., “Energy storage systems for transport and grid applications,” IEEE Transaction on Industrial Electronics, Vol.57, Issue 12, December 2012, pp.3881-3895, ISSN:0278-0046, DOI:10.1109/TIE.2010.2076414.

[30] Kusko, A., and Dedad, J., “Short-term and long-term energy storage methods for standby electric power systems,” Industry Applications Conference 2005, Fortieth IAS Annual Meeting, Vol.4, IEEE, 2-6 October 2005, pp.2672-2678, ISSN:0197-2618, DOI:10.1109/IAS.2005.1518837.

[31] Walawalkar, R., and Apt, J., “Market analysis of emerging electric energy storage systems,” Carnegie Mellon Electricity Industry Centre, National Energy Technology Laboratory, DOE/NETL-2008/1330, July 2008.

[32] McDowall, J., “Nickel-cadmium batteries for energy storage applications,” The Fourteenth Annual Battery Conference on Applications and Advances, IEEE, 12-15

January 1999, Long Beach, CA, pp.303-308, ISSN:1089-8182, DOI:10.1109/BCAA.1999.796008.

[33] Slocum, A.H., Fennell, G.E., Dundar, G., Hodder, B.G., Meredith, J.D.C. and Sager, M.A., “Ocean renewable energy storage (ORES) system: Analysis of an undersea energy storage concept,” Proceedings of the IEEE, April 2013, Vol. 101, Issue 4, IEEE, pp.906-924, ISSN:0018-9219, DOI:10.1109/JPROC.2013.2242411.

[34] “Investigation on storage technologies for intermittent renewable energies: evaluation and recommended R&D strategy,” INVESTIRE-NETWORK (ENK5-CT-2000-20336), Storage Technology Reports (http://www.itpower.co.uk).

[35] Wong, B., Snijders, A., and McClung, L., “Recent Inter-Seasonal Underground Thermal Energy Storage Applications in Canada,” EIC Climate Change Technology, IEEE, 10-12 May 2006, Ottawa, ON, pp.1-7, E-ISBN:1-4244-0218-2, DOI:10.1109/EICCCC.2006.277232.

[36] Boicea, V.A., “Energy storage technologies: The past and the present,” Proceedings of the IEEE, November 2014, IEEE, Vol. 102, Issue 11, pp.1777-1794, ISSN:0018-9219, DOI:10.1109/JPROC.2014.2359545.

[37] Bose, J.E., Ledbetter, C.W., and Partin, J.R., “Experimental results of a low-cost solar assisted heat pump system using earth coil and geothermal well storage,” Proceedings of the Fourth Annual Heat Pump Technology Conference, 1979, Stillwater, Oklahoma State University.

[38] Wang, H., and Qi, C., “Performance study of underground thermal storage in a solar-ground coupled heat pump system for residential buildings,” Journal of Energy and Buildings, 2008, Vol.40, Issue 7, pp.1278-1286, DOI:10.1016/j.enbuild.2007.11.009.

[39] Wang, H., and Zhao, J., “Center solar heating technology with seasonal thermal storage,” Journal of Solar Energy, 2005, Vol.108, Issue 4, pp.27-31.

[40] Paksoy, H.O., Gurbuz, Z., Turgut, B., Dikici, D., and Evliya, H., “Aquifer thermal storage (ATES) for air-conditioning of a supermarket in Turkey," Journal of

Renewable Energy, October 2004, Vol.29, Issue 12, pp.1991-1996, DOI:10.1016/j.renene.2004.03.007.

[41] Dalvi, C., “Cryogenic energy storage,” Submitted as coursework for PH240, Stanford University, December 2012.

[42] Lombardo, T., “Cryogenic energy storage,” 29 May 2013, (http://www.engineering.com/ElectronicsDesign/ElectronicsDesignArticles/ArticleID/5780/Cryogenic-Energy-Storage.aspx).

[43] Lo, C., “Reliable renewables with cryogenic energy storage,” Power Technology Market and Customer Insight, 23 July 2013, (http://www.power-technology.com/features/feature-reliable-renewables-cryogenic-energy-storage).

[44] Dunn, R.I., Hearps, P.J., and Wright, M.N., “Molten-salt power towers: Newly commercial concentrating solar storage,” Proceedings of the IEEE, Vol.100, Issue 2, February 2012, IEEE, pp.504-515, ISSN:0018-9219, DOI:10.1109/JPROC.2011.2163739.

[45] Sharma, A., Tyagi, V.V., Chen, C.R., and Buddhi, D., “Review on thermal energy storage with phase change materials and applications,” Journal on Renewable and Sustainable Energy Reviews, February 2009, Vol.13, Issue 2, pp.318-345, DOI:10.1016/j.rser.2007.10.005.

[46] “Thermal Energy Storage,” Technology Brief E17, January 2013, IEA-ETSAP and IRENA (www.etsap.org – www.irena.org).

[47] Gil, A., Medrano, M., Martorell, I., Lazaro, A., Dolado, P., Zalba, B., et al., “State of the art on high temperature thermal energy storage for power generation. Part 1 – concepts, materials and modellization,” Journal of Renewable and Sustainable Energy Reviews, January 2010, Vol.14, pp.31-55, DOI:10.1016/j.rser.2009.07.035.

[48] Liu, C., Li, F., Ma, L.P., and Cheng, H.M., “Advanced materials for energy storage,” Journal of Advanced Materials, February 2010, Vol.22, Issue 8, pp.E28-62, DOI:10.1002/adma.200903328.

[49] Bastien, J. and Handler, C., “Hydrogen production from renewable energy sources,” EIC Climate Change Technology, 10-12 May 2006, IEEE, Ottawa, ON, pp.1-9, E-ISBN:1-4244-0218-2, DOI:10.1109/EICCCC.2006.277218.

[50] Emori, H., Kawamura, T., Ishikawa, T. and Takamura, T., “Carbon-hydride energy storage system,” Humanitarian Technology Conference (R10-HTC), 2013 IEEE Region 10, 26-29 August 2013, IEEE, Sendai, pp.142-147, DOI:10.1109/R10-HTC.2013.6669031.

[51] Grant, D.C., “Short and long term energy storage for enhanced resilience of electric infrastructures,” The Fifth International Renewable Energy Congress (IREC), 25-27 March 2014, IEEE, Hammamet, pp.1-6, ISBN:978-1-4799-2196-6, DOI:10.1109/IREC.2014.6826953.

[52] Hassenzahl, W.V., “Superconducting magnetic energy storage,” Proceedings of the IEEE, Vol. 71, Issue 9, IEEE, September 1983, pp.1089-1098, ISSN:0018-9219, DOI:10.1109/PROC.1983.12727.

[53] Boyes, J.D. and Clark, N.H., “Technologies for energy storage flywheels and super conducting magnetic energy storage,” Power Engineering Society Summer Meeting, 16-20 July 2008, Seattle, WA, IEEE, Vol.3, pp.1548-1550, ISBN:0-7803-6420-1, DOI:10.1109/PESS.2000.868760.

[54] Schoenung, S.M., and Burns, C., “Utility energy storage applications studies,” IEEE Transactions on Energy Conversion, Vol. 11, Issue 3, September 1996, IEEE Power and Energy Society, pp.658-665, ISSN:0885-8969, DOI:10.1109//60/537039.

[55] Honghai, K., and Zhengqiu, W., “Research of super capacitor energy storage system based on DG connected to power grid,” International Conference on Sustainable Power Generation and Supply, 2009, SUPERGEN 2009, pp.1-6, 6-7 April 2009, Nanjing, ISBN:978-1-4244-4934-7, DOI:10.1109/SUPERGEN.2009.5348057.

[56] Wright, J.K., “Large-scale storage of electrical energy,” Electronics and Power, Vol.26, Issue 2, February 1980, IET, pp.153-157, ISSN:0013-5127, DOI:10.1049/ep.1980.0085.

[57] Roberts, B., “Performance, purpose, and promise of different storage technologies,” Power and Energy Magazine, IEEE, Vol.7, Issue 4, July-August 2009, pp.32-41, ISSN:1540-7977, DOI:10.1109/MPE.2009.932876.

[58] Pena-Alzola, R., Sebastian, R., Quesada, J., and Colmenar, A., “Review of flywheel based energy storage systems,” International Conference on Power Engineering, Energy and Electrical Drives (POWERENG), 11-13 May 2011, IEEE, Malaga, pp.1-6, E-ISBN:978-1-4244-9843-7, DOI:10.1109/PowerEng.2011.6036455.

[59] Kondoh, J., Ishii, I., Yamaguchi, H., Murata, A., Otani, K., Sakuta, K., et al., “Electrical energy storage systems for energy networks,” Journal of Energy Conversion and Management, November 2000, Vol.41, Issue 17, pp.1863-1874, DOI:10.1016/S0196-8904(00)00028-5.

[60] Fang, X., Kutkut, N., Shen, J., and Batarseh, I., “Analysis of generalized parallel-series ultracapacitor shift circuits for energy storage systems,” Journal of Renewable Energy: Generation and Application, October 2011, Vol.36, Issue 10, pp.2599-2604, DOI:10.1016/j.renene.2010.05.003.

[61] Kinjo, T., Senjyu, T., Urasaki, N., and Fujita, H., “Output levelling of renewable energy by electric double-layer capacitor applied for energy storage system ,” IEEE Transactions, Energy Conversion, March 2006, Vol.21, Issue 1, pp.221-227, ISSN:0885-8969, DOI:10.1109/TEC.2005.853752.

[62] Muyeen, S.M., Shishido, S., Ali, M.H., Takahashi, R., Murata, T., and Tamura, J., “Application of energy capacitor system (ECS) to wind power generation,” Journal of Wind Energy, July 2008, Vol.11, Issue 4, pp.335-350, DOI:10.1002/we.265.

[63] Deane, J.P., O Gallachoir, B.P., and McKeogh E.J., “Techno-economic review of existing and new pumped hydro energy storage plant,” Journal of Renewable and Sustainable Energy Reviews, May 2010, Vol.14, Issue 4, pp.1293-1302, DOI:10.1016/j.rser.2009.11.015.

[64] Castronuovo, E.D., and Pecas Lopes, J.A., “Optimal operation and hydro storage sizing of a wind-hydro power plant,” International Journal of Electrical Power and Energy Systems, December 2004, Vol.26, Issue 10, pp.771-778, DOI:10.1016/j.ijepes.2004.08.002.

[65] Kaldellis, J.K., Kavadias, K.A., and Vlachou, D.S., “Electricity load management of APS using wind-hydro solution,” 3rd Mediterranean Conference and Exhibition on Power Generation, Transmission Energy and Distribution – Med Power, 2002, Athens, Greece.

[66] Kaldellis, J.K., and Kavadias, K.A., “Optimal wind hydro solution for Aegean sea islands’ electricity demand fulfilment,” Journal of Applied Energy, December 2001, Vol.70, Issue 4, pp.333-354, DOI:10.1016/S0306-2619(01)00036-8.

[67] Leonard, W., and Grobe, M., “Sustainable electrical energy supply with wind and pumped storage – A realistic long-term strategy or utopia,” Power Engineering Society General Meeting, Vol.2, 10 June 2004, Denver, CO, pp.1221-1225, ISBN:0-7803-8465-2, DOI:10.1109/PES.2004.1373049.

[68] Rosa, L.P., and dos Santos, M.A., “Certainty and uncertainty in the science of greenhouse gas emissions from hydroelectric reservoirs (Part 2),” A report on the state of the art for the World Commission on Dams, WCD Thematic Review II.2, March 2000.

[69] Denholm, P., and Kulcinski, G.L., “Life cycle energy requirements and greenhouse gas emissions from large scale energy storage systems,” Journal of Energy Conversion and Management, August 2004, Vol.45, Issues 13-14, pp.2153-2172, DOI:10.1016/j.enconman.2003.10.014.

[70] “Basics of Turbulent Flow,” Massachusetts Institute of Technology, (www.mit.edu/course/1/1.061/www/dream/SEVEN/SEVENTHEORY.PDF).

[71] “Basic Hydraulic Principles,” Computer Applications in Hydraulic Engineering, Haestad Methods Inc., Waterbury, CT, 2002 (http://www.dynatech.nl/Basic%20Hydraulic%20Principles.pdf).

[72] Adrian, R.J., and Christensen, K.T., “Analysis and interpretation of instantaneous turbulent velocity fields,” Journal of Experiments in Fluids, August 2000, Vol.29, Issue 3, Illinois, US, pp.275-290, DOI:10.1007/s003489900087.

[73] Huggins, R.A., Energy Storage, Springer, New York/London, 2010, ISBN 978-1-4419-1024-0.

[74] Allen, R.D., Doherty, T.J., and Kannberg, L.D., “Underground pumped hydroelectric storage,” Pacific Northwest National Laboratory, U.S. Department of Energy, DE-AC06-76RLO 1830, Richland, WA, July 1984.

[75] Allen, A.E., “Potential for conventional and underground pumped-storage”, IEEE Transactions on Power Apparatus and Systems, , Vol. 96, Issue 3, 19-23 September 1976, IEEE, pp.993-998, ISSN:0018-9510, DOI:10.1109/T-PAS.1977.32413.

[76] Allen, A.E., and Larson, W.E., “Developments in underground pumped-storage,” Edison Electric Institute, May 1974.

[77] Pickard, W.F., “The History, Present State, and Future Prospects of Underground Pumped Hydro for Massive Energy Storage,” IEEE, Vol. 100, No. 2, February 2012, pp.473-483, ISSN:0018-9219, DOI:10.1109/JPROC.2011.2126030.

[78] Sorensen, K.E., “Underground reservoirs: Pumped storage of the future?” Journal of Civil Engineering, March 1969, Vol.39, Issue 3, pp.66-70.

[79] Uddin, N., “Preliminary design of an underground reservoir for pumped storage,” Journal of Geotechnical and Geological Engineering, November 2003, Vol.21, Issue 4, pp.331-355, DOI:10.1023/B:GEGE.0000006058.79137.e2.

[80] Uddin, N., “Geotechnical issues in the creation of underground reservoirs for massive energy storage,” Proceedings of the IEEE, Vol. 100, Issue 2, February 2012, IEEE, pp.484-492, ISSN:0018-9219, DOI:10.1109/JPROC.2011.2161969.

[81] Gordon, J.L., “Hydraulic turbine efficiency,” Canadian Journal of Civil Engineering, NRC Canada 2001, Vol.28, pp.238-253, DOI:10.1139/cjce-28-2-238.

[82] Williams, A.A., “The turbine performance of centrifugal pumps: A comparison of prediction methods,” Part A: Journal of Power and Energy, Proceedings of the Institution of Mechanical Engineers, February 1994, Vol.208, Issue 1, pp.59-66, DOI:10.1243/PIME_PROC_1994_208_009_02.

[83] Charbeneau, R.J., “Groundwater Hydraulics and Pollutant Transport,” Upper Saddle River, New Jersey, Prentice Hall, ISBN 0139756167, 2000, pp.48-114.

[84] Batterton, S., “Water hammer: An analysis of plumbing systems, intrusion and pump operation,” MSc Civil Engineering, Virginia Polytechnic Institute and State University, Blacksburg, Virginia, July 2006.

[85] Parmakian, J., Waterhammer Analysis, New York, Dover Publications, 1963.

[86] Hansen, A.G., “Fluid Mechanics,” Journal of Fluid Mechanics, June 1968, Vol.32, Issue 4, Cambridge University Press, DOI:10.1017/S0022112068211060.

[87] Powers, J.M., “Control Volume Derivations for Thermodynamics,” University of Notre Dame, AME327, 2003 (www3.nd.edu/~powers/ame.50531/equation.pdf).

[88] Street, R.L., Watters, G.Z., and Vennard, J.K., Elementary Fluid Mechanics, 7th Edition, Wiley, 1996, ISBN:978-0-471-01310-5.

[89] “Sub-surface pumped hydroelectric storage,” Energy Storage Association, Washington, USA. (http://energystorage.org/energy-storage/technologies/sub-surface-pumped-hydroelectric-storage).

[90] “Grid scale energy storage,” Gravity Power, Goleta, Canada. (http://www.gravitypower.net/technology-gravity-power-energy-storage).

[91] Topper, R., Barkmann, P.E., Bird, D.A. and Sares, M.A, “Artificial Recharge of Groundwater in Colorado – A Statewide Assessment,” Colorado Geological Survey, Environmental Geology 13, Department of Natural Resources, Denver, Colorado, 2004.

[92] Woodford, A., Rosewarne, P., and Girman, J., “How Much Groundwater Does South Africa Have?” National Groundwater Resource Assessment 2 (GRA 2), SRK Consulting and Department of Water Affairs and Forestry, South Africa, 2005, (http://www.srk.co.za/files/File/newsletters/groundwater/PDFs/1_A_Woodford.pdf).

[93] “A Groundwater Mapping Strategy for South Africa,” Directorate Geohydrology publication, Department of Water Affairs and Forestry, August 2002, Pretoria, South Africa.

[94] Vegter, J.R., Seymour, A.J., and Simonic, M., “Groundwater Resources of the Republic of South Africa. A Set of 7 Maps,” Water Research Commission and Department of Water Affairs and Forestry, 2005.

[95] Vegter, J.R., “Groundwater Resources of South Africa: An explanation of a set of national groundwater maps,” Water Research Commission Report No. TT 74/95, Pretoria, South Africa, 1995.

[96] Abiye, T.A., Mengistu, H., and Demlie, M.B., “Groundwater Resource in the Crystalline Rocks of the Johannesburg Area, South Africa,” Journal of Water Resource and Protection, April 2011, Vol.3, pp.199-212, DOI:10.4236/jwarp.2011.34026.

[97] Buchanan, M., “Hypothesizing the Highly Fractured Defuse South African Transvaal Aquifer (SATVLA),” IUCN WCPA Task Force on cave and Karst, Cave Research Organization of South Africa – CROSA, Hampshire, United Kingdom, 2005.

[98] “Hydrology of Upper Crocodile River Sub-System,” Department of Water Affairs and Forestry (DWAF), Report No. PA200/00/1492, Vol.1-2, DWAF, 1992, Pretoria, South Africa.

[99] Barnard, H.C., “An Explanation for the 1:500 000 Hydrogeological Map of Johannesburg 2526,” Department of Water Affairs and Forestry, 2000, Pretoria, South Africa.

[100] Bredenkamp, D.B., and Xu, Y., “Perspectives on Recharge Estimation in Dolomitic Aquifers in South Africa,” In: Xu, Y., and Beekman, H.F., Eds., Groundwater Recharge Estimation in Southern Africa, UNESCO, p.207, 2003.

[101] “Derivation of a Numerical Model for a Cumulative Water Balance of the Central Rand Basin,” Ferret Report, Council for Geosciences, 2005, Pretoria, South Africa.

[102] “Numerical Modelling of Seepage Potential at Three Ingress Areas of the Central Rand Basin of the Witwatersrand Goldfields,” Africa Geo-Environmental Services (AGES) Report, Council for Geosciences, 2005, Pretoria, South Africa.

[103] Adams, S., Titus, R., Pietersen, K., Tredoux, G., and Harris, C., “Hydrochemical characteristics of aquifers near Sutherland in the Western Karoo, South Africa,” Journal of Hydrology, January 2001, Vol.241, Issues 1-2, pp.91-103, DOI:10.1016/S0022-1694(00)00370-X.

[104] Rosewarne, P., Woodford, A., Goes, M., Talma, S., O’Brien, R., Tredoux, G., Esterhuyse, C., Visser, D., and van Tonder, G., “Recent Developments in the Understanding of Karoo Aquifers and the Deeper Underlying Formations,” Karoo Groundwater Expert Group, 2013, (http://gwd.org.za/sites/gwd.org.za/files/01_Peter%20Rosewarne_Recent%20Developments%20in%20the%20Understanding%20of%20Karoo%20Aquifers.pdf).

[105] Woodford, A.C., and Chevallier, L., “Hydrogeology of the Main Karoo Basin: Current Knowledge and Future Research Needs,” WRC Report No. TT 179/02, 2002, Pretoria, South Africa.

[106] “Huge ancient freshwater aquifer under seabed,” Posted by: Saving Water SA – partnered with Water Rhapsody conservation systems, May 2010, (http://www.savingwater.co.za/2010/05/10/08/huge-ancient-freshwater-aquifer-under-seabed/)

[107] Lohe, C., and Houben, G., “TC Namibia: Groundwater for the North of Namibia,” BGR Projects,

(http://www.bgr.bund.de/EN/Themen/Wasser/Projekte/laufend/TZ/Namibia/ceb_fb_en.html).

[108] Jager, M., “Namibia – Groundwater Management in the North of Namibia,” Technical Cooperation with Namibia Kalahari: Hydrogeology and Sedimentology of the Cuvelai-Etosha Basin, Southern African Science Service Centre for Climate Change and Adaptive Lad Management (SASSCAL), BGR Projects, Project-No.: 2013.2472.2, (http://www.bgr.bund.de/EN/Themen/Zusammenarbeit/TechnZusammenarb/Projekte/Laufend/Afrika/2011_2013-2472-2_Namibia_Grundwassermanagement_en.html).

[109] “Electricity Supply and Demand Management Options for Namibia. A Technical and Economic Evaluation,” Ministry of Mines and Energy, Renewable Energy and Energy Efficiency Capacity Building Programme (REEECAP), March 2008 (http://www.reeei.org.na/admin/data/uploads/Namibia%20Electricity%20Supply%20Demand%20Options.pdf).

[110] Struckmeier, W.F., Gilbrich, W.H., Gun, Jvd., Maurer, T., et al., “WHYMAP and the World Map of Transboundary Aquifer Systems at the scale of 1: 50 000 000,” Special Edition for the 4th World Water Forum, Mexico City, March 2006, BGR, Hannover and UNESCO, Paris.

[111] Jean Boroto, R.A., “Limpopo River: steps towards sustainable and integrated water resources management,” Regional Management of Water Resources, Proceedings of a symposium held during the Sixth IAHS Scientific Assembly at Maastricht, The Netherlands, July 2001, IAHS Publication No.268, 2001.

[112] Hobbs, P.J., and Esterhuyse, C.J., “A preliminary evaluation of the groundwater resources of the upper Limpopo River valley, North West Transvaal,” Department of Water Affairs and Forestry Report Gh3278, 1983, Pretoria, South Africa.

[113] Davies, J., “Lesotho Lowlands water supply feasibility study – Hydrogeology,” British Geological Survey Report CR/03/176C, 2003.

[114] Meyer, R., Talma, A.S., Duvenhage, A.W.A., Eglington, B.M., et al., "Geohydrological investigation and evaluation of the Zululand Coastal Aquifer," Water Research Commission Report 221/1/01, 2001, Pretoria, South Africa.

[115] Madlener, R., and Specht, J.M., "An Exploratory Economic Analysis of Underground Pumped-Storage Hydro Power Plants in Abandoned Coal Mines," FCN Working Paper No. 2/2013, Institute for Future Energy Consumer Needs and Behavior, RWTH Aachen University, February 2013.

[116] Nanahara, T., and Takimoto, A., "A Study on Required Reservoir Size for Pumped Hydro Storage," IEEE Transactions on Power Systems, February 1994, Vol.9, Issue 1, pp.318-323, ISSN:0885-8950, DOI:10.1109/59.317595.

[117] Coetzee, H., Nengobela, N.R., Vorster, C., Sebake, D., and Mudau, S., "South Africa's strategy for the management of derelict and ownerless mines," Conference: Mine Closure 2008, Proceedings of the third international seminar on mine closure, Johannesburg, South Africa.

[118] "The National Strategy for the Management of Derelict and Ownerless Mines in South Africa," Department of Mineral Resources, 2009, Pretoria, South Africa.

[119] McCarthy, T.S., and Pretorius, K., "Coal Mining on the Highveld and its Implications for Future Water Quality in the Vaal River System," Proceedings of the International Mine Water Conference, 19-23 October 2009, Pretoria, South Africa, ISBN:978-0-9802623-5-3.

[120] Wagner, H., "Pillar design in coal mines," Journal of the South African Institute of Mining and Metallurgy, January 1980, Vol.80, Issue 1, pp.37-45.

[121] Norden, C., and Ismail, J., "Defining a representative overall equipment effectiveness (OEE) measurement for underground bord and pillar coal mining," Journal of South African Institute of Mining and Metallurgy, December 2012, Vol.112, Issue 10, pp.845-851, ISSN:2225-6253.

[122] Kaldellis, J.K., “An integrated time-depending feasibility analysis model of wind energy applications in Greece,” Journal of Energy Policy, March 2002, Vol.30, Issue 4, pp.267-280, DOI:10.1016/S0301-4215(01)00089-1.

[123] Kavadias, K.A., and Kaldellis, J.K., “Storage system evaluation for wind power installations,” Proceedings of the international conference of wind power for the 21st century, 2000, Paper OR7.3.

[124] Kaldellis, J.K., Kavadias, A.K., and Filios, A., “Techno-economic evaluation of large energy storage systems used in wind energy applications,” European Wind Energy Conference and Exhibition, February-March 2006, EWEC-2006, Athens, Greece.

[125] Kaldellis, J.K., Zafirakis, D., and Kavadias, K., “Techno-economic comparison of energy storage systems for island autonomous electrical networks,” Journal of Renewable and Sustainable Energy Reviews, February 2009, Vol.13, Issue 2, pp.378-392, DOI:10.1016/j.rser.2007.11.002.

[126] Ochieng, G.M., Seanego, E.S., and Nkwonta, O.I., “Impacts of mining on water resources in South Africa: A review,” Scientific Research and Essays, December 2010, Vol.5, Issue 22, pp.3351-3357, ISSN:1992-2248.

[127] Adams, R., and Younger, P.L., “A Strategy for Modelling Ground Water Rebound in Abandoned Deep Mine Systems,” Journal of Ground Water, March 2001, Vol.39, Issue 2, pp.249-261, DOI:10.1111/j.1745-6548.2001.tb02306.x.

[128] Oelofse, S., “Mine Water Pollution – Acid Mine Decant, Effluent and Treatment: A Consideration of Key Emerging Issues that may Impact the State of the Environment,” Department of Environmental Affairs and Tourism (DEAT), March 2008, (http://www.hsph.harvard.edu/mining/files/South_Africa.pdf).

[129] Pratt, S.E., “All that glitters … Acid mine drainage: The toxic legacy of gold mining in South Africa,” Earth: The Science Behind the Headlines, 23 September 2011, (http://www.earthmagazine.org/article/all-glitters-acid-mine-drainage-toxic-legacy-gold-mining-south-africa).

[130] “Water Treatment in South Africa: Water for All,” Massachusetts Institute of Technology, (http://12.000.scripts.mit.edu/mission2017/water-treatment-in-south-africa/).

[131] Johnson, D., and Fourie, C.J.S., “Conference Paper for the Geothermal Potential of South African Deep Mines,” Southern African Energy Efficiency Convention (SAEEC), November 2013, ISBN:978-0-620-58204-9.

[132] Watzlav, G.R., and Ackerman, T.E., “Underground Mine Water for Heating and Cooling using Geothermal Heat Pumps,” Journal of Mine Water and the Environment, February 2006, Vol.25, Issue 1, pp.1-14, DOI:10.1007/s10230-006-0103-9.

[133] Cassell, B., “FERC license sought for 260-MW pumped storage project in N.Y.,” Generation Hub, 10 April 2013, (http://generationhub.com/2013/10/04/ferc-license-sought-for-260-mw-pumped-storage-proj).

[134] Moriah Hydro Corporation; Notice of Preliminary Permit Application Accepted for Filing and Soliciting Comments, Motions To Intervene and Competing Applications, A Notice by the Federal Energy Regulatory Commission, Federal Register: The Daily Journal of the United States Government, 6 January 2010, (https://www.federalregister.gov/articles/2010/01/14/2010-524/moriah-hydro-corporation-notice-of-preliminary-permit-application-accepted-for-filing-and-soliciting).

[135] Acres International Corporation, “Summit hydroelectric pumped storage project: Report on investigations from the mine,” Report prepared for Summit Energy Storage, Inc. Vol.1-2, 1993.

[136] Broch, E., Tunnels and Underground Works for Hydropower Projects: Lessons learned in home country and from projects worldwide, April 2010, International Tunneling and Space Association, ISBN:978-2-9700624-4-8.

APPENDIX A

Aquifer classification of South Africa

APPENDIX B

Aquifer vulnerability of South Africa

APPENDIX C

Aquifer susceptibility of South Africa

APPENDIX D

Groundwater and aquifers in Namibia